A GRAVITY INVESTIGATION OF EASTERN IRON COUNTY, MICHIGAN

by

David Ray Paddock

A THESIS

Submitted to
Michigan State University
in partial fulfillment of the requirements
for the degree of

MASTER OF SCIENCE

Department of Geology

1982

ABSTRACT

A GRAVITY INVESTIGATION OF EASTERN IRON COUNTY, MICHIGAN

by

David Ray Paddock

A gravity survey was conducted in the Iron River-Crystal Falls district (IR-CF) to determine whether the "Paint River Group" is correlative with other parts of the Marquette Range Supergroup (MRS), the structure of the boundary, and, whether IR-CF belongs to MRS, is a greenstone belt, or is trapped or obducted ocean crust. Two hundred gravity measurements were taken, modified Bouguer corrected, including removal of till effects, and reduced to datum using a bedrock density of 2.91 gm/cc. These data supplemented previously existing data which were linearly transformed to agree with the above reductions. Subsurface structure was modelled using a Talwani 2D gravity routine assuming laterally uniform thickness of formations. The existing U.S.G.S. interpretation is most consistent with the observed gravity. Interpretation of the IR-CF as an "uplifted" or "downdropped" fault-block would require a minimum lateral thickening of 2.1 and 3.8 kilometers, respectively; a minimum of 3.8 kilometers is required to model the Kiernan Sills as ophiolites.

DEDICATION

This work is dedicated to the friends with whom I shared many 100 mile (and shorter) bicycle rides: David Michael Riggs, Robin Theresa Cole, Jay Brian Silber, and April Poelvoorde.

ACKNOWLEDGEMENTS

I thank Dr. Hugh F. Bennett for his guidance, advice, and suggestions concerning a thesis topic which was somewhat forced upon him. Hugh's stints as tennis opponent were also appreciated; although they were too infrequent for both of us.

I thank Kazuya Fujita for his drafting of most of the figures in this work, for his friendship, for the use of his Decwriter IV and personal library, and for his suggestions during the two years this study took place.

Thanks go to Dr. Jim Trow for his seemingly limitless knowledge of and familiarity with the Lake Superior region and for his invariably cheery disposition.

Dr. F. W. Cambray is to be thanked for his patience in approving my continual requests for more computer money.

I would like to thank Mike Gottler for his help and company in the 1981 field work for this study, and to thank Robin Cole for her help in the 1980 OCT field session. Special thanks go to Jay Brian Silber, April Poelvoorde, Kazuya Fujita, and Cynthia Lynn Cordes for their understanding friendship and for getting me through the hard times.

I would like to thank David K. Larue for data prior to publication (actually, they were used without his knowledge).

TABLE OF CONTENTS

LIST OF TABLES

LIST OF FIGURES

LIST OF PLATES

STRATIGRAPHIC NOMENCLATURE

Xg = Middle Proterozoic granites

Xmin = Early Proterozoic mafic intrusives, including the Peavy Pond Complex

gab = gabbro

um = ultramatics

Xp = Early Proterozoic, "Paint River Group"

sed = oceanic sediments

Xpf = Early Proterozoic, "Paint River Group", Fortune Lake Slate

Xpfs = Early Proterozoic, "Paint River Group", Fortune Lake Slate south member

Xpr = Early Proterozoic, "Paint River Group", Riverton Iron Formation

Xpd = Early Proterozoic, "Paint River Group", Dunn Creek Slate

gs = greenstone

Xb = Early Proterozoic, Baraga Group, generally does not include Badwater Greenstone

bas = basalt

Xbb = Early Proterozoic, Baraga Group, Badwater Greenstone

Xbm = Early Proterozoic, Baraga Group, Michigamme Formation

Xba = Early Proterozoic, Baraga Group, Amasa Formation

Xbh = Early Proterozoic, Baraga Group, Hemlock Formation

Xm = Early Proterozoic, Menominee Group

Xcr = Early Proterozoic, Chocolay Group, Randville Dolomite

Wd = Archean, Dickinson Group

Wg = Archean, granitic rocks

Wgn = Archean, granite gneiss

Wbcg = Archean, Bell Creek Gneiss

1. INTRODUCTION

1.1 The Problem

Beginning in the late 1950's, a number of papers were published concerning the structure, stratigraphy, and tectonics of the Iron River-Crystal Falls district and its environs (James, 1958; James and others, 1968; Pettijohn and others, 1969; Cambray, 1977). These papers do not reach a consensus in their interpretation of the Iron River-Crystal Falls district (IR-CF).

In an attempt to discern which geologic model(s) were most feasible, a gravity survey was conducted in eastern Iron County, Upper Peninsula of Michigan. The survey samples the eastern boundary and the eastern half of the northern boundary of the IR-CF district. The resulting data were then modelled using a Talwani two-dimensional gravity program (Talwani and others, 1959).

1.2 Geologic Setting

The Iron River-Crystal Falls district is a triangular-shaped syncline of early Proterozoic (Precambrian X) metavolcanics and metasediments which belong to the $\sim$2.0 Ga old (Cannon, 1978) Marquette Range Supergroup. The apices of the triangle are roughly located at Iron River, Crystal Falls, and the Michigan-Wisconsin border at US-141, with an arm extending southeast along the state line for some distance. Regionally, the Marquette Range Supergroup rests unconformably on Archean (Precambrian W) gneisses, metavolcanics, and granites whose ages vary from in excess of 3.0 Ga to about 2.6 Ga (Cannon, 1978). Also, present in the study area are intrusive rocks emplaced during two separate (?) events. The first

are early Proterozoic intrusives of mafic composition which were emplaced during deposition of the Marquette Range Supergroup (2.0 Ga) (Cannon, 1978). The other intrusives are of varying composition and synchronous with the Penokean Orogeny (1.9 Ga) (Cannon, 1978). Scattered remnants of Paleozoic rocks cover only a tiny percentage of outcrop area, which is itself a small percentage of the total study area.

The region has been interpreted as an ancient passive margin, with Marquette Range Supergroup sediments and volcanics deposited both in grabens and on platformal or interbasinal areas (Cambray, 1977; Larue and Sloss, 1980). Outcrops of Archean rocks on anticlines and domes are common and are generally of large area. Although the trends of folds in both the Archean and Proterozoic rocks are NW-SE, the frequent crossfolding and overturning of beds observed in the Proterozoics suggest that they have been more severely deformed than their Archaean counterparts (James and others, 1968). Folds in the Proterozoic beds are nearly isoclinal and beds generally dip at more than sixty degrees (James and others, 1968). Faults are mostly high angle thrusts (James and others, 1968), but are of unknown age. The two major unconformities are above and below the early Proterozoic rocks (Cannon, 1978).

1.3. Previous Works

1.3.1. Geologic Works

Several significant United States Geologic Survey publications have been written concerning the Iron River-Crystal Falls district and its environs (Clements and Smyth, 1899; Gair and Weir, 1956;

James, 1958; Bayley, 1959; James and others, 1961; Weir, 1967; James and others, 1968; Dutton, 1971). The modern study of the geology of Iron and Dickinson Counties began with the introduction of a new stratigraphic column (James, 1958; Figure 1), which is still generally accepted today.

The premier work on the area is James and others (1968), which includes a fine geologic map, litholigic descriptions and thicknesses, a simple Bouguer gravity map, chemical analyses (including a whole-formation density determination of the Riverton Iron Formation), some magnetic coverage, descriptions of structural style, and dissent by co-author Pettijohn in structural interpretation:

> It is the opinion of one of the authors (FJP) that the folds in the Michigamme Slate are unrelated to those in the Badwater Greenstone and Dunn Creek Slate and that in fact they are separated by a northerly trending fault marked by the Little Tobin Lake granite dike and similar dike-like bodies to the north. This inferred fault would terminate to the north or be displaced along the Cayia fault and, for much of its length, would separate Michigamme Slate to the east from Dunn Creek Slate to the west. In this view, the Badwater Greenstone might not be a continuous mass; rather it might reach bedrock surface on a series of anticlines comparable to that in Sec. 19, T.42N., R.32W., and the adjacent part of Sec. 24, T.42N., R.33W.

Publication of James and others (1968) was quickly followed by the release of investigations by the Michigan Geologic Survey (e.g., Pettijohn and others, 1969; James and others, 1970; Weir, 1971; Pettijohn, 1972) which contain essential information not included by James and others (1968).

Although additional interpretations of the structure, stratigraphy, and tectonics of the area began to be published during

Middle Proterozoic			Granitic rocks		gr
Early			Mafic intrusives		min
		Paint	Fortune Lakes Slate		sl
			Stambaugh Slate		mag sl
		River	Hiawatha Graywacke		gw
			Riverton Iron Formation		if
	Marquette	Group	Dunn Creek Slate		sl
			Badwater Greenstone		gs
		Baraga	Michigamme Formatin		sl
		Group	Amasa Formation		sl-if
Proterozoic	Range		Hemlock Formation		gs
		Menominee	Vulcan Iron Formation		gf
		Group	Felch Formation		sl
	Supergroup		Saunders Formation	Randville Dolomite	dm
		Chocolay		Sunday Quartzite / Sturgeon Quartzite	qzt
		Group		Fern Creek Formation	cgl
		Dickinson		Margeson Creek	
Archean					var
		Group		Gneiss	

gr = granite, min = mafic intrusives, sl = slate, mag = magnetic, gw = graywacke, if = iron formation, gs = greenstone, dm = colomite, qzt = quartzite, cgl = conglomerate, var = variable. (James, 1958; Larue, 1980, personal communication)

Figure 1
James' pre-Keweenawan stratigraphy

the late 1970's, the stratigraphic interpretations most directly affecting the Iron River-Crystal Falls district were first proposed (although not published) in the late 1950's. The first proposal suggests that the Paint River Group consists of strike-fault repetitions of facies of parts of the Baraga and Menominee Groups (Trow, 1960, Figure 2). This hypothesis requires some "uplift" of the rocks in IR-CF to obtain the desired repetition of lighologies. The second interpretation suggests the stratigraphic equivalence of the Paint River Group and the Menominee Group (Cambray, 1977). Structurally, this model requires uplift of the Iron River-Crystal Falls district so that the older Menominee (Paint River) Group shares its present erosional surface with that of the younger Baraga Group, which virtually surrounds the IR-CF district in map view.

The final stratigrapnic interpretation, based upon observations in Baraga County (north of the present study area) correlates the Baraga Group with the Menominee Group (Mancuso, 1975).

The most recent tectonic interpretations envision the granitic terrain of N. Wisconsin as the basal part of a volcanic arc complex beneath which oceanic lithosphere subducted. In this view, IR-CF is remnant ocean floor and overlying sediments which escaped subduction beneath Wisconsin when that subduction zone ceased with a continent-continent or continent-arc collision at the close of the early Proterozoic (Cambray, 1980; Larue, 1981, 1982).

Figure 2. Trow's pre-Keweenawan stratigraphy.

	Iron River and Crystal Falls (Iron River Facies)	Amasa Oval (Amasa Facies)
Upper Precambrian		Keweenawan gabbro and diabase
	Granitic intrusive rocks	Granitic intrusive rocks
	Metagabbro and metadiabase	Metagabbro and metadiabase
	Fortune Lakes Slate	
	Stambaugh formation	
		Michigamme formation
	Hiawatha graywacke	
	Unconformity	
Middle Precambrian	Riverton formation	Amasa-Fence River formation
	Dunn Creek slate	a slate
	Badwater Greenstones	Hemlock formation
	Jumbo exploration	Bird iron-bearing member
	Basal greenstone interbedded	
	Saunders formation	Gair and Wiers "Goodrich"
	Unconformity	
		Randville dolomite
	Unconformity	
Lower Precambrian	Basic volcanics grade into migmatites south of Iron River	Hargeson Creek gneiss

Eastern O.E.1247 (Amasa Facies)	Old Menominee Range (Norway Facies)	Marquette Range Column from Leith, Lund, and Leith (1935)
intrusives		
Granitic intrusive rocks	Granitic intrusive rock	Granitic intrusive rocks
Metagabbro and metadiabase	Metagabbro and metadiabase	Metagabbro and metadiabase
	Michigamme formation	Upper Slates
	Turners exploration	Bijiki iron-formation
Michigamme formation		
		Lower slates
	Michigamme formation	Clarksburg volcanics
		Greenwood iron formation
		Goodrick quartzite
Hamilton Creek formation	Vulcan formation	Negaunee iron formation
a slate	Felch formation	
Quinnesec formation	Badwater greenstones	Siama slate
Rominger's silica ferruginous rock	(not present everywhere)	
	Dolomite breccia E. of Aragon	Ajibik quartzite
		Wewe slate
	Randville Dolomite	Kona dolomite
McAllister dolomite		
	Sturgeon quartzite	Mesnard quartzite
	Fern Creek formation	"Lake Enchantment" formation (not mentioned in USGS P.P. 189)
Miscauno formation grades southwestward into the Beecher gneiss	Dickinson group grades into granite gneiss	Granite, syenite, peridotite and Palmer gneiss

1.3.2. Geophysical Works

The only previously published detailed gravity survey of IR-CF is that of Bacon and Wyble (1952). Bacon and Wyble (1952) includes density determinations for the Badwater Greenstone and also cites some density determinations performed by Zinner and others (1949) on "younger" rocks. Terrain corrections were not deemed necessary within their accuracy and no mention is made of bedrock density assumed for Bouguer correction.

Leney (1966) presents the work of Bacon and Wyble (1952) as an example of the usefulness of gravity methods in iron-ore exploration and includes several histograms of rock densities for the mining district immediately to the east of the study area.

Gravity profiles across various troughs of the Marquette Range (north of the present study) by Cannon and Klasner (1974) provide densities and general methods for the present study. A related work is the interpretation of the Witch Lake 15' quadrangle by Cannon and Klasner (1976). Their area slightly overlaps the present study area. The density determinations by Cannon and Klasner (1974, 1976) include the only density determinations for the Hemlock Formation and Amasa Formation.

Finally, Klasner and Jones (1979) produced a simple Bouguer gravity map of the 1° x 2° Iron River quadrangle. Although Klasner and Jones (1979) used considerable data from Bacon and Wyble (1952), they also reoccupied many of Bacon and Wyble's stations and reportedly obtained measurements in close agreement (0.4 mgal) with the earlier study (Klasner, personal communication).

1.4 Study Area

The stratigraphic, structural, and tectonic models described above were tested through the measurement and interpretation of the gravity field in eastern Iron County, Michigan, U.S.A. The areal extent of the survey is approximately 1200 km^2. The survey area includes the eastern half of the IR-CF district and the southwest flank of the Amasa Oval.

The study area lies within the Iron River and Iron Mountain 1° x 2° quadrangles and consists of the Witch Lake and Ned Lake 15' quadrangles and the Naults, Florence West, Florence East, Lake Mary, Crystal Falls, Fortune Lakes, Amasa, Kelso Junction and Kiernan 7 1/2' quadrangles. The area is bounded by 45°52'30" and 46°17'30" north latitude and by 88°07'30" and 88°30'00" west longitude (see figure 3).

The gravity survey was tied to the Iron River, Michigan pendulum gravity station (q.v., Duerksen, 1949). This station was subsequently reoccupied by gravimeter and tied to the Madison fundamental gravity base, improving the accuracy of the Iron River station by a factor of 3 (Woollard and Rose, 1963).

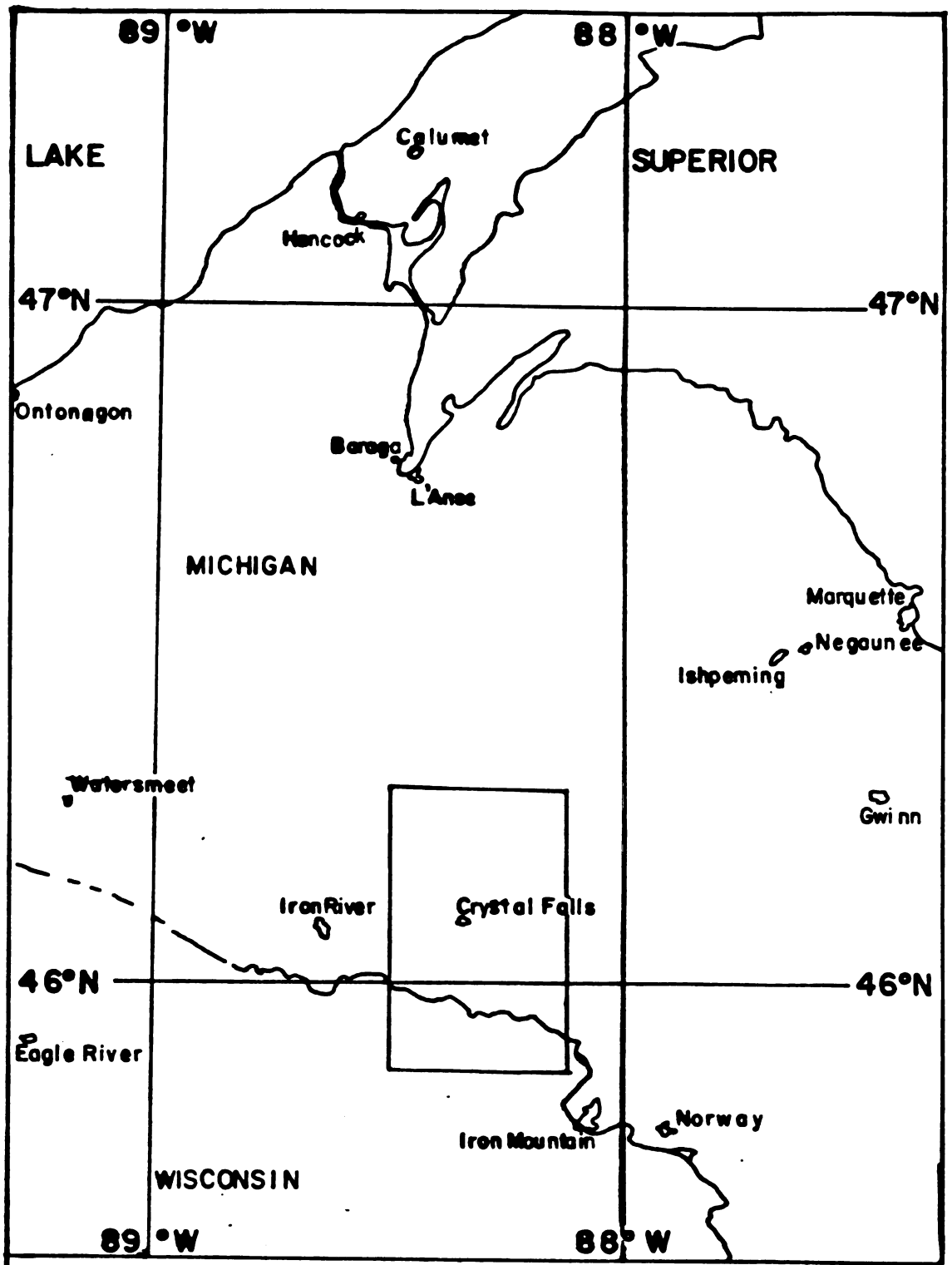

Figure 3
SCALE 1:1,000,000
INDEX MAP

2 FIELD WORK

2.1 Time

The data for this study were obtained during three different surveys. The first was a combination gravity-elevation survey from 1980 SEP 03 to 1980 SEP 16. The second survey only determined elevations; it lasted from 1980 OCT 11 to 1980 OCT 12. The third survey measured gravity and elevation from 1981 JUN 28 to 1981 JUL 02.

2.2 Instruments

Relative gravity measurements were made with a LaCoste and Romberg Gravity Meter number G-180, which reads to the nearest 0.01 milligals. Elevation measurements during 1980 SEP were made using a Wallace and Tiernan altimeter (Model No. FA112, Serial No. WP17401). This altimeter is marked in units of ten feet and will hereafter be referred to as altimeter A.

A second Wallace and Tiernan altimeter (identification "U.S. Army, no. 6 -- 3833"; hereafter referred to as altimeter B) was used in conjunction with altimeter A during the 1980 OCT field work. Altimeter B is also marked in units of ten feet.

Three altimeters were used during 1981 field work. Altimeters A and B were supplemented by yet another Wallace and Tiernan altimeter (serial number 45 - 7731B; altimeter C), marked in units of two meters.

2.3 The Surveys

2.3.1 line location and station spacing

Survey measurements of gravity and elevation were made along eleven lines, four oriented north-south and seven oriented east-west.

Two of the north-south lines parallel strike and are located east of the Iron River-Crystal Falls district while the otner two are oriented perpendicular to strike and sample the eastern half of the northern boundary of tne Iron River-Crystal Falls district.

Four of the east-west lines parallel strike to the north of the IR-CF district; the remaining three are oriented perpendicular to strike and test the eastern boundary of the Iron River-Crystal Falls district (figure 4).

Lines oriented parallel to strike are located only in areas where gravity contours and geologic strike meet at high angles. Line lengths vary from 2 to 20 kilometers. Lines oriented perpendicular to strike are longer.

Parallel lines were placed approximately five kilometers apart. Because geologic models for this study extend as deep as 35 kilometers, and because differences in tne gravity field on two adjacent parallel lines (separated by 5 kilometers) will be primarily due to geologic differences in the uppermost five kilometers of the respective geologic columns, only one north-south and one east-west line were modeled (see figure 5). Although perpendicular to one another, both modeled lines were oriented roughly perpendicular to strike, as is required by the two-dimensional method (compare figures 4 and 5).

Station spacing varied inversely with the amount of resolution desired in a particular area. Station spacing varied from 0.3 km to 1.0 km, but averages 0.7 km on the two lines which were modeled.

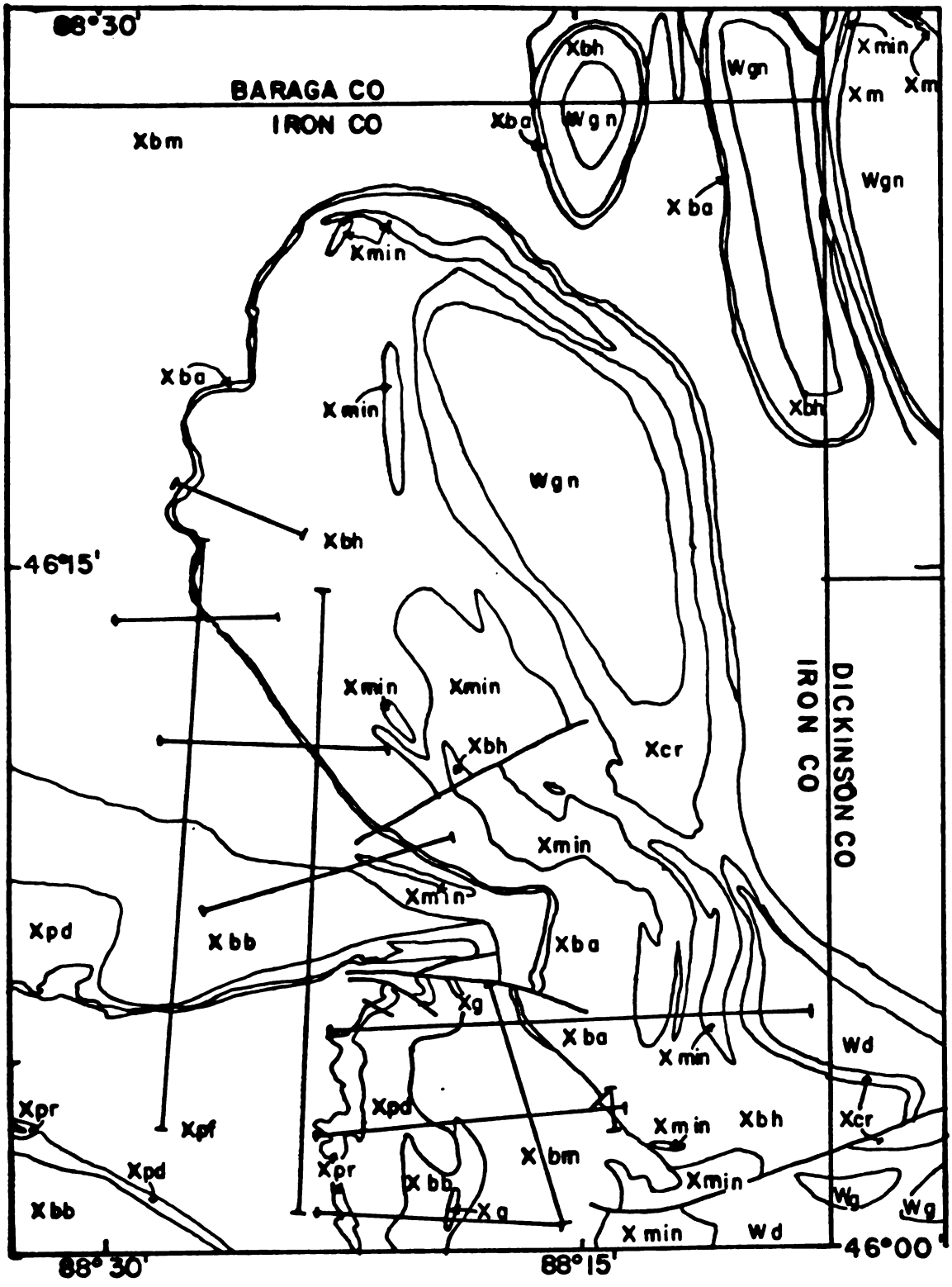

Figure 4

Geologic map showing location of gravity lines

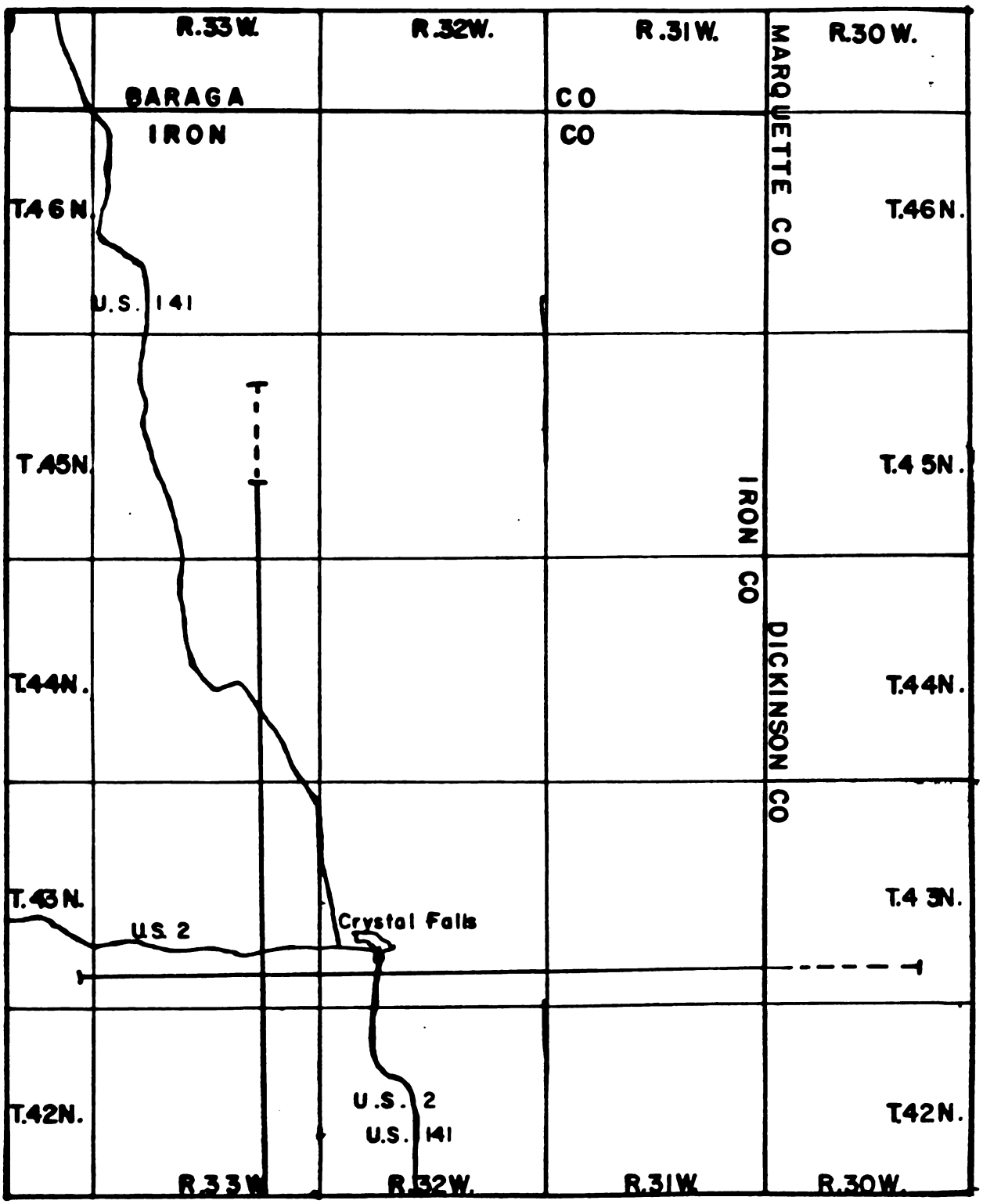

Figure 5

Reference map showing modelled profiles

2.3.2 base stations and loops

The gravity survey was tied to the 1940 Iron River Pendulum Gravity Station (see Duerksen, 1949). The most accurate gravity determination of that station was by Woollard (Woollard and Rose, 1963). That occupation of that station was by a gravimeter loop tied to the Madison Fundamental Gravity Base. Woollard's gravimeter value is accurate to $\pm$ 0.6 mgals relative to Madison (which itself is accurate to $\pm$ 1.2 mgal), whereas the accuracy of the pendulum gravity determinations by the U.S. Coast and Geodetic Survey for 1940-1941 is $\pm$ 1.7 milligals relative to Madison (Woollard and Rose, 1963).

The Iron River gravity station (IR) was tied to station 1F of the present study by Gravity Loop 1. Gravity Loop 1 was open for 3 hours, 18 minutes and has an average drift rate of 0.03 mgal per hour. This loop was not repeated.

All gravity measurements for this study are indirectly tied to IR through station 1F. In the interest of time, not all gravity loops were tied to station 1F. This method of "floating" the base station is illustrated in Figure 6.

Gravity Loop	Stations Occupied
Gravity Loop I	IF-IR-IF
Gravity Loop 2	IF-continue survey-IP-IF
Gravity Loop 3	IP-continue survey-IP

Figure 6

DIAGRAM OF "FLOATING" BASE

STATION METHOD OF LOOPING

Table 1

GRAVITY LOOP LENGTHS (h:m:s)

survey	minimum	maximum	mean	standard deviation	n
1980SEP	1:44:30	5:46:00	3:53:00	1:00:00	26
1981	0:24:55	4:25:55	2:34:25	1:18:25	14

Table 2

GRAVITY DRIFT RATES

(assumed linear, absolute values, mgal/hr)

survey	minimum	maximum	mean	standard deviation	n
1980SEP	0.00	0.11	0.03	0.04	26
1981	0.00	0.25	0.07	0.12	14

Altimeter loops can be tied to any of numerous points of known elevation, eliminating the need for "floating" base stations on altimeter loops.

Gravimeter loop length and drift rate data are given in Tables 1 and 2 above; corresponding data for altimeter loops is presented in Tables 3 and 4.

Table 3

ALTIMETER LOOP LENGTHS

(hr:min:sec)

Survey	minimum	maximum	mean	standard deviation	n
1980SEP	0:42:15	5:40:00	2:33:00	1:22:00	29
1980OCT	0:08:30	1:10:00	0:32:20	0:19:00	15
1981	0:23:40	4:24:00	1:22:00	1:08:00	20

Table 4

ALTIMETER DRIFT RATES

(reals in meters/hour, assumed linear)

Survey	minimum	maximum	n	mean	standard deviation
1980SEP	00.00	10.61	29	04.18	03.17
1980OCT	00.00	63.73	15	09.05	12.74
1981	00.00	22.40	20	05.43	04.11

2.4 Data Collection

During a single occupation at a station, the gravimeter was read to the nearest .01 units (approximately .01 milligals) until two consecutive readings agreed within .02 units.

Elevation was measured to the nearest foot on altimeters A and B and to the nearest decimeter on altimeter C.

During a single station occupation, an altimeter was read until one or more of the following criteria were met: a) consecutive identical readings were obtained, b) the reading equalled the mean of the previous readings of that altimeter during that occupation of the station, or c) a large and consistent drift rate emerged over the course of 3 consecutive readings, whereupon the middle reading was adopted or the loop was discarded and reoccupied. Criterion "a" is thought to indicate that the altimeter has reached some sort of thermal equilibrium with the ground. On many stations located in bright sunshine, the placement of the altimeter on the hot ground was followed by a change in indicated altitude. It is thought that this change was due to heating of the altimeter, particularly since it was most marked in the metal-cased (as opposed to wood-cased) altimeters. Criterion "b" was found to be useful when wind conditions created a large scatter in readings without a noticeably consistent drift. Criterion "c" simply suggests that if a constant drift rate is observed over 3 readings (a time span of approximately 30 seconds), then that loop should probably be thrown out. Most altimeter drift is the result of sharp changes in barometeric pressure (compare tables 3 and 4). When a weather front of sufficient intensity to change altimeter readings by 2 feet in 30 seconds is included in an

altimeter loop which assumes linear drift between its end point, a large amount of elevation error is likely to result.

3 DATA REDUCTION

3.1 Drift Corrections, Translation from Gravity Meter Units to Milligals, and Translation to Absolute Milligals

3.1.1 gravity

Gravimeter readings were drift corrected assuming linear drift within each loop. These drift corrected readings were then multiplied by the appropriate factor to change the readings in gravimeter units to milligals. A constant was then added to all milligal values to tie the survey to the 1960 value of the Iron River gravity station. Gravity field strengtn at each station is listed in Appendix B.

3.1.2 elevation

Whenever possible, gravity stations were located at points of known elevation. When this was not possible, the station elevation was estimated by one of the two methods below:

1. Elevations were interpolated from topographic map contours (contour interval 6.1 meters (10 feet)). (Preferred method, used only for stations not located on hills, in depressions or on saddles.)

2. Elevations were determined solely on the basis of altimeter data. (Method used for stations located on hills, in depressions, or on saddles.)

Station elevations are listed in Appendix B.

Root-mean-square error due to drift correction on altimeter loops were $\pm$ 2.4 meters for altimeter A, $\pm$ 3.29 m for altimeter B, and $\pm$4.27 m for C. No system of averaging or weighting the values of

the various altimeters could be found which would give better accuracy than that attained using altimeter A alone.

3.1.3 errors in drift correction

Drift corrections for each meter (the gravimeter, and altimeters A, B, and C) were analysed to estimate the accuracy of the corrections. The gravimeter drift correction for 1980 and 1981 were analysed separately since 1981 gravity measurements had been made by an assistant, M. T. Gottler.

Error estimates were made by finding a sequence of stations containing 3 stations which had previously been occupied and forming a "floating" loop with these three stations. The length of this "floating" loop (in time) was required to be less than the maximum loop length of the sample set from which the stations were chosen (see subsection 2.3.3 for data on loop lengths). The "floating" loop was then drift corrected and the previous value for the intermediate station was compared with the new value derived by the drift correction on the new loop (see Figure 7).

Only one such series of stations from the 1980 data formed a sufficiently short loop. Error for that loop was 0.02 milligals.

Gravity Loop 22

Station	4P	other stations	3M	other stations	40
value	6.384				2.658

value for 3M calculated to be 6.71 mgal.

Gravity Loop 23 & 24

Station	40	other stations	3M	other stations - 3I
value	2.658			2.574

value for 3M calculated to be 6.69 mgal.

difference between two gravity determinations: 0.02 mgal.

Figure 7

Figure showing method of evaluating accuracy of drift corrections

Two series of stations from the 1981 data lent themselves to this method, yielding a root-mean-square error of $\pm$ 0.16 mgals, to which those data are considered accurate. These assigned accuracies are consistent with the results of experiments performed to determine the maximum repeatability of gravity measurements. Those experiments sought to determine how closely gravity measurements at one station

would agree when the gravity meter was required to be releveled after each measurement (a book was successively inserted under each of the three legs of the gravimeter to guarantee that a large change in leveling was required). The standard deviation was found to be 0.017 milligals.

3.1.4 elevation error

Whenever possible, gravity stations were located at points of known elevation. Stations located at points whose elevations are labeled on 7 1/2 minute or 15 minute quadrangle topographic maps are assigned an accuracy of $\pm$ 0.2 meters. Stations whose elevation could be determined from highway construction plans are supposedly accurate to $\pm$ 0.02 meters (Michigan Department of Transportation).

It was found that points not located on local elevation maxima, minima, or saddles could be linearly interpolated between elevation contours to $\pm$ 1.5 meters rot-mean-square error. Points located on such saddles and extrema could be interpolated to an accuracy of only $\pm$ 3.9 meters; therefore, elevation of points located on local elevation extrema or saddles were approximated by use of altimeter A, whose accuracy is $\pm$ 2.4 meters (subsection 3.1.3, drift error).

Average elevation accuracy is $\pm$ 1.1 meters, producing a $\pm$ .35 milligal error.

3.2 Latitude Corrections

After reducing the gravity data to absolute values (see subsection 3.1.1), the data was normalized to a latitude of 46°00'00". Latitude was determined to the nearest second (30 meters)

for all stations. The 1967 International Formula for gravity variation with latitude is (Telford and others, 1976)

$g = g_o(1 + \alpha \sin^2(\phi) + \beta \sin^2(2\phi))$ where $g_o = 978031.8$ mgals

Φ = latitude

$\alpha = 5.3024 \times 10^{-3}$

$\beta = 5.8 \times 10^{-6}$

Differentiation to obtain the latitudinal correction, yields:

$$dg = g_o(\alpha\ 2\sin(\phi)\cos(\phi)d\phi + \beta\ 2\sin(2\phi)\cos(2\phi)2d\phi)$$

$$= g_o(2\alpha\sin(\phi)\cos(\phi) + 4\beta\sin(2\phi)\cos(2\phi))d\phi$$

$$\frac{dg}{d\phi} = g_o(\alpha\sin(2\phi) + 2\beta\sin(4\phi))$$

Latitude corrections are approximately 0.8199 milligals per kilometer. Relative latitude corrections are estimated to be accurate to 0.020 mgal.

Latitude and latitude corrections are listed in Appendix B.

3.3 Till Thickness

The largest density contrast in the geologic column is between glacial deposits and bedrock. Therefore, it is thought that till distribution strongly influences the gravitational field. Because this study seeks to test theories involving bedrock, an attempt was made to remove the effect of till thickness variations from the observed gravity field.

Till thickness data are available for points occupied by water wells, mines and mineral explorations, and for areas subjected to seismic surveys. Not all water wells and seismic surveys extend to bedrock; these are useful in providing <u>minimum</u> till thickness at their locations (See plate 1).

Till thickness data are concentrated in highly populated areas

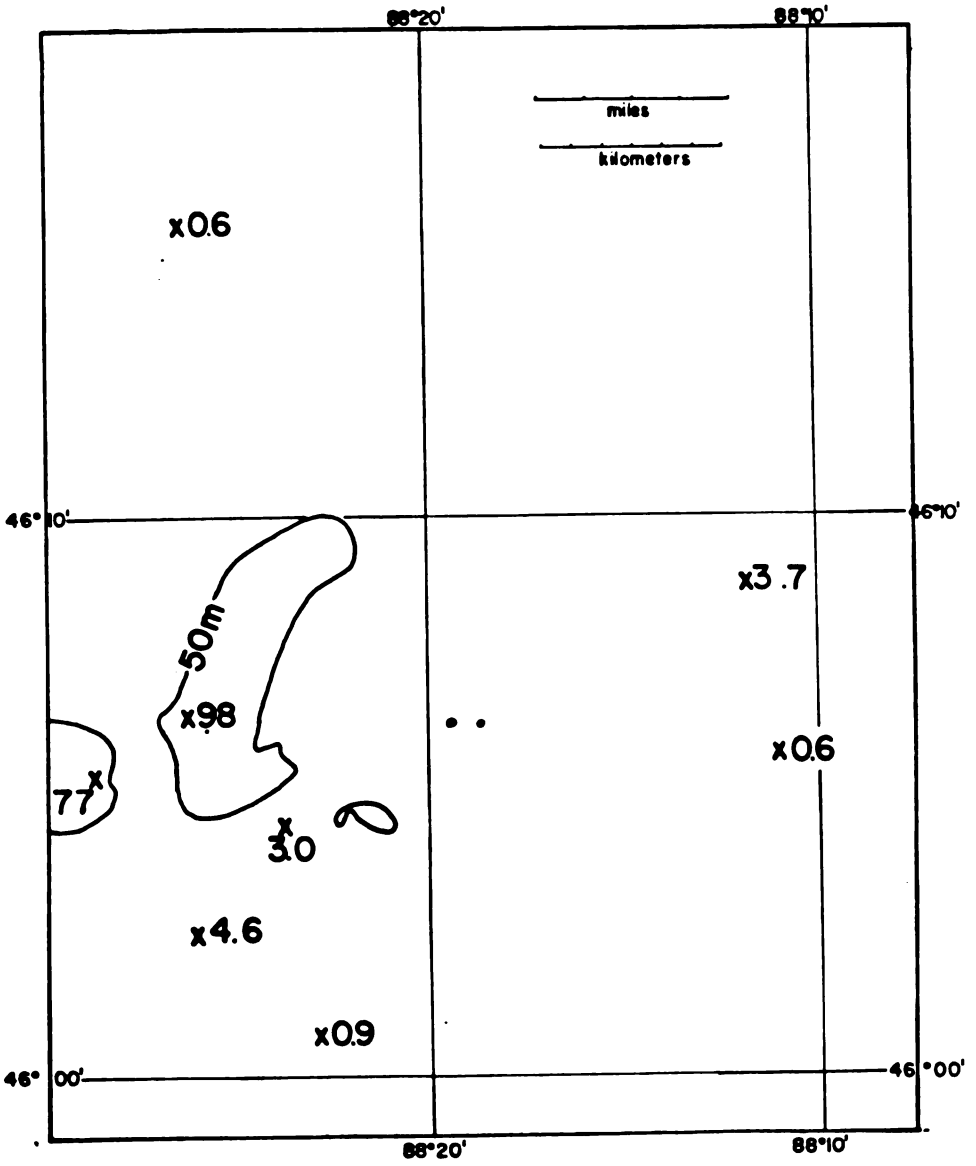

Figure 8

Contour map of till thickness (meters)

(Appendix 5). Most water wells are located near dwellings. Towns are located near mines and their mineral explorations. Roads, along which seismic surveys are located, connect these towns.

The problem of poor till-thickness-data distribution is compounded by the sharp variation in thicknesses over short distances. We must assume that the steep slopes of the till isopach map (figure 8 and plate 1) in areas at good control also exist in areas of poorer control. Till thickness varies from 0 to at least 98 meters in the study area. The thickness at each gravity station is listed to the nearest 0.25 meters, althouth it is probably only accurate to an average of $\pm$ 3.75 meters ($\pm$ 0.14 milligals). Till thickness at each station is tabulated in Appendix B.

3.4 Free Air Correction

Gravity data were reduced to mean sea level using a correction factor of 0.3085 milligals per meter of elevation.

The Free Air anomaly and modified Bouguer anomaly have a similar shape in the study area (figures 9 and 10). This is caused by small elevation effects (approximately 100m) and large effects of surface bedrock density variation (approximately 0.5 grams per cubic centimeter).

Free Air anomalies in the study area (35 by 35 kilometers) range from a minimum of +6 milligals to a maximum of +60 milligals. Recent glacial unloading and a resultant lack of isostacy would produce negative Free Air anomalies. These effects are not observed over the relatively small scale of the survey.

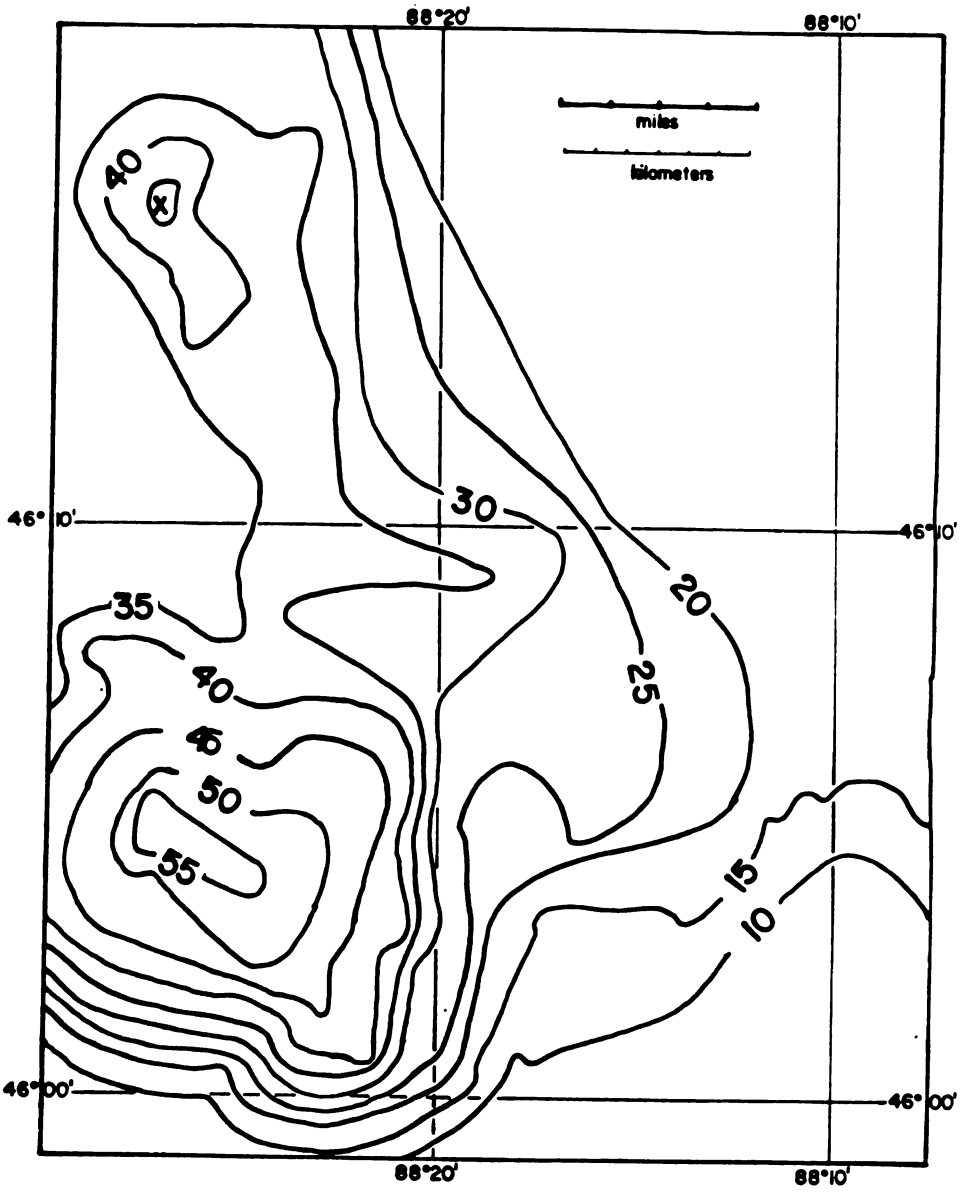

Figure 9

Contour map of Free Air anomaly (mgal)

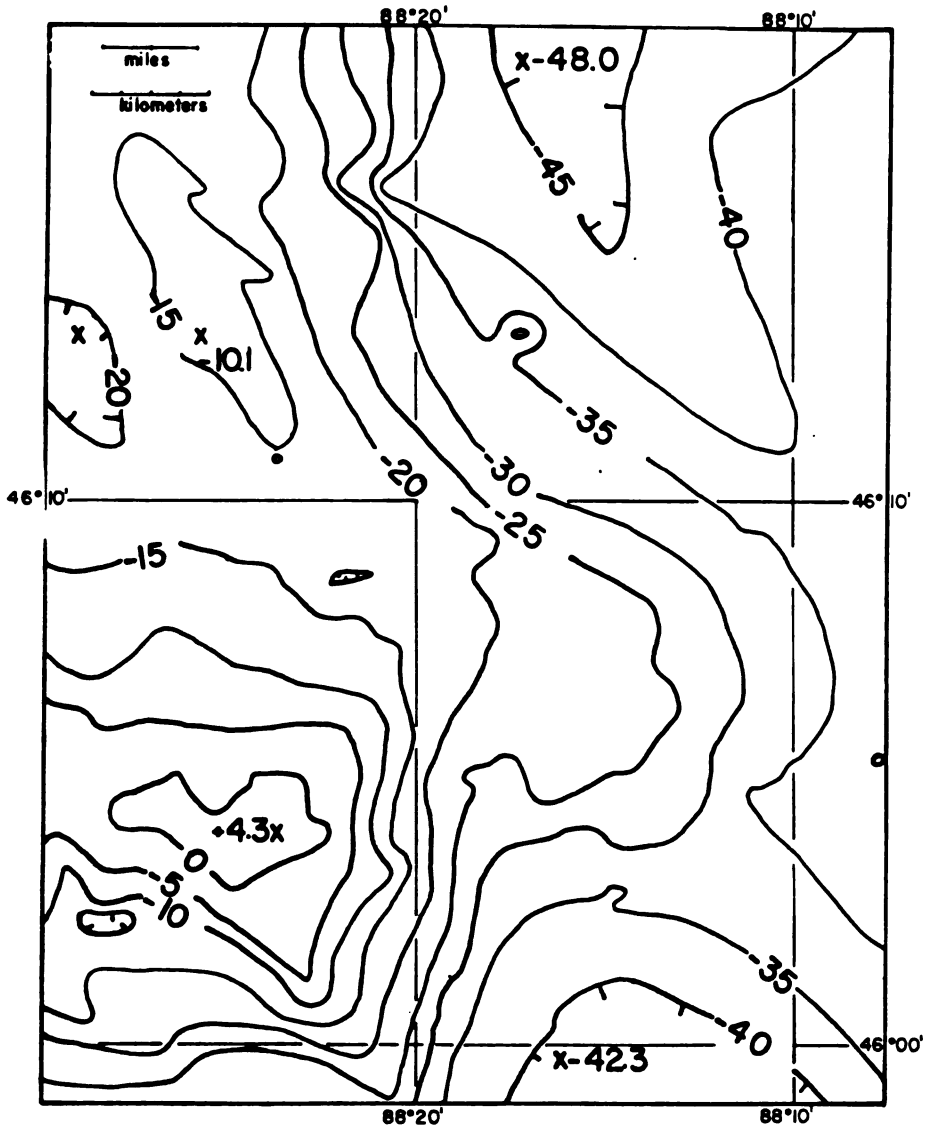

Figure 10

Contour Map of Modified Bouguer Anomaly

3.5 Bouguer Corrections

Once Free Air corrected, the data were modified-Bouguer corrected down to a datum of 395.3 meters above sea level. The modified Bouguer anomaly for each station was then calculated by comparing the modified-Bouguer corrected value with the theoretical value for an elevation of 395.3 meters. Because of the uncertainty in bedrock density, it was decided that as little bedrock should be corrected for as was feasible. For this reason, a datum of 395.3 meters was chosen as it was believed that the lowest bedrock elevation for the study would be 395.3 meters.

A modified Bouguer correction was made in two steps. The first step was to remove the gravitational effect of the till using the till thicknesses determined previously (see section 3.3) and a till density of 2.0 grams per cc (Zinner and others, 1949). The second step was to remove the remaining bedrock from stations whose bedrock elevations were above the 395.3 meter datum, and to add bedrock to those few stations with bedrock elevations below the 395.3 meter datum. Bedrock density was assumed to be 2.84 grams per cubic centimeter. Density data obtained from Cannon and Klasner (1976) after simple Bouguer corrections revealed that a bedrock density of 2.91 would have been more appropriate. The error resulting from improper assumed bedrock density was not completely corrected for. Uncorrected error does not exceed $\pm$ 0.02 mgal.

3.6 Terrain Corrections

Terrain corrections were not deemed necessary within the $\pm$ 0.6 mgal average accuracy of this study. Bacon and Wyble (1952) found inadequate topography there to justify a terrain correction when an

accuracy of $\pm$ 0.3 was desired. To test this, a terrain correction was calculated for a point located on the middle of the cliff next to U.S 141 at the Paint River. This is the steepest terrain in the study area, yet its terrain correction is approximately 0.1 milligals (zones B through H), supporting Bacon and Wyble's (1952) findings.

3.7 Correlation of Bouguer Anomalies Between This Study and Other Studies

Simple Bouguer anomaly maps by Bacon and Wyble (1952, 1966) and Klasner and Jones (1979) include gravity stations within eastern Iron County which were not occupied during field work for this study. The data set for this study was enlarged by incorporating the data of Bacon and Wyble (1952 1966) and Klasner and Jones (1978). Unfortunately, the only readily available form of their data was simple Bouguer anomaly maps.

An attempt was made to correlate Bacon and Wyble's (1952, 1966) and Klasner and Jones' (1979) simple Bouguer anomalies with the anomalies of the present study at stations which were co-occupied. A simple constant could not be added or subtracted from their values (in order to bring them into line with the data obtained by this study) since their assumed bedrock density, till density, till thickness, elevation, etc. may have been different from those assumed by this study. A multiple linear regression on Bouguer anomaly, elevation, and till thickness was performed to remove effects of differing Bouguer corrections:

$t = a + bx + cy + dz$, where a, b, c, d are constants determined by regression: x = Bouguer anomaly according to other survey

y = elevation according to the present study

z = till thickness according to the present study

t = Bouguer anomaly according to the present study.

The data of Bacon and Wyble (1952, 1966) and Klasner and Jones (1979) were correlated to the present study separately, in case any difference in reduction exists between those two sets of data.

The resulting function correlating the present study to Bacon and Wyble (1952, 1966) is:

$$t = 5.91 + 1.03x - 0.007300y + 0.00473z,$$

where: t = Bougner anomaly according to the present study

x = Bougner anomaly accoridng to Bacon and Wyble

y = elevation according to the present study

z = till thickness according to the present study.

The function was obtained using 57 co-occupied stations. The correlation coefficient, R^2, was .9834.

Fifty six of Klasner and Jones (1978) stations were co-occupied by the present study. The function correlating their Bouguer anomalies to those of the present study is:

$$t = -3.65 + 1.05x + 0.003263y + 0.00571z$$

The correlation coefficient for this function is $R^2 = .9928$.

Root-mean-square differences between predicted and observed values were calculated for both correlation functions on the data set from which the function had been derived. Root-mean-square differences were 1.3 mgal for Bacon and Wyble's (1952, 1966) values and 1.0 mgal of Klasner and Jones' (1978) Bouguer anomalies. Bouguer anomalies adopted from Bacon and Wyble (1952, 1966) or Klasner and Jones (1978) are passed through the proper correlation function, then assigned an accuracy of $\pm$ 1.3 or $\pm$ 1.0 mgal.

3.8 Error Summary

Gravity values from 1980 field work are accurate to ± 0.02 milligals relative to the Iron River datum. Those from 1981 are accurate to ± 0.16 milligals.

Free Air anomaly accuracies average ± 0.4 mgals, while relative modified simple Bougner anomalies accuracy averages ± 0.6 mgals. Gravity values on an absolute scale are accurate to ± 1.9 mgals. The ± 1.9 mgal accuracy is attributable to the ± 1.2 mgal accuracy of the Madison Fundamental Gravity Base, the ± 0.6 mgal accuracy of the Iron River Station (Wollard and Rose, 1963), and the 0.1 accuracy of this study's stations relative to Iron River.

4 MODELLING

4.1 Procedures

Gravity models were calculated for various two-dimensional subsurface-geology models using the method of Talwani and others (1959). Computations were performed using a CDC Cyber 750 computer. A listing of the FORTRAN IV computer program used for modelling is presented in appendix 4. Models of the geology of eastern Iron County, Michigan, USA, were primarily based upon the differing interpretations by James and others (1968), Pettijohn (James and others, 1968; Pettijohn and others, 1969), Cambray, (1977, and personal communications 1980-81), Trow (1960), and Larue (personal communication, 1981).

Models were constrained by surface geology, including mine geology, exploration drill holes, mean and standard deviation in density of each formation (table 5), formation thicknesses (table 6), and thickness of the crust. Models were also required to match where the north-south and east-west profiles crossed, since this is a constraint which must be met in nature. Profiles will not automatically match using two-dimensional modelling, due to deviations from two-dimensionality of the geologic configuration, and also due to lithologic changes (especially in density) between the two profiles. Although structure and density were varied to match the observed gravity, formation thicknesses (as listed in table 6) were adhered to as much as possible and in addition to being kept near the mean densities listed in table 5, formation densities were allowed to vary only within approximately 2.5 standard deviations.

TABLE 5
Density Data

Formation	p	st.dev.	range	n	source
Fortune Lakes Slate	2.84	±.25		1	p from Free Air anomaly correlation. St dev from Michigamme Slate
Stambaugh Formation	2.98	±.05	2.98-2.98	1	Bacon and Wyble (1952)
Hiawatha Graywacke	2.73	±.23	2.57-2.89	2	Bacon and Wyble (1952)
Riverton Iron Formation	3.21	±.029	chemical analysis	6	James et al. (1968)
Dunn Creek Slate	2.77	±.18	2.64-3.00	4	Bacon and Wyble (1952
Badwater Greenstone	2.87	±.02	2.84-2.91	11	Bacon and Wyble (1952)
	2.97	±.005	2.97-2.97	1	Carlson (1974)
	2.87	±.06	2.84-2.97	12	Total
Michigamme Slate	2.99	±.25	2.15-3.55	98	Leney (1966)
	2.89	±.17	2.71-3.09	6	Cannon and Klasner (1976)
	2.72	±.05	2.64-2.79	7	Cannon and Klasner (1976)
	2.97	±.25	2.15-3.55	111	Total
Amasa Formation	3.18	±.35	2.91-3.81	4	Cannon and Klasner (1976)
felsic	2.67	±.09	2.55-2.74	4	Cannon and Klasner (1976)
Hemlock Formation mafic	2.96	±.10	2.82-3.11	6	Cannon and Klasner (1976)
total	2.84	±.17	2.55-3.11	10	Total

TABLE 5 (continued)

Formation	p	st.dev.	range	n	source
Metagabbro	2.91	±.06	2.81-2197	9	Cannon and Klasner (1976)
	2.93	±.03	2.89-2.97	5	Carlson (1974)
	2.92	±.05	2.81-2.97	14	Total
Randville Dolomite	2.86	±.14	2.65-3.10	32	Leney (1966)
	2.84	±.005	2.84-2.84	1	Cannon and Klasner (1976)
	2.86	±.14		33	Total
Dickinson Group Undifferentiated	2.89	±.06	2.77-3.10	126	Clark (1966)
Margeson Creek Gneiss	2.64	±.08	2.50-2.73	13	Cannon and Klasner (1976)
Mafic Gneiss	3.08	±.20	2.85-3.33	4	Cannon and Klasner (1976)

TABLE 6

Thickness of Formations on Modelled Profiles

Formation	north-south profile thickness(m)	References	east-west profile thickness(m)	References
Fortune Lakes Slate	1600	James et al. (1970)	1600 (west) 220 (east)	James et al. (1970)
Stambaugh Formation	30	James et al. (1968)	20 (west) 38 (east)	Pettijohn (1972)
Hiawatha Graywacke	10	James et al. (1970)	25 (west) 10 (east)	James et al. (1970) Pettijohn (1972)
Riverton Iron Formation	200	James et al. (1970)	23(west) 160 (east)	James et al. (1970) Pettijohn (1972)
Dunn Creek Slate	300	Pettijohn (1970)	120 (west 485 (east)	James et al. (1970) Pettijohn (1972)
Badwater Greenstone	3700	James et al (1968	2600 (west) 0 (east)	James et al. (1968) James et al. (1968)
Michigamme Slate	1800	James et al. (1968)	1800	James et al. (1968)
Amasa Formation	200	Weir (1967)	200	Weir (1967)
Hemlock Formation (Upper)	3300	Bayley (1959) Clements & Smyth (1899)	3000	Bayley (1959)
West Kiernan Sill	1600	Weir (1967)	1500	Weir (1967)
Hemlock Formation (Middle)	700	Bayley (1959) Clements & Smyth (1899)	600	Bayley (1959)
East Kiernan Sill	1000	Bayley (1959)	900	Bayley (1959)
Hemlock Formation (Early)	400	Bayley (1959) Clements & Smyth (1899)	300	Bayley (1959)
Randville Dolomite	600	Bayley (1959)	600	Bayley (1959)
Dickinson Group Undivided	0	Foose (1978), Cannon (1978)	2000	Bayley (1959), Cannon (1978), James (1958), James et al. (1961)

In order for any model to be considered succesful, the parameters were varied until the r.m.s. residual relative to the observed gravity was less than 3.2 mgal. This figure represents an estimate of the error in the residual and is derived by adding the average uncertainty of the observed simple Bouguer gravity anomaly ($\pm$0.8 milligals) to the uncertainty of the calculated gravity ($\pm$2.4 mgal, produced by round-off of depth to the nearest 100 meters and of density to the nearest 0.01 grams per cubic centimeter).

4.2 Geologic Interpretations

All models are consistent with surface geologic observations of James and others (1968), Pettijohn and others (1969), James and others (1970), Pettijohn (1970), Wier (1971), Pettijohn (1972), Foose (1978), and Cannon (1978). The models are (numbers correspond to subsection):

1. The United States Geologic Survey interpretation
2. The Pettijohn interpretation
3. The Paddock interpretation
4. The Trow interpretation
5. The Greenstone Belt interpretation
6. The Trapped Ocean Crust Interpretation
7. The Larue interpretation
8. The "Badwater ophiolite" interpretation

4.2.1 The United States Geologic Survey interpretation

The United States Geologic Survey suggests that the IR-CF district is not fault bounded (James and others, 1968), or, if the district is fault bounded, that those faults do not reach the present erosional surface. Stratigraphy for the USGS model is identical to

that given in Table 1. A rough block diagram across the north and east margins of the eastern half of the Iron River-Crystal Falls district (hereafter referred to as the Crystal Falls district) can be found in Figure 11. The two front vertical sides of the block diagrams represent sections along which the two-dimensional profiles were modeled; this will also be true for the block diagrams which illustrate models of other interpretations.

The United States Geological Survey's interpretation (James and others, 1968; Bayley, 1959; Wier, 1967; Gair and Wier, 1956; Cannon, 1978; Foose, 1978) was found to match the observed gravity within the required RMS residual using the densities and structure illustrated in figures 12 and 13 for the north-south and east-west profiles, respectively. Densities required to fit the observed gravity within an RMS residual of 3.2 mgal averaged 1.34 standards of deviation from the means.

4.2.2 the Pettijohn interpretation

Pettijohn (1969; and James and others, 1968) retains James' (1958) stratigraphy but interprets the Little Tobin Lake granites as evidence of a fault which "would separate Michigamme Slate to the east from Dunn Creek slate to the west. In this view, the Badwater Greenstone "...only reaches...bedrock surface on a series of anticlines" (Pettijohn, 1969). Pettijohn proposed no such fault boundaries for any of the other margins of the Iron River-Crystal Falls district. A block diagram illustrating this interpretation is given in figure 14.

Pettijohn's interpretation fails to match the observed gravity on the east-west profile under the assumption that individual

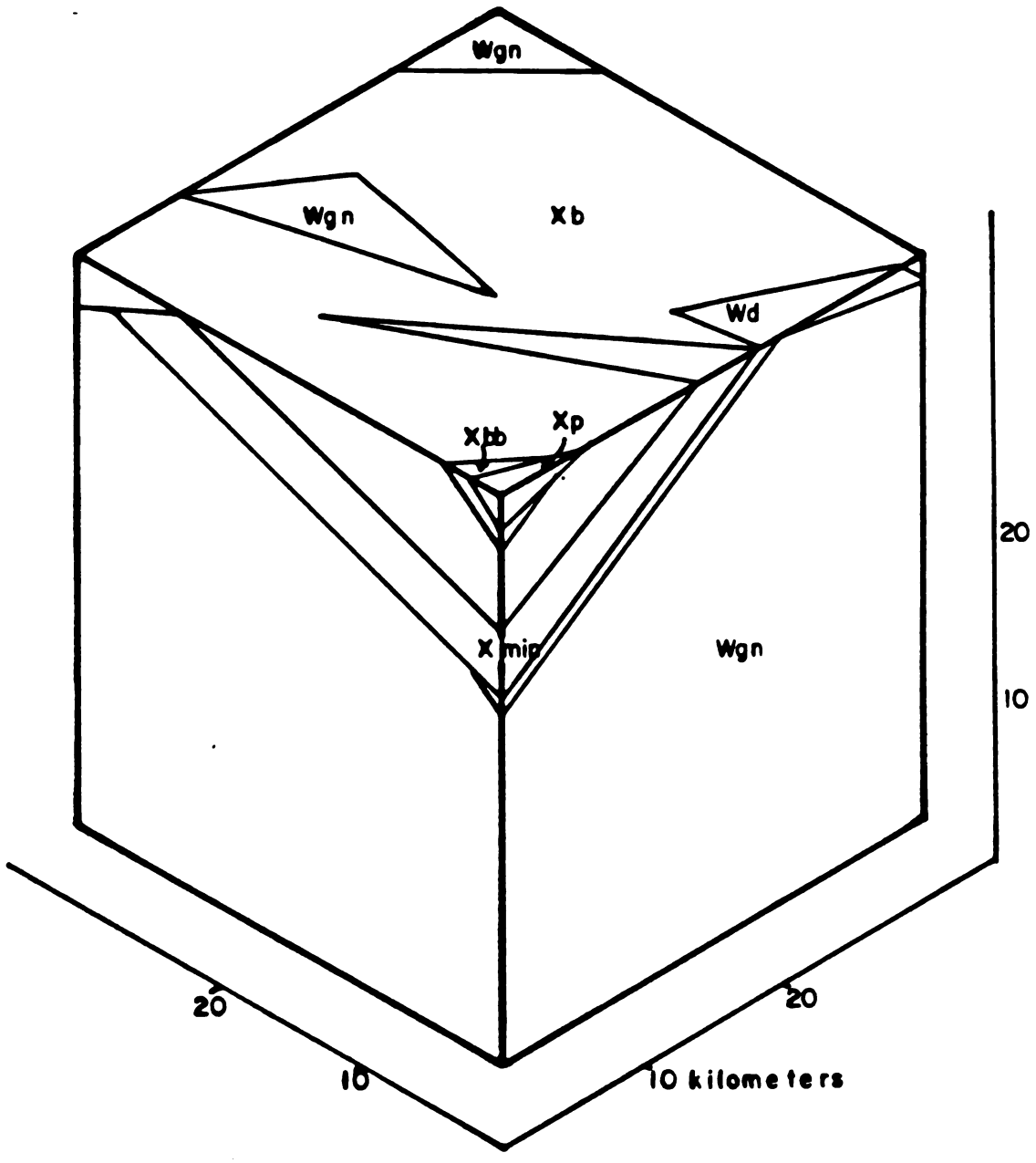

Figure 11

Block diagram of U.S.G.S. interpretation

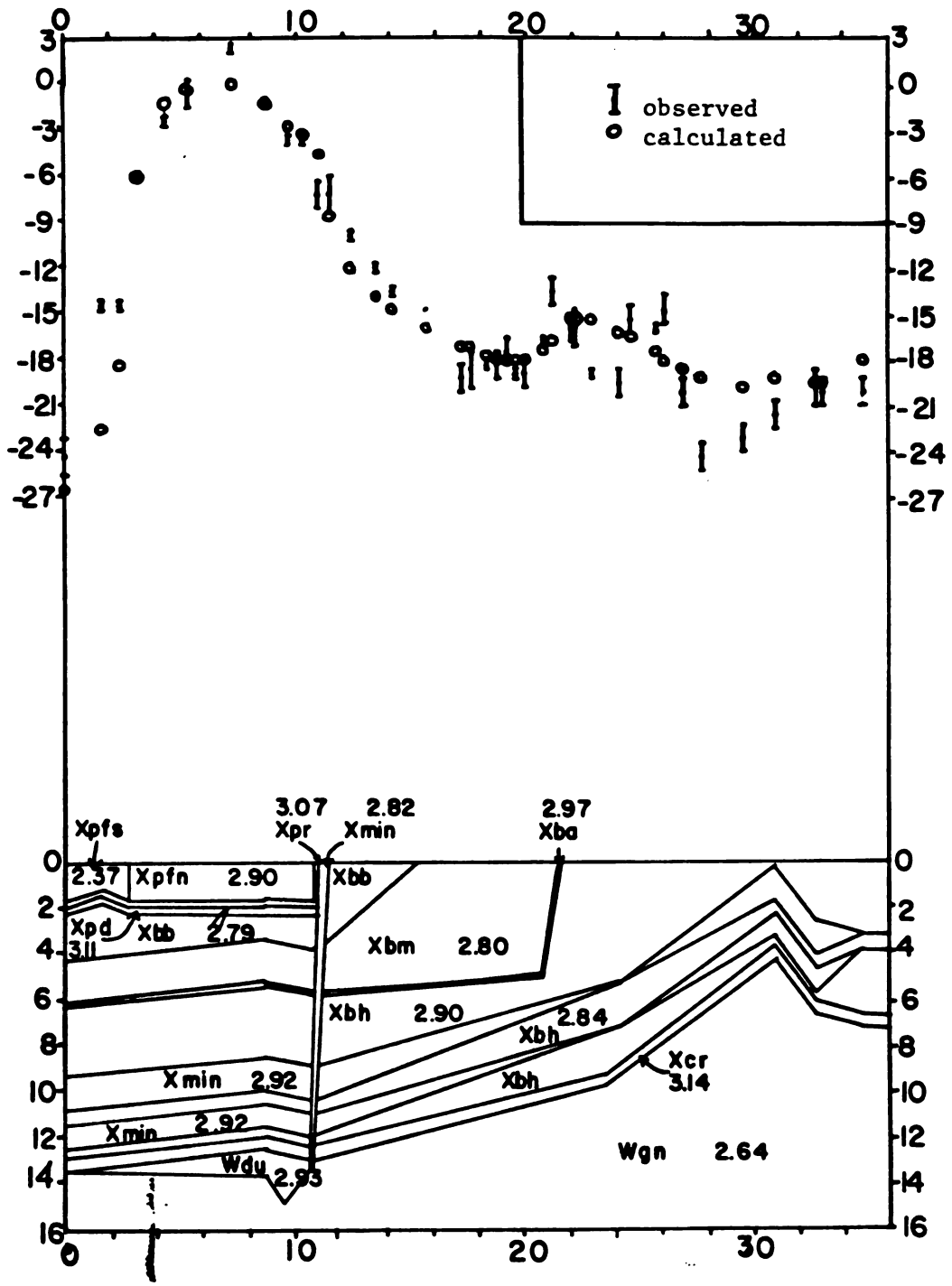

Figure 12

North-south gravity profile of U.S.G.S.-Pettijohn interpretation

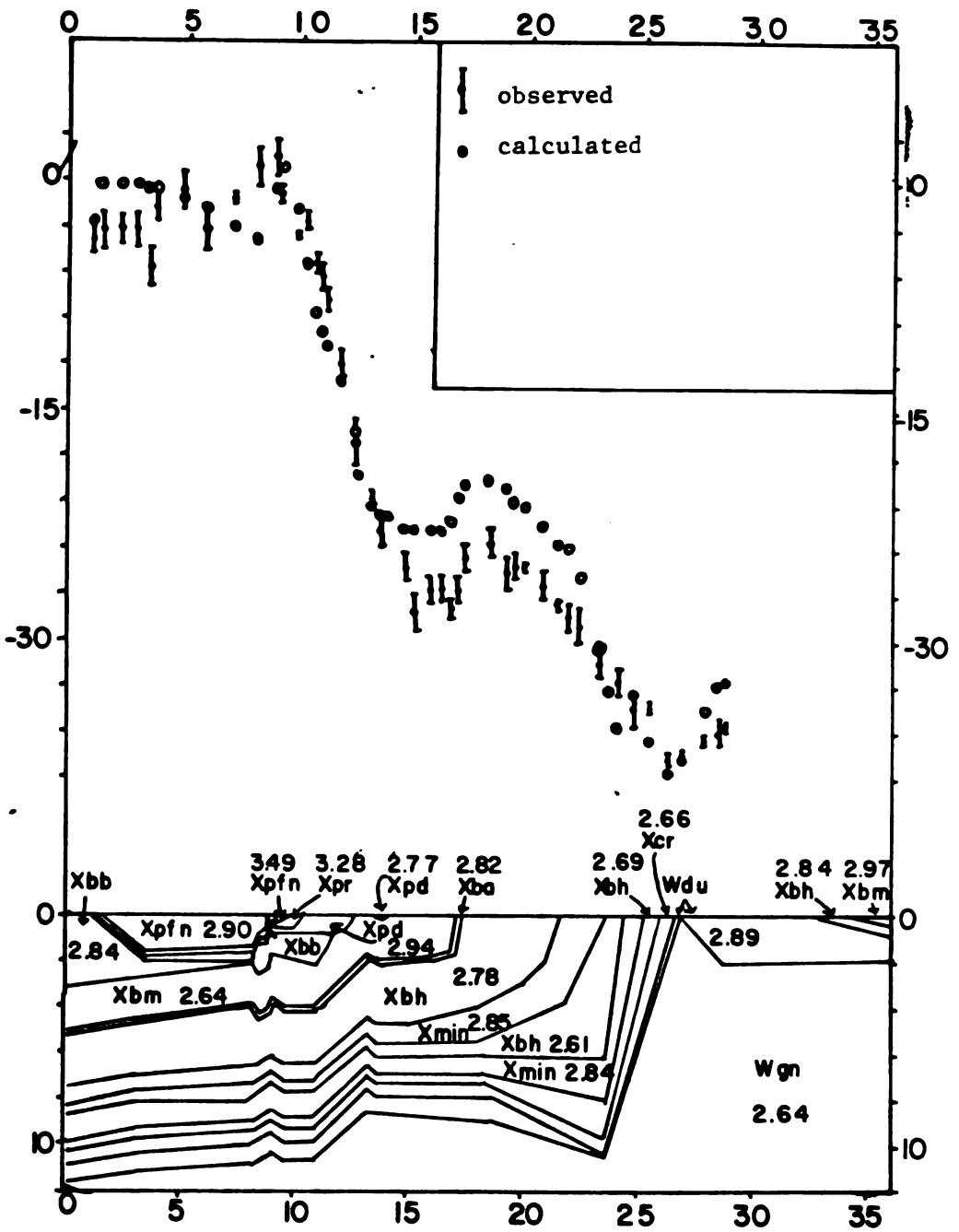

Figure 13

East-west gravity profile of U.S.G.S. interpretation

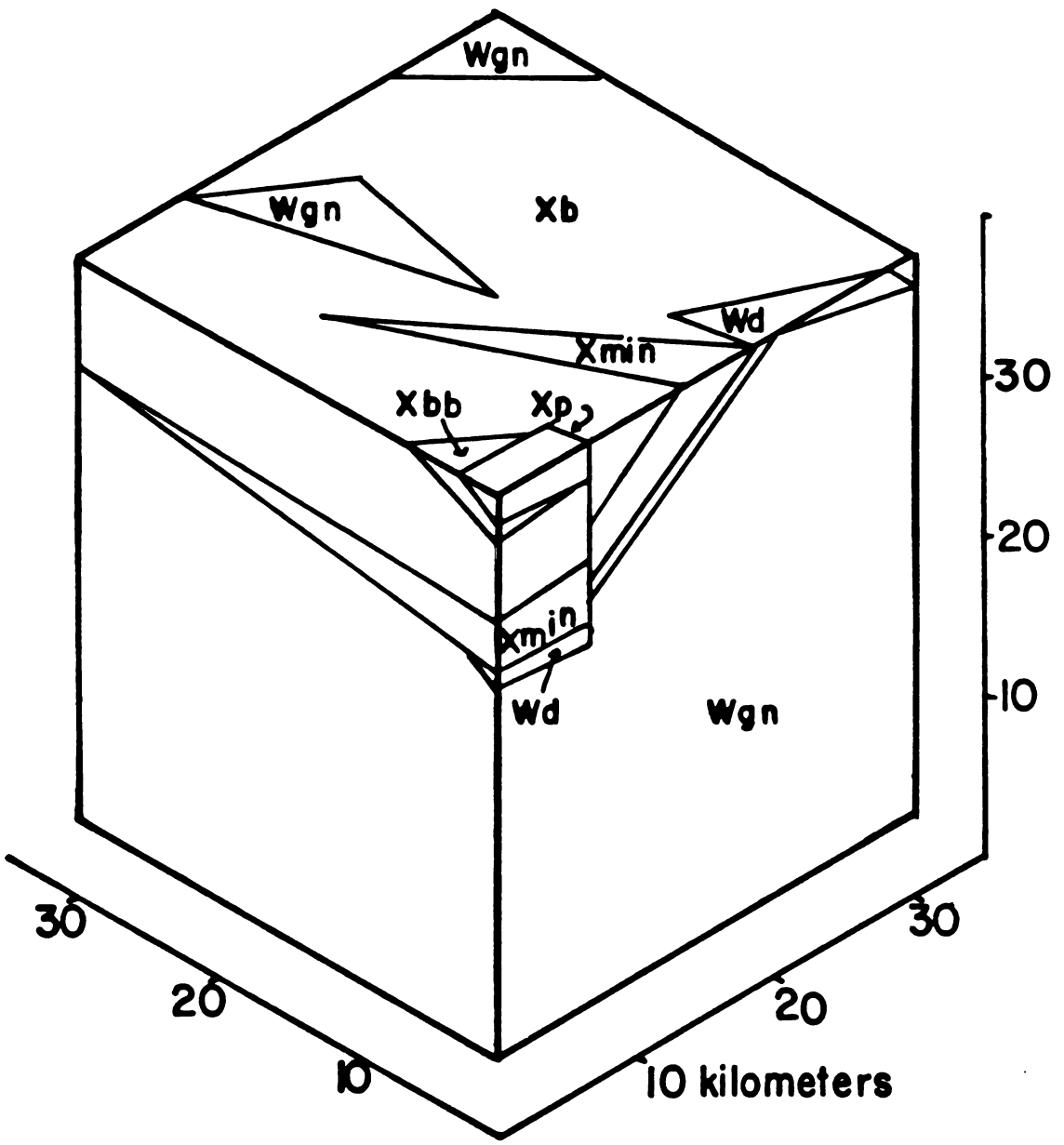

Figure 14

Block diagram of Pettijohn interpretation

formations do not thicken appreciably laterally (see figure 15).

The root-mean-square residual for the final computer model of the east-west profile was 5.6 milligals.

Attempting to fit the gravity through the thickening of formations would require the addition of at least 10 kilometers of 2.82 gram/cubic centimeter material to the western portion of the east-west profile (the left portion of figure 15). This thickening would have to be uniformly distributed along the north-south profile, and would probably ruin the previously adequate fit shown in figure 12.

4.2.3 the Paddock interpretation

The author retains James' (1958) stratigraphy and Pettijohn's (1969; James and others, 1968) fault-bounded eastern margin, but suggests the existence of faults bounding the entire Iron River-Crystal Falls district. Such a series of faults would separate Dunn Creek Slate from Michigamme Slates on the east margin of the district and would therefore, lie at either the Dunn Creek-Badwater Greenstone contact or the Badwater Greenstone-Michigamme Slate contact on the northern margin of the Iron River-Crystal Falls district. It was found that the second option was more successful at matching the gravity, and that the fault contact dips 10 and 15 degrees to the south. This interpretation is illustrated in figure 16.

The author's interpretation fails to match the observed gravity on the east-west profile within the required r.m.s. residual of 3.2 mgals under the assumption that no formation appreciably thickens laterally. The final computer model of the east-west profile of this interpretation had a root-mean-square residual of 4.4 milligals (see figure 17). The interpretation might be further modelled on the

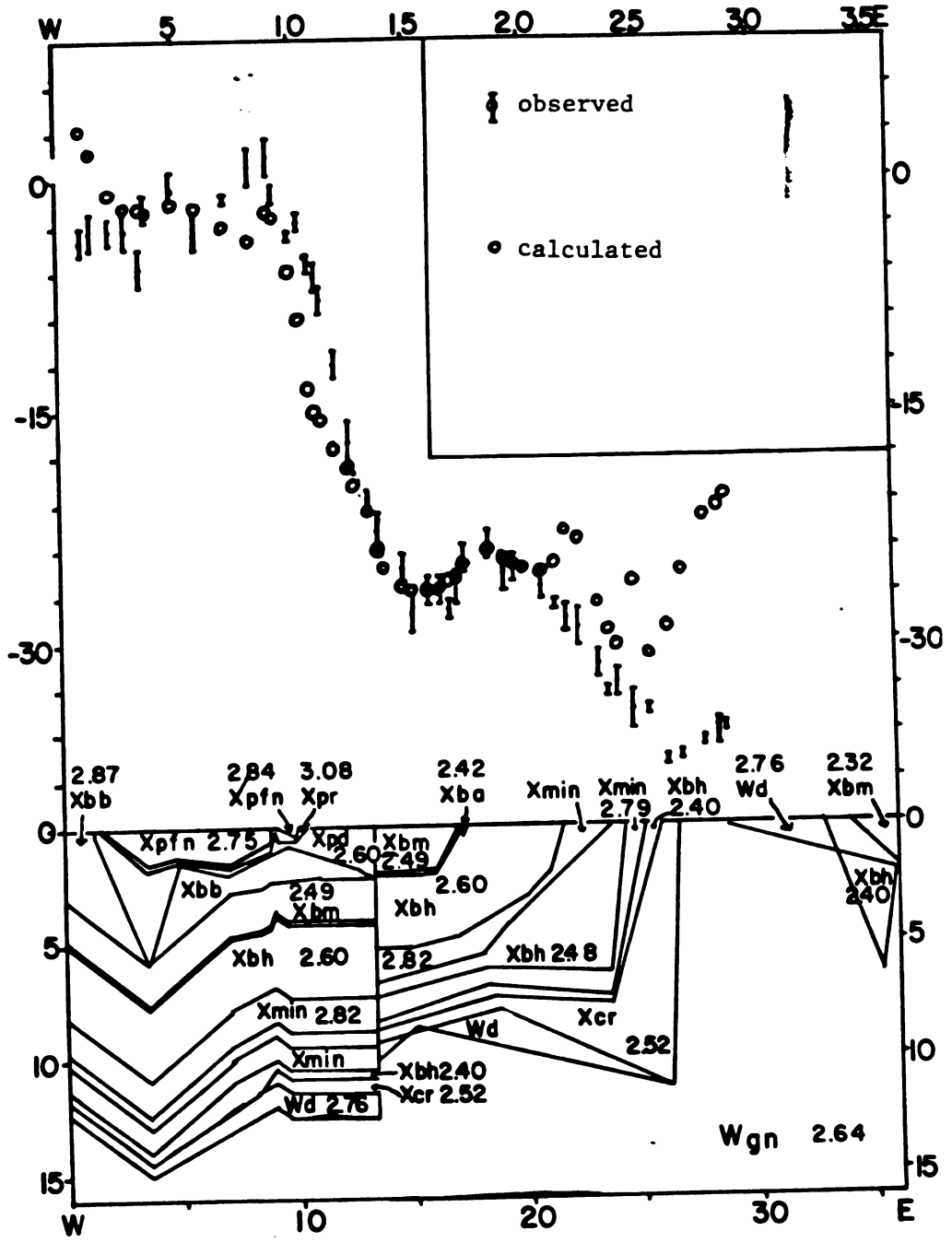

Figure 15

East-west gravity profile of Pettijohn interpretation

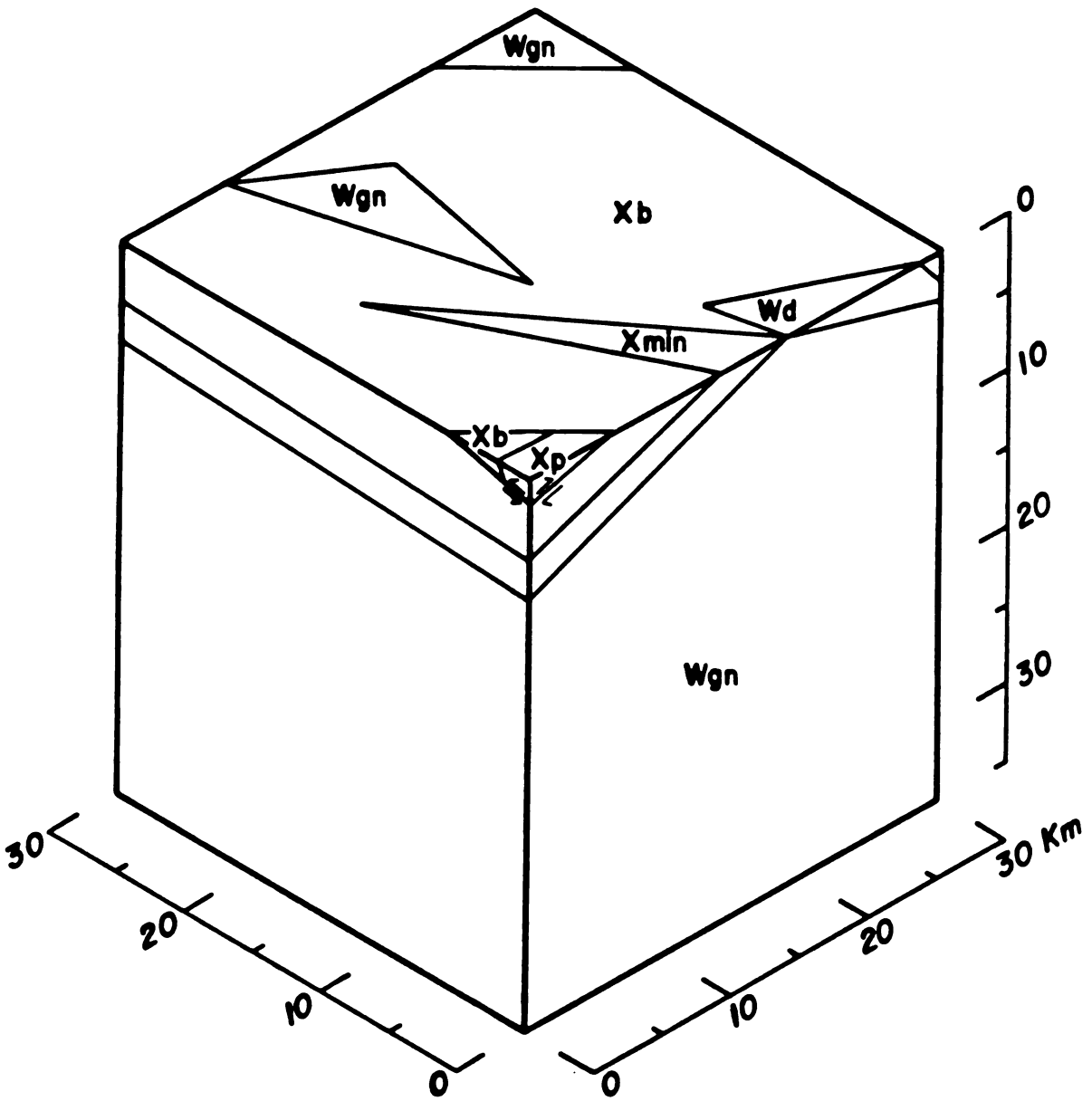

Figure 16

Block diagram of Paddock interpretation

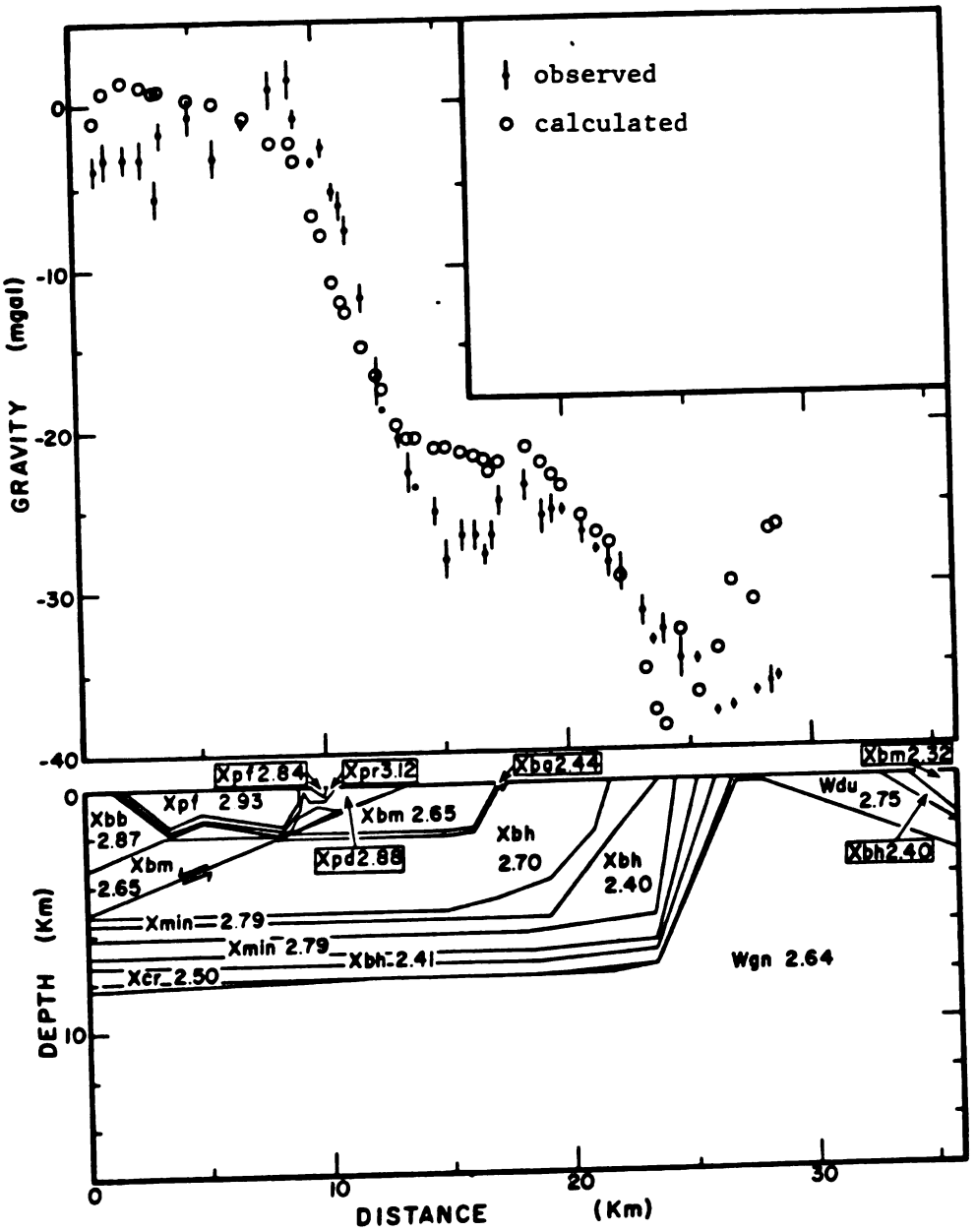

Figure 17

East-west gravity profile of Paddock interpretation

east-west profile by thickening the West Kiernan Sill (density 2.82) by approximately 3.8 kilometers in the Iron River-Crystal Falls district. The area north of IR-CF would also receive this additional mass, but those areas to the east would not. While this additional mass would presumably improve the fit of the east-west profile, it would also probably ruin the previously acceptable fit of the north-south profile (figure 18).

4.2.4 the Trow interpretation

Trow (1960) interprets the Paint River Group as repetitions of facies of parts of the Baraga and Menominee Groups (see Figure 2). In the context of the Iron River-Crystal Falls district (IR-CF), Trow's interpretation is identical to the author's (see subsection 4.2.3) except that Trow requires non-existence of the Michigamme Formation, the Amasa Formation, and the Hemlock Formation from below the IR-CF (see figure 19). Trow's model fails because the Badwater Greenstone-Hemlock Formation is required to have a high density where it outcrops between x = 0 and x = 1.3 km on Figure 20, while needing a low density where it outcrops between x = 17.4 kilometers and x = 21.6 kilometers. The density used in figure 17 (2.70 grams per cubic centimeter) is a good compromise between the two requirements, but will not adequately fit the observed gravity. Solving this inadequacy by thickening the West Kiernan Sill requires replacement of at least 2.1 kilometers of Hemlock Formation with sills.

4.2.5 The Greenstone Belt interpretation

Cambray (personal communication, 1980-81) has noted the similarity between the Iron River-Crystal Falls district and greenstone belts. Both contain sequences of basalt, slates and iron

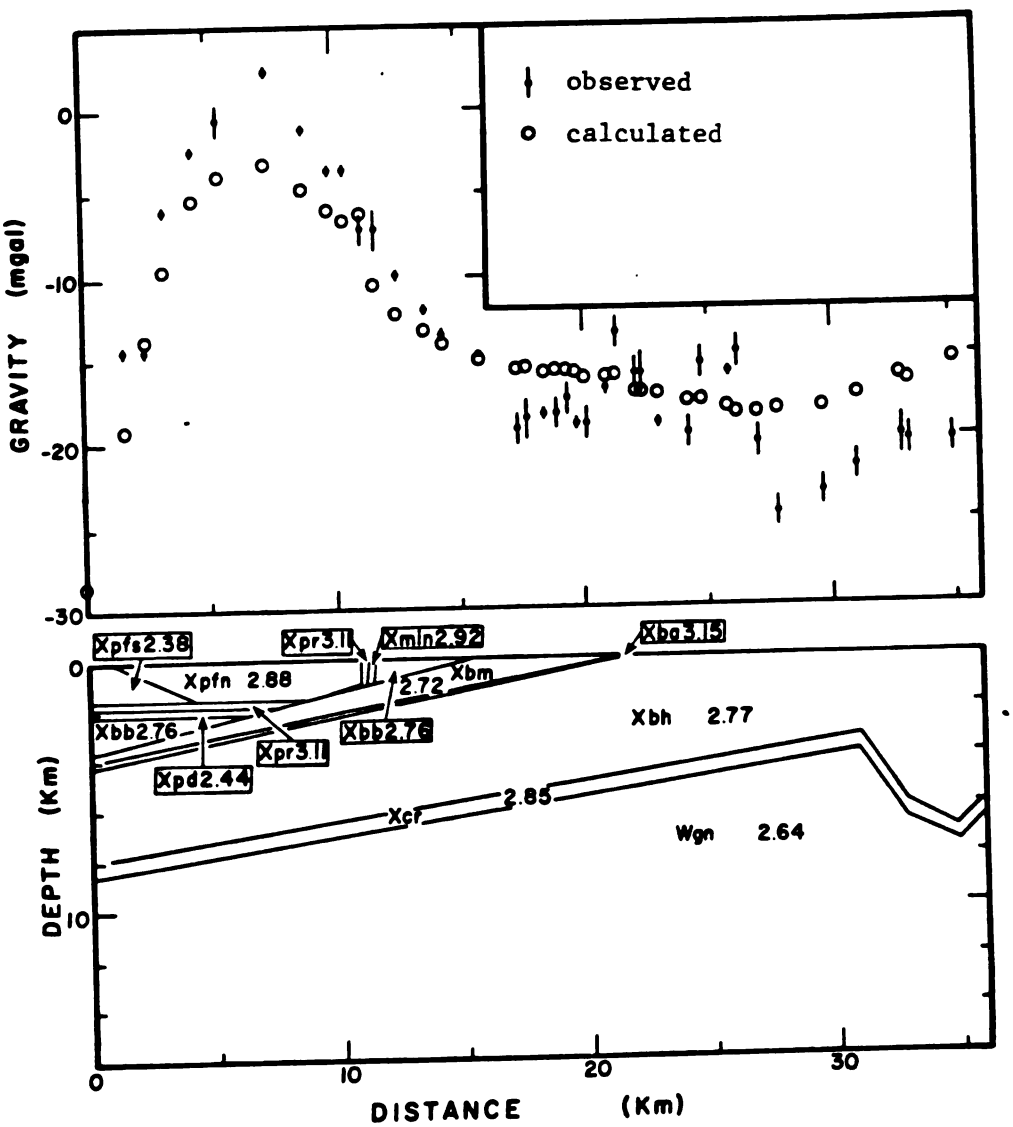

Figure 18

North-south gravity profile of Paddock interpretation

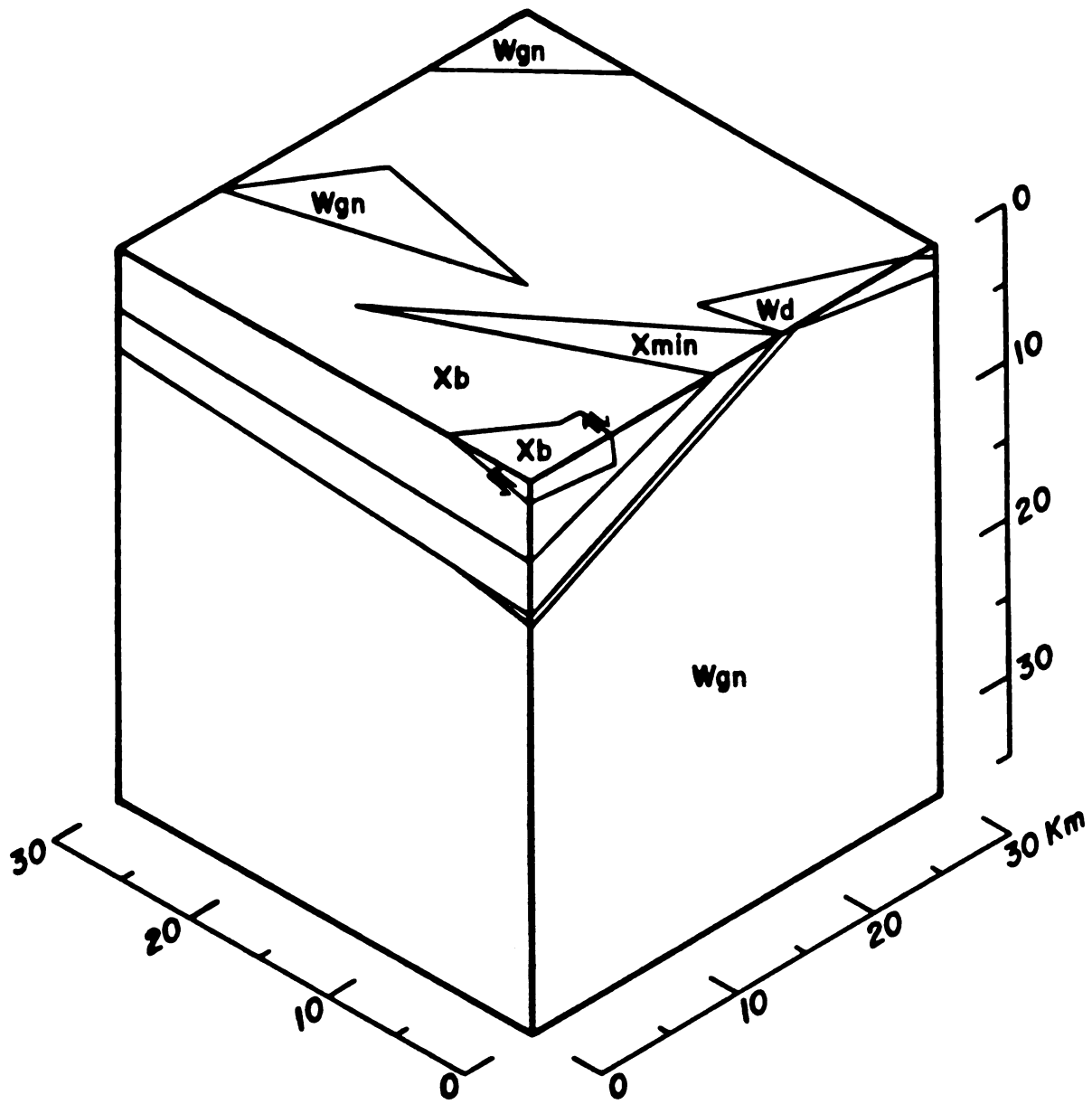

Figure 19

Block diagram of Trow interpretation

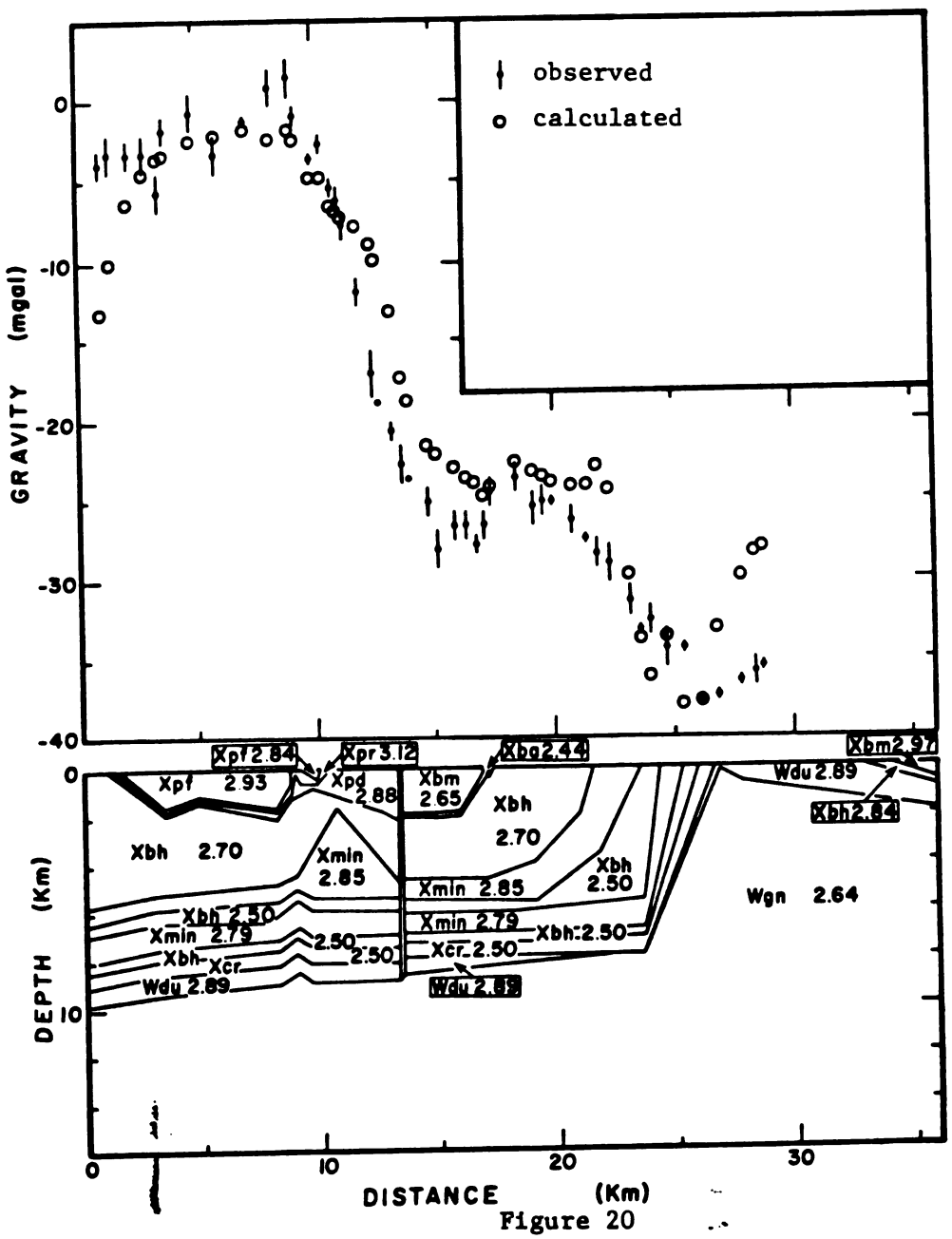

Figure 20

East-west gravity profile of the interpretation

formations. Interpreting the IR-CF district as a greenstone belt requires fault bounding all margins of the district at the Badwater Greenstone-Michigamme Slate "contact". The possibility of extensive thickening of the Badwater Greenstone also exists since greenstones regularly extend to a depth of 25 kilometers (Windley, 1977). The greenstone belt interpretation is illustrated in figure 21.

The greenstone-belt model is inconsistent with the shallow dip gravitationally required on the contact separating the Badwater Greenstone from the Michigamme Slate on the northern margin of the Iron River-Crystal Falls district.

4.2.6 The Trapped Ocean Crust interpretation

Cambray (personal communication, 1979) interpreted the Iron River-Crystal Falls district as trapped ocean crust which has escaped subduction (figure 22). The ocean crust was created either directly as a result of spreading between Michigan and Wisconsin in early Proterozoic time, or as the result of back-arc spreading as the proposed ocean floor between Michigan and Wisconsin was subducted to the north (VanSchmus, 1976). The ocean crust in the Iron River-Crystal Falls district would escape subduction due to the peculiar geometry of the area. Unfortunately, this interpretation is inconsistent with the shallow dip (10° to 15°) gravitationally required on the contact between the Badwater Greenstone and Michigamme Slate on the northern margin of the Iron River-Crystal Falls district.

4.2.7 the Larue interpretation

Larue (personal communication, 1981) interprets eastern Iron County, Michigan, USA as a large number of overthrusting ophiolites

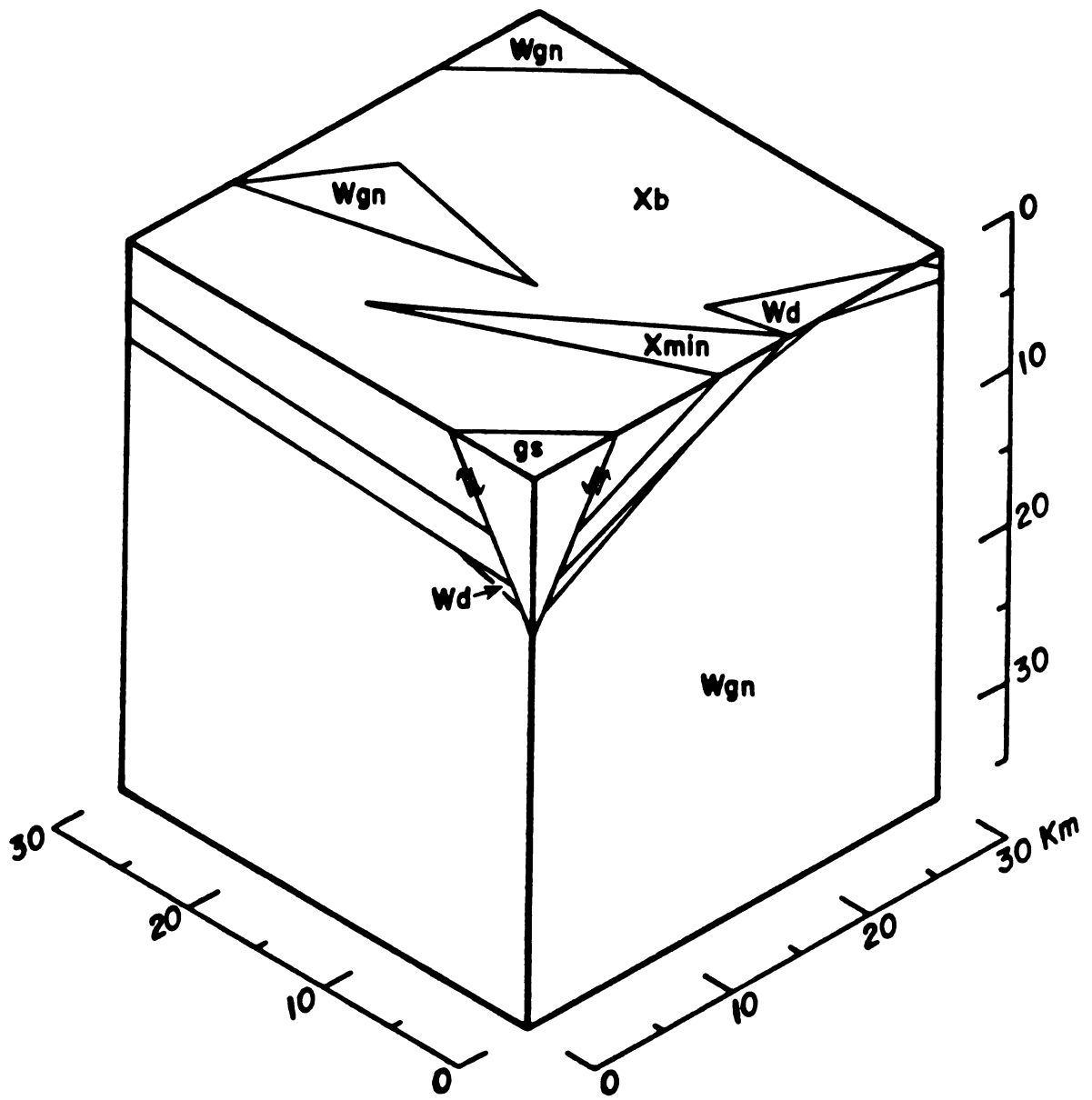

Figure 21

Block diagram of greenstone belt interpretation

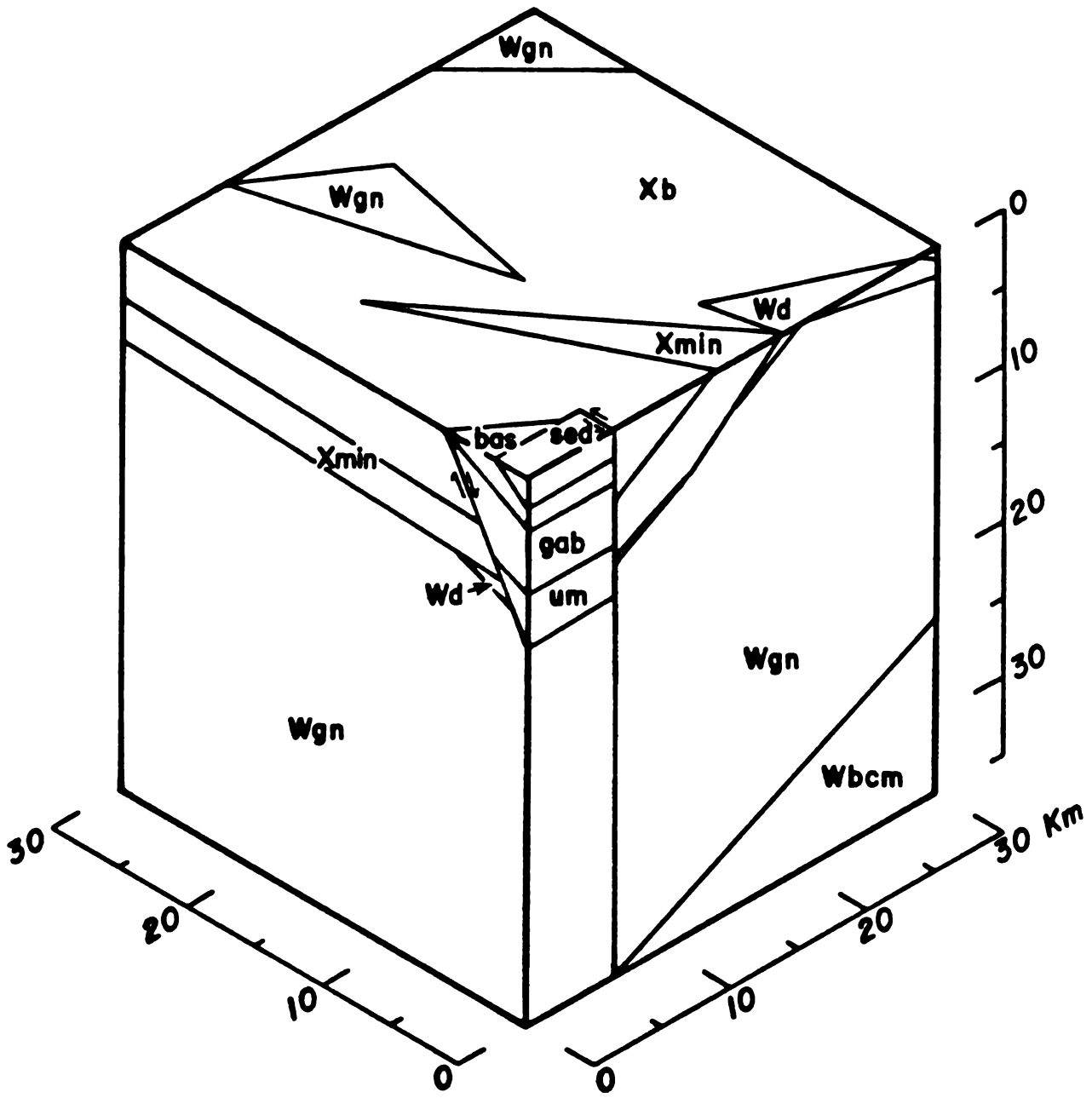

Figure 22

Block diagram of trapped ocean crust interpretation

terminating at the edge of a stable cratonic margin. These ophiolites would lie upon thinned continental crust, but would terminate at the edge of thicker (and more stable) cratonic crust to the northeast (Larue, personal communication, 1981; 1982). A block view of these ideas is found in figure 23.

Larue's interpretation was found to be virtually identical to the Paddock model, except that thrust faults were inserted along appropriate contacts. For this reason, Larue's interpretation was not tested separately. The model fails for the same reasons as the Paddock interpretation, and can possibly be remodelled using the same additional thickness as the Paddock interpretation (see subsection 4.2.3).

4.2.8 the "Badwater ophiolite" interpretation.

A second ophiolite interpretation views the Badwater Greenstone as an ophiolite whose remains are found in topographic lows of the underlying rock. This model requires the removal of the Badwater greenstone from the stratigraphic column and placing it instead at the top of the column above the Fortune Lakes Slate. Its stratigraphic position with respect to the Little Tobin Lake granite trend would be ambiguous. The ophiolite could be obducted over continental crust of any of the previously mentioned models. The "Badwater ophiolite" model fits best when the continental crust is as described by Trow (see subsection 4.2.4, see figure 24). The interpretation matches the north-south gravity profile very well (figure 25), but fails to fit the east-west profile within an RMS error of 3.2 milligals (figure 26). The Badwater "ophiolite" interpretation might be viable through the thickening of the Kiernan Sills by 17 kilometers. However, the Kiernan Sills have a maximum observed thickness of approximately four kilometers.

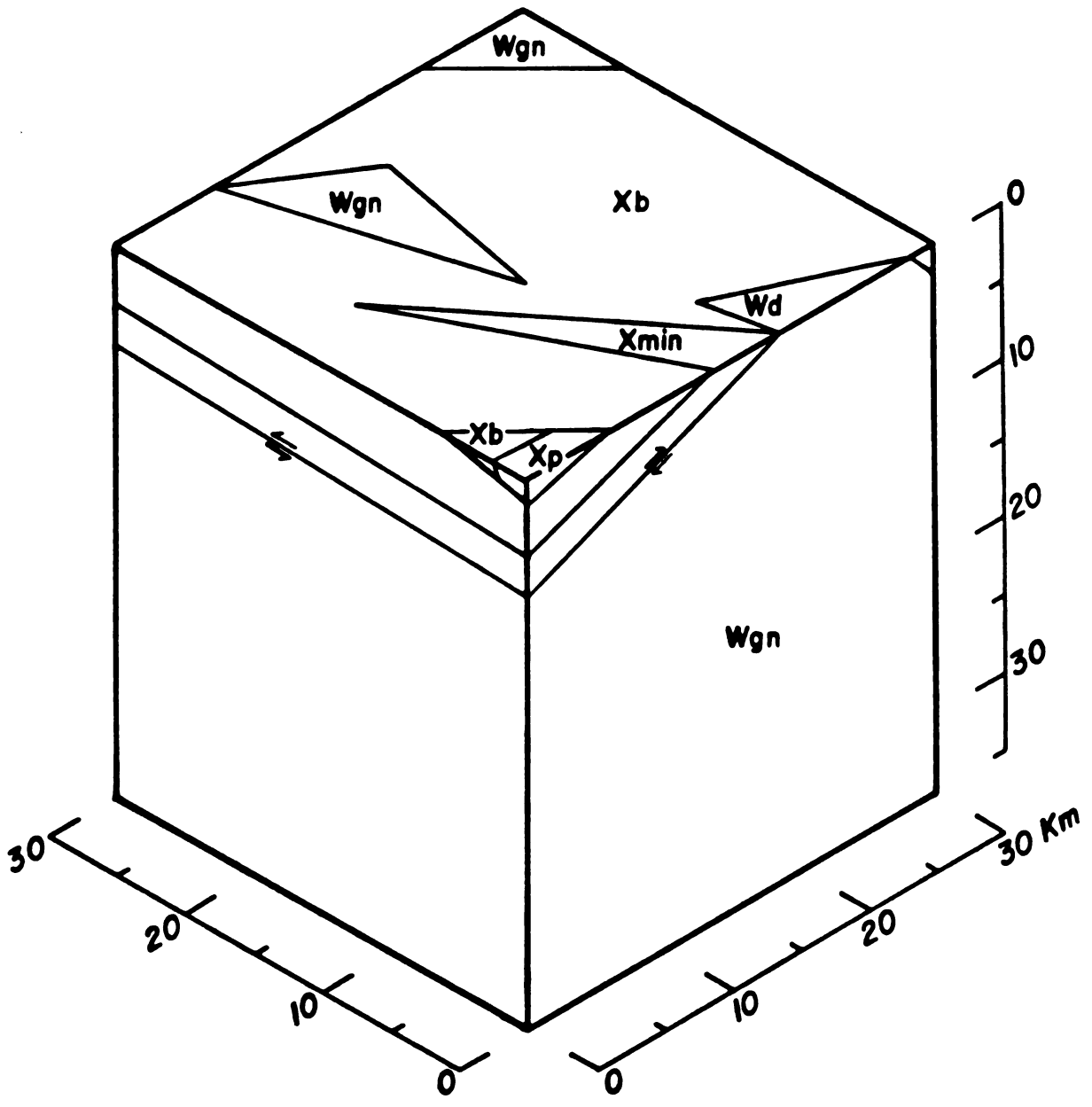

Figure 23

Block diagram of Larue interpretation

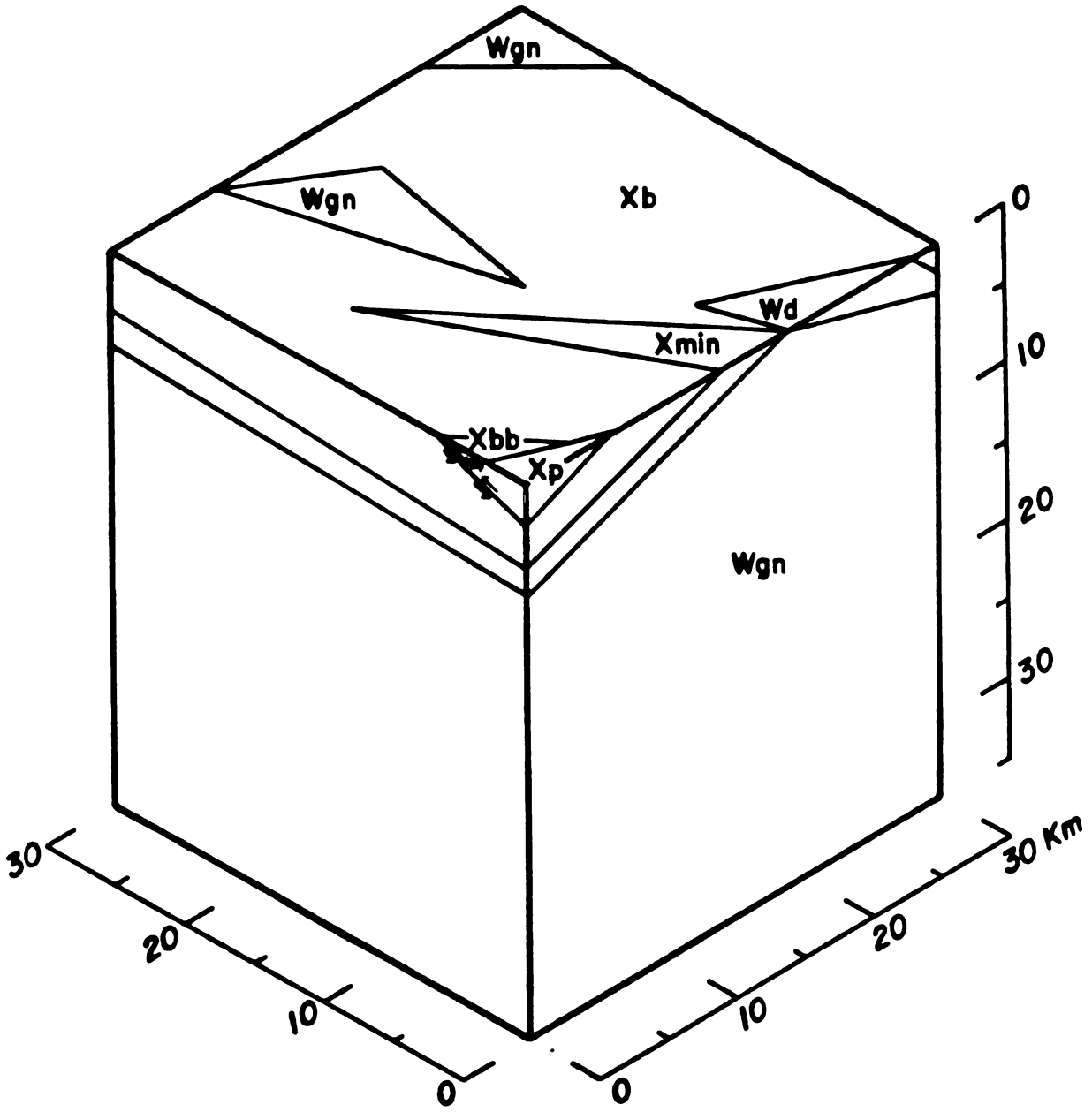

Figure 24

Block diagram of "Badwater ophiolite" interpretation

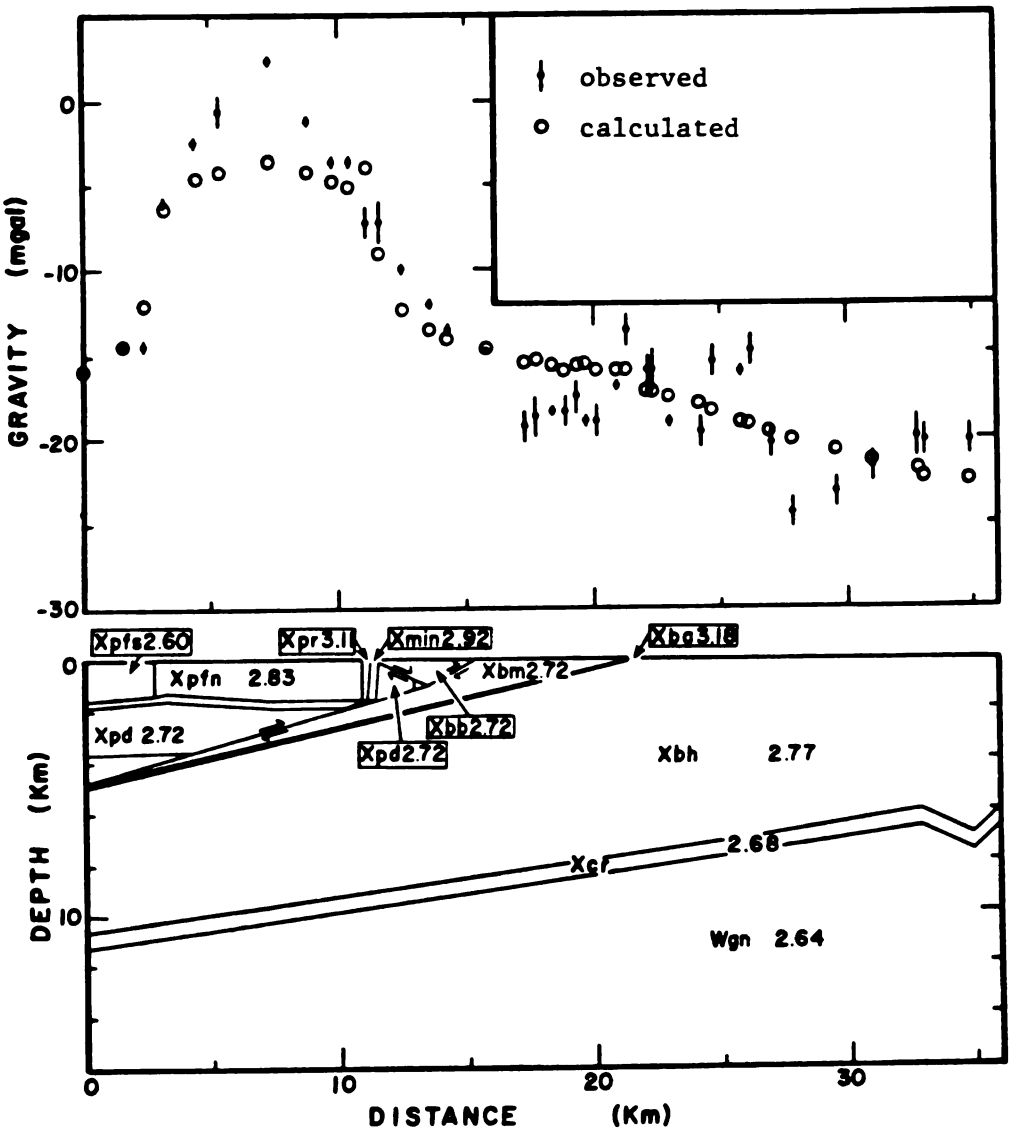

Figure 25

North-soucth gravity profile of "Badwater ophiolite" interpretation

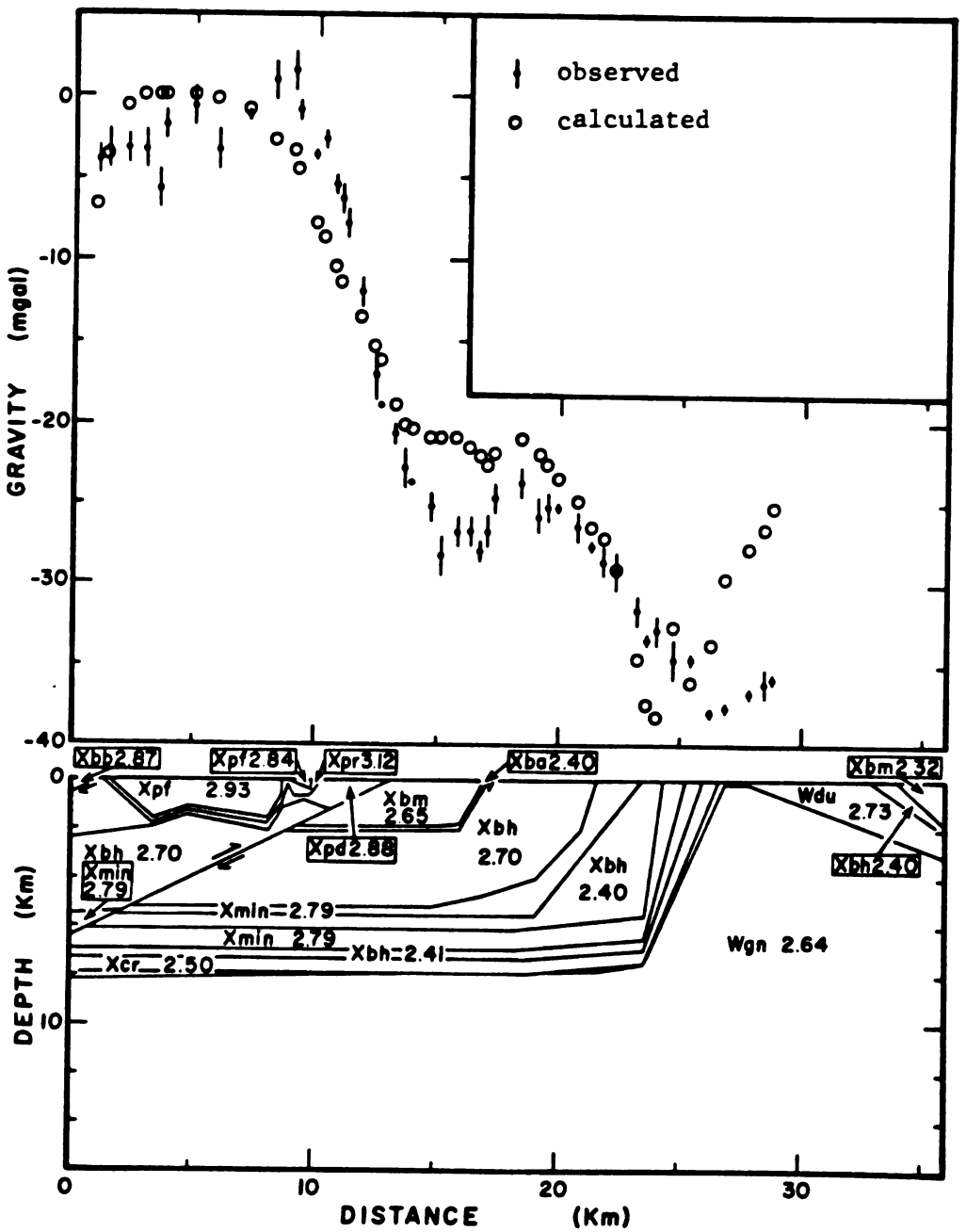

Figure 26

East-west gravity profile of "badwater ophiolite" interpretation

4.3 Detailed Gravity Survey Across the Riverton Iron Formation

A detailed gravity survey (with stations spaced every 300 meters) was performed along CR-424 through Alpha, Michigan. That survey revealed that a negative residual anomaly of approximately 0.3 milligals occurs where the Riverton Iron Formation reaches bedrock surface. Figure 24 illustrates the results of that survey, with surface lithology and density from Table 5 indicated along the bottom margin. Computer modelling of this profile predicts a positive gravity anomaly of 1.5 milligals over the Riverton Iron Formation. The inability of this detailed survey to detect the iron formation is thought to result from unmapped variations in till thickness. This detailed survey had only four stations located over the iron formation. It is believed that over a larger set of gravity measurements, the iron formation would probably be visible as a positive residual anomaly.

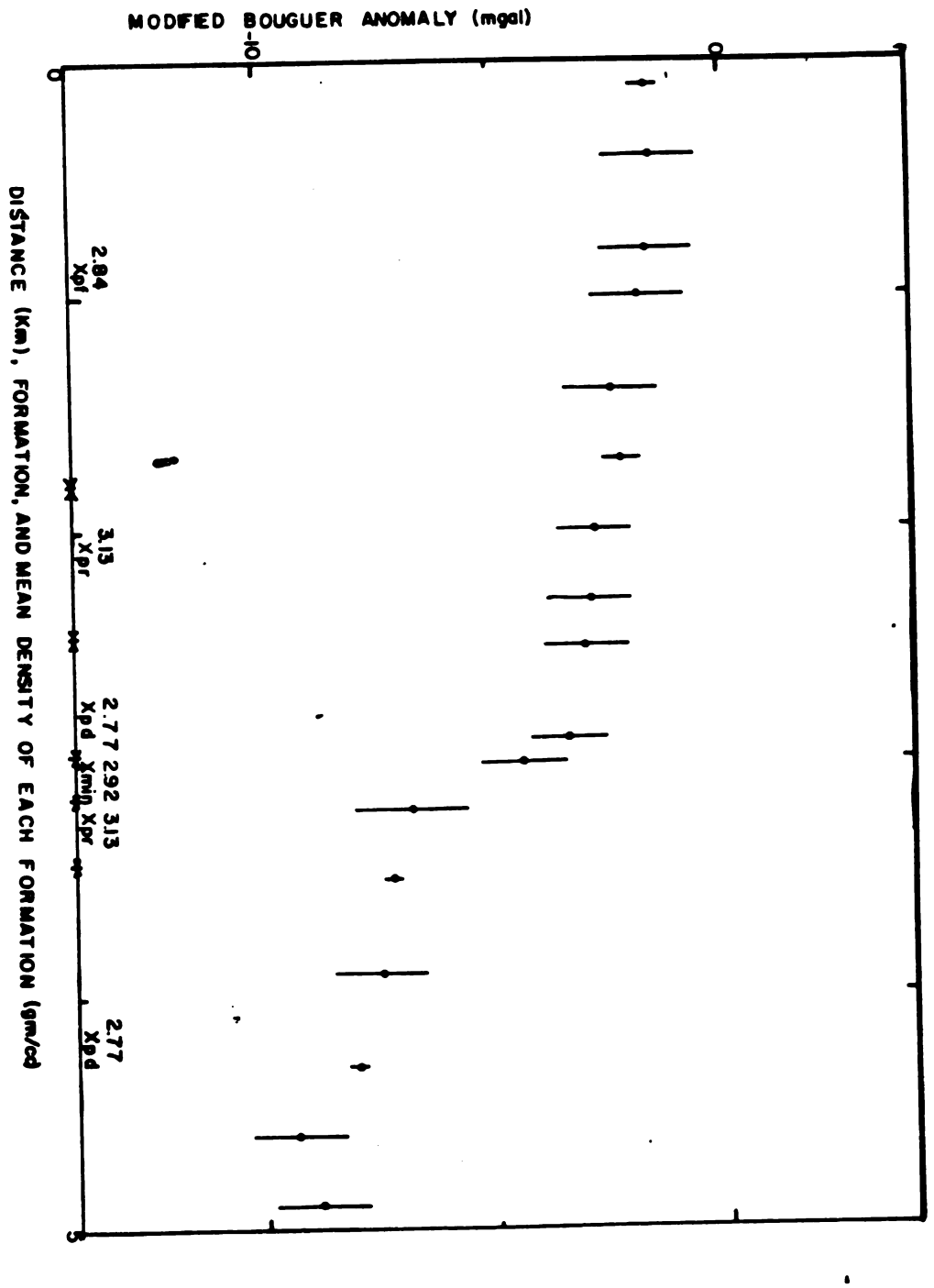

Figure 27

Gravity profile of line A across Riverton Iron Formation

5 SUMMARY, CONCLUSIONS AND RECOMMENDATIONS

5.1 Summary

Carefully collected and reduced gravity measurements in eastern Iron County provided gravity values, Free Air anomalies and modified Bouguer anomalies accurate to about 0.1, 0.35 and 0.6 milligals, respectively, relative to the Iron River datum. Modified Bouguer anomalies were supplemented by simple Bouguer anomalies from Bacon and Wyble (1952) and Klasner and Jones (1979). Since the three sets of data had been corrected in different ways, a correlation function was created to bring the simple Bouguer anomalies of a Bacon and Wyble (1952) and Klasner and Jones (1979) into agreement with the anomalies of this study. Accuracy of correlation-function values is $\pm$ 1.3 milligals and $\pm$ 1.0 milligals for input from Bacon and Wyble (1952) and Klasner and Jones (1979), respectively. Final accuracy of this enlarged set of simple Bouguer anomalies averages $\pm$ 0.8 mgal. This includes approximately 200 points from the present study, and another 100 each from Bacon and Wyble (1952) and Klasner and Jones (1979).

Modified Bouguer anomalies were interpreted to determine which of several different geologic models by the United States Geologic Survey, Pettijohn, the author, Trow, Cambray, and Larue best fit the observed gravity (see Chapter 4). Modelling was two-dimensional using the method of Talwani and others (1959) on a CDC Cyber 750 computer. All models were consistent with known surface geology, including outcrop data, mine geology, diamond drill hole data, water well data, and seismic surveys. In particular, lateral variation from the thickness observed or inferred from the outcrop of each

formation was minimized. In order to fit the theoretical model to the observed gravity, additional structure was introduced and densities varied within a range of $\pm$ 2.49 standard deviations for the north-south profile and $\pm$ 2.56 standard deviations on the east-west profile according to the number of stations on the profile.

5.2 Conclusions

Modelling revealed that the existing USGS interpretation (Gair and Wier, 1956; Bayley, 1959; Weir, 1967, James and others, 1968; Cannon, 1978; Foose, 1978) will fit the observed gravity under the assumption that no formation appreciably thickens laterally. That interpretion holds that IR-CF is not fault bounded (at least at the surface), and that none of the geologic features in eastern Iron County, Michigan, is an ophiolite.

None of the remaining seven interpretations (see Chapter 4) were able to match the observed gravity within a root-mean-square residual of 3.2 milligals under the assumption that the thickness of each formation is fairly uniform laterally. Of these seven interpretations, three are potentially salvageable through lateral thickening of the proper formations. Trow's (1960) interpretation would require a replacement of at least 2.1 kilometers of Hemlock Formation with West Kiernan Sill under IR-CF and to the north of IR-CF with no replacement to the east of IR-CF. The other potentially salvageable models are the author's and Larue's (1982, personal communication) interpretations. These two models are virtually identical, except for the insertion of thrust faults along the proper lithologic contacts to accommodate Larue's (1981, personal communication) ophiolites. These interpretations would both require

replacement of at least 3.8 kilometers of Hemlock Formation with Kiernan Sill. This replacement would be restricted to the Iron River-Crystal Falls district and to the area north of the district with no thickening of the Kiernan Sills east of the IR-CF district. In the case of the author's and Larue's interpretation, thickening of the sills may help to fit the east-west profile, but might also harm the acceptably small residual currently existing on the north-south profile.

Pettijohn's interpretation and the "Badwater ophiolite" interpretation (see chapter 4) are both salvageable through lateral thickening of high-density formations, but both require an unrealistic additional thickness (10 kilometers and 17 kilometers, respectively). The remaining two models, the "Greenstone Belt" and "Trapped Ocean Crust" interpretations were found to be inconsistent with the ten to fifteen degree southern (apparent) dip of the Badwater Greenstone-Michigamme Formation (fault?) contact obtained by gravity modeling the northern margin of IR-CF.

A feature not specifically modelled, but which was required in the U.S.G.S. model (and some other models as well) was the crustal thinning of the south half of Iron Conty, Michigan suggested by Larue (1980, personal communication). That thinning can be seen on figure 12 at x=28 kilometers and on figure 13 at x=26 km.

Another required feature was the subdivision of Cannon's (1978) Fortune Lakes Slate into two separate lithologies, labelled X_{pfn} (Fortune Lakes Slate (north)) and X_{pfs} (Fortune Lakes Slate (south)) on figures 12, 18, and 25. Although densities for the "north" and "south" members are labelled 2.90 and 2.37,

respectively, on figure 1, a density of 2.56 for the "southern" member would give a better fit. The "southern" member of the Fortune Lakes Slate produces an intense magnetic low in addition to the gravity low illustrated on figure 12. This magnetic low can be traced from Chicagon Lake southeast into Wisconsin (q.v. U.S.G.S. Geophysical Investigations Map GP607). The approximate extent of the "southern" member can be seen on older geologic maps, where it is labelled "Paint River Group Undivided" (q.v. Dutton and Linebaugh, 1967, or James and others, 1968). The "southern" member is probably at the base of the Fortune Lakes Slate, but is only evident on the east half of the southern margin of the basin. Its thickness there is approximately a kilometer; presumably, the "southern" member is missing elsewhere in the district.

5.3 Recommendations

The best ways to test the eight interpretations presented in Chapter 4 is through drill holes. The required depth of these holes (tens of kilometers) lead one to suggest that the endeavor might be best assigned to the Midcontinent Drilling Project. Cores through the center of the Iron River or Crystal Falls districts, through the Dunn Creek Slate, and through the Hemlock Formation/Kiernan Sill complex would be the most desirable. They would test for stratigraphy, fault boundaries, and ophiolites, respectively. The drawback of such an undertaking is the occasional inability of cores to reveal faults (q.v. Weir, 1971). A less expensive investigation would be the detailed field study of the Little Tobin Lake Granites to determine whether or not Pettijohn's fault actually exists. The

emphasis of such a study should be on evidence for shearing (Trow, personal communication, 1981).

To further investigate the ophiolite theories for eastern Iron County, a chemical analysis might be done on each of what should be identical "thrust sheets" along M-69 between Crystal Falls and Sagola. Observations and chemical analyses by Bayley (1959) suggest that these sheets are significantly different. In addition, the similarity in stratigraphy between the Hemlock Formation in Lake Mary and Ned Lake quadrangles (Bayley, 1959; Foose, 1978) strongly suggests that the Hemlock Formation actually is a distinct formation rather than a series of thrust sheets.

Investigation should be made of the "southern" member of the Fortune Lakes Slate mentioned in the previous section. The gravity and magnetic lows above this member could be the result of rocks with low magnetic susceptibility and density or perhaps a thick body of glacial deposits.

The final recomendation is that more density determinations be made for the southern Lake Superior region. No density determinations for the Fortune Lakes Slate (and its "southern member"), the Kiernan Sills or the Dickinson Group currently exist.

REFERENCES

REFERENCES CITED

Bacon, L. O., and Wyble, D. O., 1952, Gravity investigations in the Iron River-Crytal Falls mining district of Michigan: Am. Inst. Mining Metall. Engineers Trans., v. 193, Tech. Paper 3383L, p. 943-979.

Bayley, R. W., 1959, Geology of the Lake Mary Quadrangle, Iron County, Michigan: U.S. Geol. Survey Bull. 1077, 112 p.

Cambray, F. W., 1977, The geology of the Marquette district, a field guide: Michigan Basin Geological Society, 62 p.

Cannon, W. F., 1978, Geologic map of the Iron River 1°x2° Quadrangle, Michigan and Wisconsin: U.S. Geol. Survey Open File Map 78-342, Scale 1:250,000.

Cannon, W. F., and Klasner, J. S., 1976, Geologic map and geophysical interpretation of the Witch Lake Quadrangle, Marquette, Iron, and Baraga Counties Michigan: U.S. Geol. Survey Map I-987, scale 1:62,500.

Carlson, B. A., 1974, A gravity study of the geology of northeastern Wisconsin (Ph.D. thesis): Michigan State University, 120 p.

Clark, S. P., Jr., ed., 1966, Handbook of physical constants (rev. ed.): Geol. Soc. America Mem. 97, 587p.

Clemens, J. M., and Smyth, H. L., Jr., 1899, The Crystal Falls iron-bearing district of Michigan: U.S. Geol.Survey Mon. 36, 512 p.

Duerksen, J. A., 1949, Pendulum gravity data in the United States: U.S. Coast and Geodetic Survey Spec. Pub. 244, 218 p.

Dutton, C. E., 1971, Geology of the Florence area, Wisconsin and Michigan: U.S. Geol.Survey Professional Paper 633, 54 p.

Foose, M. P., 1978, Preliminary geologic map for the Ned Lake Quadrangle, Michigan: U.S. Geol. Survey Open File Report 78-386, scale 1:62,500.

Frye, K., 1974, Modern Mineralogy: Englewood Cliffs, New Jersey. Prentice-Hall, Inc. 325 p.

Gair, J. E., and Weir, K. L., 1956, Geology of the Kiernan Quadrangle, Iron County, Michigan: U.S. Geol Survey Bull 1044, 88 p.

James, H. L., 1958, Stratigraphy of pre-Keweenawan rocks in parts of northern Michigan: U.S. Geol. Survey Prof. Paper 314-C, p. 27-44.

James, H. L., Dutton, C. E., Pettijohn, F. J., and Weir, K. L., 1968, Geology and ore depostis of the Iron River-Crystal Fall district, Iron County,Michigan: U.S. Geol Survey Prof. Paper 570, 134 p.

James, H. L., Pettijohn, F. J., and Clark, L. C., 1970, Geology and magnetic data between Iron River and Crystal Falls, Michigan: Michigan Geol. Survey, Report of Investigation 7, 17p.

Klasner, J. S., and Jones, W. J. 1979, Simple Bouguer gravity map and geologic interpretation: Iron River 1°x2° quadrangle, Northern Michigan and Wisconsin: U.S. Geol. Survey Open File Report 79-1564.

Larue, D. K., 1981, (unpublished preliminary version of Larue, 1982), Evolution of a purported early Proterozoic passive margin, Lake Superior region.

Larue, D. K., 1982 (in press), Three early Proterozoic terranes in the southern Lake Superior region bearing on passive margin sedimentation and plate collision.

Larue, D. K., and Sloss, L. L., 1980, Early Proterozoic sedimentary basins of the Lake Superior region, Geol Soc. America Bull. 91, p. 450-452, 1936-1874.

Leney, G. W., 1966, Field studies in iron ore geophysics in Mining Geophysics, vol. 1, Soc. Expl. Geophysicists, p. 319-417.

Mancuso, J. J., Lougheed, M., and Shaw, R., 1975, Carbonate-apatite in Precambrian cherty iron-formation, Baraga County, Michigan: Econ. Geol., v. 70, p. 583-586.

Pettijohn, F. J., 1972, Geology and magnetic data for southern Crystal Falls area, Michigan: Michigan Geol. Survey, Report of Investigation 9, 31 p.

Pettijohn, F. J., Gair, J. E., Weir, K. L., and Prinz, W. C., 1969 Geology and magnetic data for Alpha-Brule River and Panola Plains area, Michigan: Michigan Geol. Report of Investigation 10, 12 p.

Talwani, M., Worzel, J. L., and Landisman, M., 1959, Rapid gravity computations for two-dimensional bodies with application to the Mendocino Submarine Fracture Zone: J. Geophys. Res., vol. 64, pp. 49-59.

Telford, W. M., Geldart, L. P., Sheriff, R. E., and Keys, D. A., 1980, Applied geophysics: New York, Cambridge University Press, 860 p.

Trow, J.W., 1960, Final report on Outside Exploration 1247 (unpublished): Cleveland Cliffs Iron Company.

Weir, K. L., 1967, Geology of the Kelso Junction quadrangle, Michigan: U.S. Geol. Survey Bull. 1226, 47 p.

_____, 1971, Geology and magnetic data for northeastern Crystal Falls area, Michigan: Michigan Geol. Survey, Report of Investigation 11, 14 p.

Windley, B. F., 1977, The Evolving Continents: N.Y., Wiley, 385 p.

Woollard, G. P., and Rose, J. C., 1963, International gravity measurements: Tulsa, Soc. Expl. Geophys. Spec. Pub.

APPENDICES

APPENDIX I

STATION	STATION LOCATION
1R	On the playgrounds of Central School (no longer used) on Cayuga Street between Second and Third Streets. The station is 37.5 meters N60°W of the "Iron River 1940" standard gravity reference mark. The mark is set flush in the concrete sidewalk along the east side of the school, 2 meters due magnetic south of the north end of the walk. The station is also 33.8 meters due magnetic west of the west curbing of Second Street, 38.4 meters due magnetic east of the center of the brick stack at the boiler room, 15 meters due magnetic north of the north side of the school, and 37.8 meters N5SW of the northeast corner of the school (Duerksen, 1949).
1A	North side of CR424 at center of Wood Lot Rd.
1B	JCT Woodlot Road and circa 1940's two track, center of both.
1C	Center of two track at drive to building south of southern more point of southwest lobe of Third Lake, at end of pea gravel.
1D	From U.S. 2, go 1220 m "south" on CR639. Take two-track south from CR639 for 1300 meters. Center of intersection. Map elevation labeled 1526 feet.
1E	At entrance to driveway on CR639, 1020 meters "south" of U.S. 2. East side of CR639, center of driveway.
1F	On BM just north of JCT U.S. 2 and CR639. Witness post.
1G	At curve 1440 meters north of U.S. 2 on Oss Road. Ctr of both roads.
1H	Corner of sections 17, 18, 19 and 20, ctr of Oss Rd, 2640 m N of U.S. 2.
1I	At top of sub-hill with 1518 BM "X", NE, NE, NE, Sec 18, T43N, R33W.
1N	At apex of curve on Gibson Lk Rd, 1180 m from new U.S. 141.
1O	BM N of JCT CR643 and Raunio Rd. Elev. 1428 ft.
1P	On west side of Snuff Country Road, 580 meters north of CR643, at junction with chained off 2-track.
1Q	Ctr of JCT Maki Rd and Snuff Country Rd, elev. 1484 feet.
1R	BM 1440, SE of JCT Park Cty Rd and Maple Ave., between telephone pole & stop sign.

APPENDIX I (cont)

STATION	STATION LOCATION
1S	Apex of curve, ctr of rd, Kahma Ave., 200 m E of new U.S. 141, elev. 1451 ft.
1T	200 m N of Corral Rd on old U.S. 141. Ctr of old 141. Close as possible to old house.
1U	1600 meters north of Corral Rd on new U.S. 141, then west until reaching a topographic high.
2-B	Ctr of JCT of Carney Dam Rd and Rainbow Tr. Elev. 1420 ft.
2-A	JCT of Carney Dam Rd and Bara Rd. Ctr of both rds. Elev. 1459 feet.
2A	JCT Carney Dam Rd at Buck Lk. Pk. Rd. Ctr of both rds.
2B	JCT CR424 at N bd. dirt rd, .7 km west of Buck Lk Rd. Elev. 1486.
2C	Just off pavement on W side of Tobin-Alpha Rd at Alpha Cr.
2D	JCT of McClaren and Bible Camp Rds. Ctr of both roads.
2E	Center of junction, Bible Camp Road at Idelwild Road. Elevation 1482 ft.
2F	JCT of Fortune Lake Camp Road at Bible Camp Road. West side of Bible Camp Road. Ctr of Fortune Lake Camp Road.
2G	JCT New Bristol Rd at U.S. 2. Ctr New Bristol Rd, N side of U.S. 2. 1451 ft.
2H	Ctr of Knivila Rd at N side of Lind Rd. Elev. 1397 ft.
2I	Ctr of Ron's Rd at W side of Knivila Rd. Elev. 1398 ft.
2J	Ctr of driveway to 283 Knivila Rd at W side of Knivila Rd. Elev. 1430 ft.
2K	Ctr of N bd 2-track at N side of Sheltrow Rd, 400 m E of Paint River Public Access. Elevation 1372 ft. N1/2, sec 11, T43N, R33W.
2L=9H	Center of driveway to 547 Sheltrow Road at southwest side of Shertrow Road.
2M=8C	At benchmark "X" on a concrete culvert, west side of old U.S. 141, 40 meters south of Swan Lake Road.

APPENDIX 1 (cont)

STATION	STATION LOCATION
2N=8E	At entrance to 159 S Casagranda Rd driveway, SE side of S. Casagranda Rd. Elev. 1457. PLEASE NOTE ELEV IS 1457, NOT 1557.
2O	Ctr of N Casagranda Rd at section line, 500 m N of U.S. 141. Elev. 1453.
2P	Ctr of Premo Cr. Rd at E. side of old U.S. 141. Not at BM.
2Q	BM 1512 ft at Balsam Sta. SE of JCT of 2-track and CMS+P&P RR.
2R	Where Carlson Rd enters section 12. 1600 m road distance from Premo Cr. Rd.
2S	Take left fork at end of Carlson Rd. Follow trail to end of clearing.
2T	Ctr of C&NW RR at S side of Buck Lk Truck Tr. Elev. 1526 ft.
2U	From Buck Lk Truck Tr at Buck Lk-Premo Lk Cr, go "west" along Buck Lk Truck Tr through a right-hand turn to a sharp left-hand turn around a topographic high. Center of trail at the apex. Traffic extremely dangerous.
3A	SE1/4, SW1/4, sec. 35. On 2-track, 273 m "NE" of station 3B, at JCT w/new trail not on topo map. Ctr new 2-track, SE track of mapped two track.
3B	3600 m from M-69 along Hope Mine Rd at JCT of Hope Mine Rd and mapped two track. 400 m "SE" of station 3C. NE side of Hope Mine Rd., ctr. of mapped 2-track.
3C	At bend in Hope Mine Rd, 2400 m S of M-69 (3200 m along Hope Mine Rd from M-69). 400 m S of ctr of sec 34 and 35 bdry. E side of Hope Mine Rd across from last fence post on E side of rd. TRAFFIC EXTREMELY DANGEROUS.
3D	Ctr of E1/2, sec 34, T43N., R.32W., 2000 meters south of M-69 (2400 meters along Hope Mine Rd from M-69)
3E	1/8th mile (200m) east of the center of section 34, T.43N., R.32W.
3G1	S bd on Old Lk. Mary Rd, cross Blaney Cr, then follow Old Lk Mary Rd 940 meters further "south". At exit to right-hand curve, left tire track.

APPENDIX 1 (cont)

STATION	STATION LOCATION
3G2	S bd. on Old Lk. Mary Rd., cross Blaney Cr., then follow Old Lk Mary Rd 720 meters further sourth. At south bound left-hand curve. Center of road.
3H	Ctr of SW1/4, SE1/4, sec 33, T.43N., R.32W. On floor of waste control lagoon.
3I	NE side of Kimball Rd at ctr Dunn Cr. bridge.
3J	Center of Kimball Rd at center of Iron County Recreation Trail. Elev. 1304 ft.
3K	Center of Iron County Recreation Trail at center of Dunn Creek bridge.
3L	Center of trail. Between two ponds. E1/2, sec. 32, T.43N., R.32W.
3M	North tiretrack of Wiggins Road at west side of U.S. 2 - U.S. 141. ELEV 1314.4 feet.
3N	North tiretrack of Wiggins Road at center of driveway to 128 Wiggins Road.
3O	Center of boundary, sections 31 and 32, T.43N., R.32W.
3P	At end of Valley View Road, south tiretrack, one meter past pine tree.
3Q	Southwest side of Valley View Road at powerline.
3R	West side of Carpenter Road at old light-duty road. Old road blocked by stop sign.
3S	450 meters "west" of Carpenter Road, measured along light duty road.
3T	Center of gravel at intersection of Tobin-Alpha Road and Idlewild Road. Elev. 1413 ft.
3U	N side of Idlewild Rd. at ctr of abandoned RR, just E of Dunn Cr.
4A	N edge of pavement at ctr of driveway to 135 S. Shore Rd.
4B	East side of Lake Mary Road at center of South Shore Road. Elev. 1357 ft.
4C	W track of Old Lk. Mary Rd. at ctr of ski pathway. SW1/4, SE1/4, SE1/4, sec 12.

APPENDIX 1 (cont)

STATION	STATION LOCATION
4D	Also station 10K. Old Lk Mary Rd at fork to Paint River. Elev. 1348 ft. SE, NW, SE.
4E	At end of fork to Paint River from 4D. Center of turn-around clearing.
4F	From corner of Little Bull Road and Lake Mary Road, proceed west 1300 meter (approx). From there take two-track "west" instead of following Little Bull road south. After 160 meters, take left fork. Follow main road. Makes two T's to the right. Stop at second T. Pace 690 meters 318°.
4G	S1/8, W1/4, sec 11, T.42N., R.32W.
4H	South track of Panola Plains Road at south-bound two-track. Elev. 1312 ft.
4I	North track of Panola Plains Road at center of Mud Lake Road. Elev. 1318.
4J	South track of Panola Plains Road at southwest track of two-track to Tim Bowers Pond.
4K	South track of Panola Plains Road at section line (9 and 10). Vegetation change.
4L	North track of Panola Plains Road at north-bound two track. E1/2, section 9.
4L1	Center of Panola Plains Road at center of section 9, T.42N., R.32W.
4M	From 4N, go "east" 360 meters through right-left "S" curve. At entrance to the next right-hand bend, on south tire track of Panola Plains Road.
4N	Panola Plains Road at barely visible old two-track which crosses at very low angle. Elevation is 1361. South side of Panola Plains Road at center of old two-track.
4O	Center of Iron County Recreation Trail at center of Panola Plains Road.
4P	South side of CR424, directly in front of house, 151 CR424.
4Q	Center of Hill Farm road at east side of Stager Lake Road.
4R	South side of CR424 where center of old Stager Lake Rd would have been. 1428.
4S	N side of CR424 at ctr of Book Rd. Elev. 1407 ft.

APPENDIX 1 (cont)

STATION	STATION LOCATION
4T	East side of Mastadon Road at center or Iron County Recreation Trail. Elevation 1398.
4U	Ctr of Mastadon Rd at ctr of Alpha Cr.
5A	At ctr of intersection near BM "X" 1337, E1/2, sec 26, T.42N., R.32W.
5B	Center of both runways, Iron County Airport, elevation 1340 ft.
5C	Northwest end of main runway, Iron County Airport. ctr of runway.
5D	North side of County Airport Road at south side of two-track where County Airport Road bends from WNW-ESE to NW-SE. SW, NE, NE, sec 27.
5E	NE1/4, sec 27, at apex of road, 340 meters northwest of unfindable BM1337.
5F	South side of County Airport Road at center of two track, 120 meters west of creek to Mallard Lake.
5G	N side of Co. Airport Rd. at ctr of old light duty rd. 180 m W of 5F.
5H	170 m E of 7 Springs Pond 2-track along main 2-track. N track, in ctr of straight between two E bd right-handers. SE1/4, NE1/4, sec 28.
5I	S side of main 2-track at ctr of 7 Springs Pond 2-track. SE, NE, sec. 28.
5J	70 m N of point INCORRECTLY labeled 1317 feet elevation on Crystal Falls 7 1/2 Quad. 630 m S of Airport Rd. On U.S. 2-U. S. 141. ELEVATION IS 1323.6 FEET AT STATION 5J.
5K	420 m "SW" along 2-track from point INCORRECTLY labeled 1317 feet on Crystal Falls 7 1/2 Quad on top of rise. Well cleared.
5L	370 m, 340° from Rusek Dr. at bdry sect. 28 and 29. At south point of the northernmost of two kettle lakes separated by two-track.
5M	390 m "NW" of 5L along two track, at right-hander in valley.
5N	Where sec. 29 2-track changes dir from 280° to 300°. Ctr of 2-track.

APPENDIX 1 (cont)

STATION	STATION LOCATION
5O	E side of CR424 at ctr of sec. 29 2-track. Not accessible from east.
5P	Sec. corner (19, 20, 29, 30). On old RR not shown on any maps.
5Q	Iron County Recreation Trail at Stager Creek. Center of both.
5R	Center of N1/2, sec 30, T.42N., R.32W. Where road curves southeast. 1498.
5S	Top of hill, NW1/4, sec 30, T.42N., R.32W. 270 meter due west of 5R.
5T	At end of rd. to burnt-out homestead, W1/2, NW1/4, sec.30.
5U	Fenceline at center of Blockaniec Rd, 1200 m E of Buck Lk. Rd. 1549.
6D	Ctr of 2-track, 400 m E of section line (secs. 20 and 21).
6F	E side of Deer Lk Rd at ctr. of two track. W1/2, NW1/4, sec 29.
6H	N track of sec 24 two-track at acute SE bd right-hand curve. SW1/4.
6I	Center of sec. 23 two-track, where 2-track dir changes from 135° to 090°.
6J	E side of The Grade at ctr of Hemlock R. SE, SE, NE, sec 22.
6K	Northernmost of 3 crossings of RRCr on The Grade. Ctr cr, W side of rd.
6L	Old U.S. 141 at the section 28-29 bdry. At concrete marker.
6M	Old U.S. 141 at Chicago, Milwaukee, St. Paul, and Pacific Railroad tracks. Center of both.
7A	2T. S side of Buck Lk Truck Trail at ctr of C&NW RR. Elev. 1526.
7B	North side of Buck Lake Truck Trail at northeast-bound two-track. Sec. 3.
7C	Ctr. of Virostek Rd at ctr of DNR Rd. Elev. 1540.

APPENDIX 1 (cont)

STATION	STATION LOCATION
7D	1R. BM1440, Amasa. NE side of intersection of Pk Cty Rd and Maple Ave. Between telephone pole and stop sign.
7E	BM"X" 1457, SW of intersection Pks. Farm Rd. and Snuff Country Rd. On culvert. 0.
8A	S. side of WPA Rd. at ctr. of St. Paul Cr. Not at BM"X" 139
8B	S side of WPA Rd at ctr of C. M. St. P. & P. RR. Traffic may damage meter.
8C	2M. BM"X" 1535 on culvert, W side of old 141, 40m S of Swan Lk Rd.
8D	"E" side of U. S. 141 at ctr of Old U.S. 141, E1/2, NW1/4, SE1/4, sec 26.
8E	2N. Ctr of drive to 159 S Casagranda Rd, SE side of S. Casagranda Rd. Elev. 1457 NOT 1557. (Map shows 1557 incorrectly).
8F	Ctr of drive to 264 Clark Rd at W side of Clark Rd. Elev. 1462 ft.
8G	Ctr of drive to 210 Gibson Lk Rd at N side of rd. Elev. 1496 ft.
8H	1N. Apex of curve on Gibson Lk Rd. W1/2, NE1/4, SE1/4, sec 21.
9A	Rock Crusher Rd. at fork. Ctr of sec. 4, T.42N., R.32W. 1489.
9B	E side of Rock Crusher Rd at ctr of Finn Lady Swamp Camp driveway. 1420.
9C	E side of Paint R. Rd at 2-track running along sec 17-18 bdry. N1/4.
9D	W side of Paint R Rd at 2-track to gravel pit near sec 7-18 bdry.
9E	Ctr Soderena Rd at W side CR141. NOT at BM1389.
9F	Ctr of drive to 310 Sheltrow Rd at N side of Sheltrow Rd. Elev. 1365.
9G	2I. Ctr of Ron's Rd at W side of Knivila Rd. Elev. 1398 ft.

APPENDIX 1 (cont)

STATION	STATION LOCATION
9H	2L. Ctr of driveway to 547 Sheltrow Rd. at S side of Sheltrow Rd.
9I	SW1/4, NW1/4, sec 10, T.43N., R.33W. Main 2-track at 2-track N to river.
9J	Northernmost point on Long Lk Rd, NW1/4, sec 16, T.43N., R.33W.
10A	5B. Ctr of both runways, Iron Co. Airport. Elev. 1340 ft.
10B	5E. S side of old light duty road at apex, NE1/4 sec 27, T.42N, R.32W.
10C	E side of Diversion Canal Rd at northernmore crossing of powerline.
10D	W side of Diversion Canal Rd at Section line, 480 m N of 10C.
10E	Little Bull Rd at curve, 350 m. S of JCT Little Bull Rd and diversion Canal Rd. Outside of curve.
10F	NW side of Little Bull Rd at ctr of 2-track, near BM"X" 1355.
10G	2-track at trail (1st "T"). S side of thru rd at ctr terminating rd. Elev. 1349. Very severe mosquitoes.
10H	W side Old Lk Mary Rd at NW-SE 2-track, SE, SE, NE, Sec 13.
10I	W side of Old Lk Mary Rd at ENE-WSW 2-track, NE3, sec 13.
10J	4C. W side of Old Lk Mary Rd at ctr of ski pathway, sec 12.
10K	4D. W side of Old Lk Mary Rd at 2-track to Paint R. 1348.
10L	W side of Old Lk Mary Rd at SW bd 2-track. Elev. 1358.
10M	W side of Old Lk Mary Rd at Little Mud Lk 2-track, Elev. 1362.
10N	Ctr of Old Lk Mary Rd. 600m SE of 3C=10Q. N1/2, N1/2, SE, sec 2.
10O	E side of Old Lk Mary Rd at ctr of Hope Mine Rd. N1/2, N1/2 sec 2.
10P	Ctr Hope Mine Rd at ctr of Hope Mine Rd-Old Lk Mary Rd cutoff. 1347.

APPENDIX 1 (cont)

STATION	STATION LOCATION
10Q	3C. 400 m N of corner, secs. 34, 35, 2,3. T.42-43N. R.32W.
10R	E side Lk Mary Rd at cr., 400 m S of M-69.
10S	12O. N side M-69 at ctr of Mansfield Cutoff. Elev. 1375.
10T	12Q. Near BM 1383, sec 25.
10U	12R. South side of M-69 at creek. Approx. 2 km W of Lk. Mary Rd.
10V	BM 1386. S side of M-69 near Lohrey Ln. NW1/4, sec 27.
11A	W side of Peavy Pond Rd at kettle lk. N1/2, sec 18, T.42N., R.31W.
11B	W side of Peavy Pond Rd at 2-track to Old Lk Mary Rd. Elev. 1341.
11C	4B. E side of Lk Mary Rd at ctr S. Shore Rd. Elev. 1357.
11D	E side of Lk Mary Rd at ctr of driveway to 423 Lk Mary Rd.
12A	BM "X" 1423, SE of JCT M-69 and Camp 5 Rd. On culvert.
12B	S side of M-69 at ctr line of driveway to 2939 M-69.
12C	S side of M-69 at ctr of Kania Rd. Elev. 1404 ft.
12D	Benchmark 1377, just south of M-69, 600 meters east of station 12E.
12E	South side of M-69, across from center of Old 69 Rd. Elev. 1363.
12F	S side of M-69 at ctr of Dawson Lk Rd. Elev. 1356 ft.
12G	S slide of M-69 at ctr of Parks Cr. NW1/4, NW1/4, NW1/4, sec 34.
12H	Southside of M-69 at gas pipeline, 525 meters "east" of benchmark 1366, as measured along M-69. NE1/4, sec 33. T.42N., R.31W.
12I	BM1366, S side of M-69, NW1/4, sec 33, T.43N., R.31W.
12J	S side of M-69 at topo low near cr. E1/2, E1/2, E1/2, sec 33.

APPENDIX 1 (cont)

STATION	STATION LOCATION
12K	North side of M-69 at two-track, near center of sec 32.
12L	S side of M-69 at ctr of driveway to 2250 M-69, NW1/4, sec 32.
12M	BM 1294 on M-69 bridge over Michigamme River, west end of bridge.
12N	S side of M-69, in front of house, 2125 M-69. N1/2, sec. 31.
12O	10S. North side of M-69 at center of Mansfield Cutoff.
12P	S side of M-69 at ctr of Lk Mary Rd, W1/2, NE1/4, NE1/4, sec. 36.
12Q	10T. Benchmark 1383, SW1/4, SW1/4, SW1/4, sec. 25, T.43N., R.32W.
12R	10U. S side of M-69 at cr., approx. 2 km W of Lk Mary Rd. SE1/4.
A1	2B. N side of CR424 at ctr of N bd 2-track. Elev. 1486.
A2	300 m E of A1, N side of CR 424. E of Manito Rd. NW1/4.
A3	600 m E of A1, N side of CR424, NE1/4, NW1/4, sec 14.
A4	775 m "W" of Buck Lake Road, measured along CR424. South side of CR424. 175 meters "E" of A3, as measured along CR424.
A5	450 m W of Buck Lk Rd. S side of CR424.
A6	S side of CR424 at ctr Buck Lk Rd. Elev. 1427 ft. W of Alpha.
A7	S side of 1st St. at intermittent stream, between CR424 and 5th Ave.
A8	N side of 1st St. at ctr of 6th Ave., Alpha. CR424 goes thru traffic circle.
A9	S side of 1st St. at ctr 8th Ave. (Mastadon Rd.), Alpha.
A10	N side of 1st St. at ctr. S. Main St. (CR424), Alpha. Floods during heavy rain.
A11	North side of CR424, across from center of Stager Snowmobile Trail.

APPENDIX 2

STA	ELEV (m)	GRAVITY* (mgal)(±.06)	LAT(deg)	LAT Correct.	Free Air Anomaly(mgal)
1R	460.95 ± 0.02	980,633.10	46.0936	08.44	47.23 ± .07
1A	453.6 ± 0.2	27.08	46.0440	03.86	43.43 ± .12
1B	460.9 ± 1.5	29.14	46.0509	04.60	47.12 ± .52
1C	426.1 ± 1.5	42.66	46.0633	05.71	48.80 ± .52
1D	465.1 ± 0.2	39.14	46.0725	06.54	56.48 ± .12
1E	489.8 ± 1.5	32.00	46.0854	07.71	55.80 ± .52
1F	470.6 ± 0.2	33.24	46.0941	08.48	50.30 ± .12
1G	438.6 ± 0.2	37.28	46.1087	09.80	43.18 ± .12
1H	437.4 ± 2.4	34.17	46.1160	10.46	39.03 ± .80
1I	462.7 ± 0.2	30.47	46.1282	11.56	42.04 ± .12
1N	448.7 ± 1.5	31.18	46.1931	17.42	32.93 ± .52
1O	435.3 ± 0.2	34.02	46.2050	18.49	30.19 ± .12
1P	448.4 ± 0.2	32.32	46.2119	19.11	31.92 ± .12
1Q	452.3 ± 0.2	33.86	46.2247	20.26	32.53 ± .12
1R	438.9 ± 0.2	41.51	46.2314	20.87	36.44 ± .12
1S	442.3 ± 0.2	42.16	46.2389	21.56	37.45 ± .12
1T	468.5 ± 1.5	41.09	46.2501	22.55	43.46 ± .52
1U	503.2 ± 2.4	35.39	46.2527	22.79	48.25 ± .80

*Datum: Iron River = 980,633.10

APPENDIX 2

STA	ELEV (m)	GRAVITY (mgal)*	LAT(deg)	LAT Correct.	Free Air Anomaly(mgal)
2-B	432.8 ± 0.2	980,622.90 ± 0.16	46.0148	01.33	37.29 ± 0.26
2-A	444.7 ± 0.2	24.71 ± 0.16	.0219	01.97	38.51 ± 0.26
2A	433.1 ± 0.2	33.89 ± 0.06	.0289	02.61	45.29 ± 0.12
2B	452.9 ± 0.2	34.72 ± 0.06	.0399	03.60	51.25 ± 0.12
2C	429.2 ± 1.5	42.49 ± 0.06	.0576	05.20	50.08 ± 0.52
2D	458.4 ± 0.2	40.42 ± 0.06	.0653	05.89	56.34 ± 0.12
2E	451.7 ± 0.2	38.95 ± 0.06	.0796	07.18	51.53 ± 0.12
2F	431.6 ± 0.2	41.75 ± 0.06	.0080	07.94	47.35 ± 0.12
2G	442.3 ± 0.2	40.40 ± 0.06	.0940	08.48	48.76 ± 0.12
2H	425.8 ± 0.2	38.84 ± 0.06	.1122	10.12	40.48 ± 0.12
2I	426.1 ± .02	37.57 ± 0.06	.1226	11.06	38.36 ± 0.12
2J	435.9 ± 0.2	34.49 ± 0.06	.1282	11.56	37.78 ± 0.12
2K	418.2 ± 0.2	38.50 ± 0.06	.1420	12.81	35.10 ± 0.12
2L	460.9 ± 0.2	27.12 ± 0.06	.1517	13.68	36.00 ± 0.12
2M	467.9 ± 0.2	26.84 ± 0.06	.1661	14.98	36.59 ± 0.12
2N	444.1 ± 0.2	32.24 ± 0.06	.1776	16.02	33.62 ± 0.12
2O	442.9 ± 0.2	35.58 ± 0.06	.1886	17.01	35.59 ± 0.12
2P	445.6 ± 1.5	38.88 ± 0.06	.1918	17.30	39.45 ± 0.52
2Q	460.9 ± 0.2	31.97 ± 0.06	.2072	18.69	35.85 ± 0.12
2R	460.9 ± 1.5	32.34 ± 0.06	.2174	19.61	35.30 ± 0.52
2S	460.9 ± 1.5	32.64 ± 0.06	.2234	20.15	35.06 ± 0.52
2T	465.1 ± 0.2	36.70 ± 0.06	.2324	20.96	39.62 ± 0.12
2U	469.7 ± 1.5	32.53 ± 0.06	.2435	21.96	35.87 ± 0.52

* Datum: Iron River = 980,633.10

APPENDIX 2

STA	ELEV (m)	GRAVITY (mgal)(+0.06)	LAT(deg)	LAT Correct.	Free Air Anomaly(mgal)
3A	422.1 ± 1.5	980,621.51	46.0750	6.76	25.37 ± 0.52
3B	419.4 ± 1.5	20.02	46.0741	1.68	23.12 ± 0.52
3C	410.9 ± 1.5	21.01	46.0759	6.85	21.30 ± 0.52
3D	417.0 ± 1.5	21.15	46.0793	7.15	23.02 ± 0.52
3E	415.7 ± 1.5	21.19	46.0793	7.15	22.68 ± 0.52
3G1	401.4 ± 2.4	23.24	46.0809	7.30	20.16 ± 0.80
3G2	201.17 ± 2.4	25.03	46.0827	7.46	21.89 ± 0.80
3H	403.9 ± 1.5	24.77	46.0742	6.69	23.06 ± 0.52
3I	394.7 ± 2.4	28.00	46.0788	7.11	23.05 ± 0.80
3J	397.5 ± 0.2	28.49	46.0797	7.19	24.31 ± 0.12
3K	396.8 ± 2.4	29.19	46.0767	6.92	25.09 ± 0.80
3L	410.0 ± 1.5	28.51	46.0790	7.13	28.25 ± 0.52
3M	400.63 ± 0.02	32.34	46.0760	6.85	29.47 ± 0.07
3N	416.4 ± 2.4	30.45	46.0763	6.88	32.42 ± 0.80
3O	430.1 ± 1.5	32.94	46.0797	7.19	38.82 ± 0.52
3P	456.9 ± 1.5	32.68	46.0820	7.40	46.43 ± 0.52
3Q	455.4 ± 1.5	34.63	46.0833	7.52	47.99 ± 0.52
3R	448.1 ± 1.5	36.84	46.0801	7.23	48.23 ± 0.52
3S	429.8 ± 1.5	43.10	46.0812	7.33	48.75 ± 0.52
3T	430.7 ± 0.2	42.03	46.0798	7.19	48.10 ± 0.12
3U	424.9 ± 1.5	45.71	46.0799	7.21	49.97 ± 0.52

APPENDIX 2

STA	ELEV (m)	GRAVITY (mgal)(+0.06)	LAT(deg)	LAT Correct.	Free Air Anomaly(mgal)**
4A	405.1 ± 1.5	980,613.87	46.0518	4.67	14.56 ± 0.52
4B	413.6 ± 0.2	11.22	46.0527	4.75	14.46 ± 0.12
4C	413.6 ± 1.5	09.74	46.0474	4.28	13.45 ± 0.52
4D	410.9 ± 0.2	10.85	46.0505	4.55	13.44 ± 0.12
4E	396.5 ± 1.5	14.13	46.0460	4.15	12.71 ± 0.52
4F	410.0 ± 1.5	08.84	46.0412	3.72	11.98 ± 0.52
4G	397.2 ± 1.5	14.56	46.0456	4.11	13.36 ± 0.52
4H	399.9 ± 0.2	14.66	46.0504	4.55	13.88 ± 0.12
4I	401.7 ± 0.2	15.34	46.0520	4.69	14.96 ± 0.12
4J	413.9 ± 1.5	13.25	46.0498	4.50	16.84 ± 0.52
4K	412.7 ± 2.4	15.39	46.9514	4.64	18.46 ± 0.80
4L	409.0 ± 0.2	17.37	46.0516	4.65	19.30 ± 0.12
4L1	413.3 ± 2.4	19.79	46.0517	4.66	23.02 ± 0.80
4M	413.3 ± 1.5	21.00	46.0508	4.59	26.31 ± 0.52
4N	414.8 ± 0.2	23.29	46.0500	4.51	27.15 ± 0.12
4O	409.7 ± 1.5	28.09	46.0523	4.72	30.17 ± 0.52
4P	428.5 ± 1.5	32.00	46.0430	3.88	40.71 ± 0.52
4Q	439.8 ± 0.2	25.22	46.0401	3.62	37.68 ± 0.12
4R	435.3 ± 0.2	32.37	46.0485	4.38	42.66 ± 0.12
4S	428.9 ± 0.2	34.14	46.0455	4.11	42.73 ± 0.12
4T	426.1 ± 0.2	37.07	46.0399	3.60	45.31 ± 0.12
4U	425.8 ± 1.5	38.89	46.0418	3.77	46.88 ± 0.52

APPENDIX 2

STA	ELEV (m)	GRAVITY (mgal)(+0.06)	LAT(deg)	LAT Correct.	Free Air Anomaly(mgal)
5A	406.9 ± 1.5	980,601.39	46.0086	0.78	06.53 ± 0.52
5B	408.4 ± 0.2	03.03	46.0085	0.77	08.65 ± 0.12
5C	408.1 ± 1.5	03.80	46.0114	1.03	09.07 ± 0.52
5D	407.5 ± 1.5	05.16	46.0109	0.98	10.28 ± 0.52
5E	407.8 ± 1.5	06.72	46.0142	1.28	11.64 ± 0.52
5F	399.0 ± 1.5	07.51	46.0130	1.18	09.81 ± 0.52
5G	403.3 ± 2.4	07.38	46.0138	1.24	10.93 ± 0.80
5H	404.8 ± 1.5	06.80	46.0095	0.86	11.20 ± 0.52
5I	403.6 ± 1.5	08.38	46.0097	0.88	12.39 ± 0.52
5J	403.43 ± 0.02	10.50	46.0088	0.80	14.55 ± 0.07
5K	409.0 ± 1.5	09.97	46.0061	0.55	16.00 ± 0.52
5L	412.4 ± 1.5	12.72	46.0061	0.55	19.78 ± 0.52
5M	413.0 ± 2.4	15.59	46.0079	0.71	22.68 ± 0.80
5N	423.7 ± 1.5	16.72	46.0131	1.18	26.63 ± 0.52
5O	424.6 ± 1.5	18.02	46.0124	1.12	28.28 ± 0.52
5P	423.4 ± 1.5	20.18	46.0147	1.32	29.86 ± 0.52
5Q	420.3 ± 1.5	22.11	46.0122	1.10	31.07 ± 0.52
5R	456.6 ± 0.2	17.38	46.0116	1.04	37.59 ± 0.12
5S	477.6 ± 2.4	14.34	46.0117	1.06	41.02 ± 0.80
5T	458.7 ± 1.5	19.28	46.0108	0.98	40.21 ± 0.52
5U	472.1 ± 0.2	22.01	46.0147	1.32	46.73 ± 0.12

APPENDIX 2

STA	ELEV (m)	GRAVITY (mgal)	LAT(deg)	LAT Correct.	Free Air Anomaly(mgal)
6D	495.6 ± 1.5	980,608.40	46.2784	25.11	16.06 ± 0.62
6F	474.9 ± 1.5	17.76 ± 0.16	730	24.62	20.04 ± 0.62
6H	479.5 ± 1.5	31.87 ± 0.16	788	25.15	35.03 ± 0.62
6I	479.8 ± 1.5	32.35 ± 0.16	770	24.98	35.76 ± 0.62
6J	459.9 ± 2.4	37.96 ± 0.16	824	25.47	34.78 ± 0.90
6K	448.4 ± 2.4	41.88 ± 0.16	590	23.36	37.23 ± 0.90
6L	491.3 ± 1.5	37.20 ± 0.16	653	23.93	45.25 ± 0.62
6M	464.2 ± 1.5	39.75 ± 0.16	824	25.47	37.89 ± 0.62
7A	465.1 ± 0.2	36.69 ± 0.02	328	21.00	39.58 ± 0.12
7B	467.9 ± 1.5	37.91 ± 0.16	333	21.04	41.60 ± 0.62
7C	469.4 ± 0.2	39.29 ± 0.16	322	20.94	43.55 ± 0.22
7D	438.9 ± 0.2	41.51 ± 0.02	318	20.91	36.40 ± 0.12
7E	444.1 ± 0.2	36.88 ± 0.16	322	20.94	33.34 ± 0.22

APPENDIX 2

STA	ELEV (m)	GRAVITY (mgal)	LAT(deg)	LAT Correct.	Free Air Anomaly(mgal)
8A	424.0 ± 1.5	980,634.76 ± 0.16	46.1838	16.58	29.37 ± 0.62
8B	429.2 ± 1.5	34.51 ± 0.16	825	16.46	30.84 ± 0.62
8C	467.9 ± 0.2	26.84 ± 0.02	663	15.00	36.57 ± 0.12
8D	462.1 ± 1.5	32.30 ± 0.16	800	16.24	39.41 ± 0.62
8E	444.1 ± 0.2	32.24 ± 0.02	778	16.04	33.59 ± 0.12
8F	445.6 ± 0.2	31.43 ± 0.16	832	16.52	32.78 ± 0.22
8G	456.0 ± 0.2	30.90 ± 0.16	948	17.57	34.39 ± 0.22
8H	448.7 ± 1.5	31.54 ± 0.02	937	17.47	32.88 ± 0.48
9A	453.8 ± 0.2	29.18 ± 0.16	513	13.646	35.94 ± 0.22
9B	432.8 ± 0.2	31.10	401	12.639	32.37 ± 0.22
9C	417.9 ± 1.5	35.17	276	11.507	32.97 ± 0.62
9D	417.3 ± 0.2	36.23	302	11.743	33.60 ± 0.22
9E	425.8 ± 1.5	34.48	302	11.743	34.49 ± 0.62
9F	416.1 ± 0.2	38.07	407	12.687	34.13 ± 0.22
9G	426.1 ± 0.2	37.57 ± 0.02	230	11.099	38.32 ± 0.12
9H	460.9 ± 0.2	27.12	520	13.709	35.98 ± 0.12
9I	411.8 ± 2.4	39.93 + 0.16	408	12.702	32.66 ± 0.90
9J	436.5 ± 1.5	38.06	255	11.319	41.78 ± 0.62

APPENDIX 2

STA	ELEV (m)	GRAVITY (mgal)	LAT(deg)	LAT Correct.	Free Air Anomaly(mgal)
10A	408.4 ± 0.02	980,603.03± 0.02	46.0083	0.75	08.67 ± 0.08
10B	407.8 ± 1.5	06.72	142	1.28	11.64 ± 0.48
10C	399.3 ± 1.5	04.69± 0.16	207	1.86	06.40 ± 0.62
10D	408.4 ± 1.5	05.73±	247	2.22	09.90 ± 0.62
10E	410.3 ± 1.5	06.00±	271	2.44	10.51 ± 0.62
10F	413.0 ± 1.5	06.60±	325	2.93	11.47 ± 0.62
10G	411.2 ± 0.2	08.36±	354	3.20	12.50 ± 0.22
10H	412.7 ± 1.5	08.61±	389	3.51	12.81 ± 0.62
10I	412.7 ± 1.5	09.25±	438	3.95	13.57 ± 0.62
10J	413.6 ± 1.5	09.74± 0.02	476	4.29	13.44 ± 0.48
10K	410.9 ± 0.2	10.85±	505	4.56	13.44 ± 0.08
10L	413.9 ± 0.2	11.75± 0.16	554	5.00	13.48 ± 0.22
10M	415.1 ± 0.2	13.67±	601	5.42	16.71 ± 0.22
10N	414.8 ± 1.5	15.88±	655	5.90	18.35 ± 0.62
10O	416.7 ± 2.4	18.22±	698	6.30	20.86 ± 0.90
10P	410.6 ± 0.2	20.81±	717	6.47	21.39 ± 0.22
10Q	410.9 ± 1.5	21.01± 0.02	764	6.89	21.26 ± 0.48
10R	411.5 ± 1.5	23.01± 0.16	813	7.33	23.02 ± 0.62
10S	419.1 ± 0.2	22.54±	847	7.64	24.58 ± 0.22
10T	421.8 ± 1.5	23.92±	873	7.88	26.58 ± 0.62
10U	420.6 ± 1.5	25.89±	911	8.22	27.82 ± 0.62
10V	422.5 ± 0.2	23.28±	976	8.80	25.20 ± 0.22

APPENDIX 2

STA	ELEV (m)	GRAVITY (mgal)	LAT(deg)	LAT Correct.	Free Air Anomaly(mgal)
11A	407.2 ± 1.5	980,611.26± 0.16	46.0418	3.77	13.50 ± 0.62
11B	408.7 ± 0.2	11.03	467	4.21	13.30 ± 0.22
11C	413.6 ± 0.2	11.22 ± 0.02	528	4.76	14.45 ± 0.08
11D	404.8 ± 1.5	16.64 ± 0.16	594	5.36	16.55 ± 0.62
12A	433.7 ± 0.2	09.29 ± 0.16	873	7.88	15.61 ± 0.22
12B	432.5 ± 1.5	09.16	873	.88	15.11 ± 0.62
12C	427.9 ± 0.2	09.59	873	.88	14.12 ± 0.22
12D	419.7 ± 0.2	10.27	873	.88	12.26 ± 0.22
12E	415.4 ± 0.2	11.02	873	.88	11.70 ± 0.22
12F	413.3 ± 0.2	14.72	873	.88	14.73 ± 0.22
12G	405.4	16.69	872	.88	14.28 ± 0.90
12H	424.6 ± 1.5	14.41	847	.64	18.15 ± 0.62
12I	416.4 ± 0.2	13.68	825	.44	15.08 ± 0.22
12J	415.1 ± 1.5	16.97	811	.31	18.12 ± 0.62
12K	414.8 ± 2.4	19.75	819	.39	20.72 ± 0.90
12L	401.4 ± 1.5	23.20	828	.47	19.95 ± 0.62
12M	394.4 ± 0.2	25.74	839	.56	20.24 ± 0.22
12N	404.5 ± 1.5	24.56	847	.64	22.09 ± 0.62
12O	419.1 ± 0.2	22.54	847	.64	24.58 ± 0.22
12P	420.0 ± 1.5	22.36	847	.64	24.68 ± 0.62
12Q	421.8 ± 1.5	23.92	873	.88	26.58 ± 0.62
12R	420.6 ± 1.5	25.89	911	8.22	27.82 ± 0.62

APPENDIX 2

STA	ELEV (m)	GRAVITY (mgal)	LAT(deg)	LAT Correct.	Free Air Anomaly(mgal)
A1	452.9 ± 0.2	980,634.73± 0.02	46.0399	3.60	51.25 ± 0.08
A2	448.7 ± 1.5	35.79± 0.16	399	0	51.00 ± 0.62
A3	454.2 ± 1.5	34.73	408	8	51.55 ± 0.62
A4	458.7 ± 1.5	34.02	424	.82	52.11 ± 0.62
A5	444.4 ± 1.5	36.18	425	8	49.84 ± 0.62
A6	434.9 ± 0.2	38.19	425	4	48.93 ± 0.62
A7	431.6 ± 1.5	38.26	436	.93	47.86 ± 0.62
A8	432.8 ± 1.5	37.97	436	3	47.96 ± 0.62
A9	431.3 ± 1.5	38.54	436	3	48.05 ± 0.62
A10	426.7 ± 1.5	38.68	438	5	46.76 ± 0.62
A11	426.7 + 1.5	37.71	438	5	45.80 ± 0.62
A12	426.4 ± 2.4	35.29	439	6	43.27 ± 0.90
A13	428.9 ± 0.2	34.14 ± 0.02	457	4.12	42.72 ± 0.08
A14	430.1 ± 1.5	33.80 ± 0.16	472	.26	42.61 ± 0.62
A15	435.3 ± 0.2	32.37 ± 0.02	486	.38	42.65 ± 0.08
A16	444.4 ± 1.5	29.37 ± 0.16	505	.56	42.30 ± 0.62
A17	436.2 ± 1.5	31.53	510	.60	41.88 ± 0.62

APPENDIX 3

STATION	TILL THICKNESS	Simple Bouguer Grav.Anom.(mgal)*
IR	42.8	- 6.08 ± 0.06
1A	42.8	-09.05 ± 0.27
1B	45.8	-06.13 ± 0.82
1C	42.8	-00.81 ± 0.79
1D	42.8	-02.62 ± 0.30
1E	42.8	-01.00 ± 0.83
1F	58.0	-03.64 ± 0.32
1G	36.5	-07.74 ± 0.26
1H	55.0	-11.52 ± 1.08
1I	58.0	-10.20 ± 0.24
1N	30.5	-19.41 ± 0.80
1O	24.5	-20.76 ± 0.26
1P	24.5	-20.59 ± 0.26
1Q	24.5	-19.45 ± 0.26
1R	15.2	-15.26 ± 0.24
1S	12.2	-14.77 ± 0.24
1T	09.0	-11.98 ± 0.76
1U	18.2	-11.00 ± 1.11

*Datum 395.3 meters above mean sea level

APPENDIX 3 (Continued)

STATION	TILL THICKNESS	Simple Bouguer Grav.Anom.(mgal)*
2-B	18.2	-13.58 ± 0.39
2-A	21.2	-13.68 ± 0.40
2A	27.5	-05.30 ± 0.27
2B	30.5	-01.59 ± 0.30
2C	06.0	-00.79 ± 0.63
2D	36.5	+03.07 ± 0.23
2E	48.8	-00.52 ± 0.26
2F	70.0	-02.72 ± 0.26
2G	27.5	-02.92 ± 0.25
2H	42.8	-09.10 ± 0.18
2I	51.8	-11.25 ± 0.18
2J	55.0	-12.64 ± 0.20
2K	45.8	-13.84 ± 0.16
2L	55.0	-16.92 ± 0.32
2M	48.8	-17.38 ± 0.31
2N	30.5	-18.17 ± 0.27
2O	27.5	-16.16 ± 0.33
2P	21.5	-12.84 ± 0.76
2Q	24.5	-18.15 ± 0.27
2R	24.5	-18.70 ± 0.79
2S	24.5	-18.94 ± 0.79
2T	15.2	-15.21 ± 0.25
2U	21.2	-19.29 ± 0.76

APPENDIX 3 (Continued)

STATION	TILL THICKNESS	Simple Bouguer Grav.Anom.(mgal)*
3A	30.5	-23.90 ± 0.78
3B	42.8	-25.93 ± 0.78
3C	42.8	-27.02 ± 0.76
3D	42.8	-25.82 ± 0.77
3E	42.8	-26.05 ± 0.77
3G1	39.5	-27.37 ± 1.12
3G2	39.5	-25.76 ± 1.12
3H	39.5	-24.68 ± 0.74
3I	39.5	-23.93 ± 1.11
3J	36.5	-22.89 ± 0.12
3K	36.5	-22.07 ± 1.11
3L	36.5	-20.01 ± 0.76
3M	36.5	-18.00 ± 0.06
3N	36.5	-16.38 ± 1.66
3O	42.8	-11.12 ± 0.79
3P	39.5	-06.36 ± 0.78
3Q	36.5	-04.93 ± 0.78
3R	51.8	-03.28 ± 0.77
3S	48.8	-01.16 ± 0.76
3T	15.2	-02.63 ± 0.22
3U	09.0	-00.28 ± 0.76

APPENDIX 3 (Continued)

STATION	TILL THICKNESS	Simple Bouguer Grav.Anom.(mgal)*
4A	27.5	-33.29 ± 0.75
4B	27.5	-34.10 ± 0.19
4C	30.5	-35.11 ± 0.77
4D	30.5	-34.89 ± 0.14
4E	33.5	-34.42 ± 0.73
4F	36.5	-36.27 ± 0.76
4G	39.5	-33.82 ± 0.73
4H	39.5	-33.53 ± 0.12
4I	39.5	-32.60 ± 0.12
4J	39.5	-32.11 ± 0.77
4K	39.5	-30.02 ± 1.15
4L	39.5	-28.88 ± 0.14
4L1	36.5	-22.51 ± 1.15
4M	36.5	-22.22 ± 0.76
4N	36.5	-21.51 ± 0.15
4O	36.5	-18.09 ± 0.76
4P	33.5	-09.12 ± 0.79
4Q	27.5	-13.70 ± 0.27
4R	33.5	-07.97 ± 0.27
4S	30.5	-07.25 ± 0.26
4T	30.5	-04.34 ± 0.25
4U	21.2	-03.06 ± 0.77

APPENDIX 3 (Continued)

STATION	TILL THICKNESS	Simple Bouguer Grav.Anom.(mgal)*
5A	30.5	-41.47 ± 0.75
5B	33.5	-39.47 ± 0.14
5C	33.5	-39.03 ± 0.75
5D	30.5	-37.76 ± 0.75
5E	30.5	-36.43 ± 0.75
5F	27.5	-37.53 ± 0.74
5G	27.5	36.76 ± 1.20
5H	24.5	-36.61 ± 0.75
5I	24.5	-35.32 ± 0.74
5J	21.2	-33.15 ± 0.07
5K	18.2	-32.17 ± 0.76
5L	15.2	-28.77 ± 0.76
5M	15.2	-25.94 ± 1.08
5N	18.2	-23.16 ± 0.77
5O	15.2	-21.72 ± 0.76
5P	12.2	-20.11 ± 0.76
5Q	12.2	-18.54 ± 0.75
5R	15.2	-16.22 ± 0.22
5S	15.2	-15.29 ± 1.07
5T	15.2	-13.86 ± 0.68
5U	03.0	-09.36 ± 0.17

APPENDIX 3 (Continued)

STATION	TILL THICKNESS	Simple Bouguer Grav.Anom.(mgal)*
6D	36.5	-41.64 ± 0.96
6F	36.5	-35.20 ± 0.95
6H	30.5	-20.96 ± 0.94
6I	27.5	-20.37 ± 0.94
6J	25.5	-19.11 ± 0.94
6K	12.2	-15.71 ± 1.24
6L	12.2	-12.80 ± 0.91
6M	18.2	-16.72 ± 0.92
7A	15.2	-15.25 ± 0.25
7B	12.2	-13.66 ± 0.90
7C	09.0	-12.00 ± 0.38
7D	15.2	-15.31 ± 0.24
7E	12.2	-19.10 ± 0.38
8A	12.2	-20.67 ± 0.90
8B	12.2	-19.82 ± 0.90
8C	48.8	-17.40 ± 0.31
8D	30.5	-14.92 ± 0.94
8E	30.5	-18.20 ± 0.27
8F	30.5	-19.19 ± 0.41
8G	30.5	-18.82 ± 0.42
8H	30.5	-19.46 ± 0.80

APPENDIX 3 (Continued)

STATION	TILL THICKNESS	Simple Bouguer Grav.Anom.(mgal)*
9A	15.2	-17.55 ± 0.39
9B	09.0	-18.82 ± 0.37
9C	30.5	-15.94 ± 0.92
9D	30.5	-15.26 ± 0.30
9E	33.5	-15.09 ± 0.93
9F	42.8	-14.63 ± 0.29
9G	39.5	-11.29 ± 0.18
9H	55.0	-16.95 ± 0.32
9I	36.5	-14.65 ± 2.12
9J	21.5	-09.42 ± 0.92

APPENDIX 3 (Continued)

STATION	TILL THICKNESS	Simple Bouguer Grav.Anom.(mgal)*
10A	33.5	-39.45 ± 0.14
10B	30.5	-36.43 ± 0.75
10C	27.5	-40.96 ± 0.88
10D	27.5	-38.23 ± 0.90
10E	27.5	-37.76 ± 0.90
10F	27.5	-37.04 ± 0.90
10G	30.5	-35.86 ± 0.28
10H	27.5	-35.68 ± 0.90
10I	30.5	-35.06 ± 0.91
10J	30.5	-35.12 ± 0.77
10K	30.5	-34.89 ± 0.14
10L	30.5	-34.10 ± 0.29
10M	30.5	-31.97 ± 0.29
10N	36.5	-30.31 ± 0.91
10O	36.5	-27.96 ± 1.30
10P	39.5	-26.91 ± 0.28
10Q	42.8	-27.07 ± 0.76
10R	30.5	-25.37 ± 0.90
10S	24.5	-24.44 ± 0.30
10T	21.2	-22.89 ± 0.92
10U	24.5	-21.39 ± 0.92
10V	24.5	-24.23 ± 0.31

APPENDIX 3 (Continued)

STATION	TILL THICKNESS	Simple Bouguer Grav.Anom.(mgal)*
11A	27.5	-34.52 ± 0.89
11B	27.5	-34.85 ± 0.28
11C	27.5	-34.11 ± 0.15
11D	27.5	-31.27 ± 0.89
12A	33.5	-34.84 ± 0.42
12B	33.5	-35.20 ± 0.94
12C	27.5	-35.85 ± 0.40
12D	24.5	-36.84 ± 0.38
12E	24.5	-37.01 ± 0.29
12F	21.2	-33.80 ± 0.29
12G	18.2	-33.59 ± 1.27
12H	15.2	-31.86 ± 0.90
12I	15.2	-33.94 ± 0.40
12J	12.2	-30.87 ± 0.89
12K	12.2	-28.23 ± 1.22
12L	12.2	-27.58 ± 0.88
12M	30.5	-26.71 ± 0.25
12N	30.5	-25.70 ± 0.89
12O	24.5	-24.45 ± 0.30
12P	24.5	-24.46 ± 0.92
12Q	21.2	-22.89 ± 0.92
12R	24.5	-21.39 ± 0.92

APPENDIX 3 (Continued)

STATION	TILL THICKNESS	Simple Bouguer Grav.Anom.(mgal)*
A1	30.5	-01.59 ± 0.30
A2	27.5	-01.44 ± 0.96
A3	24.5	-01.65 ± 0.95
A4	18.2	-01.85 ± 0.94
A5	18.2	-02.42 ± 0.93
A6	18.2	-02.20 ± 0.40
A7	18.2	-02.87 ± 0.91
A8	18.2	-02.92 ± 0.90
A9	09.0	-02.96 ± 0.91
A10	18.2	-03.38 ± 0.91
A11	18.2	-04.36 ± 0.92
A12	21.2	-06.74 ± 1.25
A13	30.5	-07.26 ± 0.26
A14	30.5	-07.52 ± 0.93
A15	33.5	-07.98 ± 0.27
A16	36.5	-09.31 ± 0.93
A17	36.5	-08.76 ± 0.93

```
APPENDIX 4
LIST,10000-15100,NS.
      PROGRAM TDG(INPUT,OUTPUT,TAPE 10,TAPE20,TAPE40,TAPE50)
C      PURPOSE
C      TO DETERMINE THE ANOMALY AT A GRAVITY STATION DUE
C      TO A GIVEN SUBSURFACE DISTRIBUTION OF ANOMALOUS
C      MASS.  GRAVITY STATIONS HAVE
C      X-COORDINATES ONLY.  ANOMALOUS MASS IS DISTRIBUTED IN
C      POLYGONS OF GIVEN DENSITY.  POLYGON APICES, DENSITY,
C      NUMBER OF STATIONS,MEAN OF OBSERVED GRAVITY ANOMALIES,
C      AND NUMBER OF POLYGONS ARE READ FROM TAPE20.
C      TAPE50 IS AN OUTPUT VERSION OF TAPE20.
C      TAPE50 WILL SHOW ANY ERRORS IN VARIABLES K, L, OR M.
C      USE TAPE50 TO CHECK INPUT WHEN K, L, OR M HAS BEEN CHANGED.
C
C    DESCRIPTION OF PARAMETERS
C      PI = 3.141592654
C      L = NUMBER OF GRAVITY STATIONS, 1.LE.L.LT.100, READ FROM TAPE20.
C      STA(K) = X-COORDINATE OF GRAVITY STATION NUMBER K,
C             READ FROM TAPE 10 IN SUBROUTINE LINE,
C             F5.1, CAN BE NEGATIVE.
C      K = COUNTER FOR LOOPS INVOLVING STATIONS,1.LE.K.LE.L.
C      M = NUMBER OF POLYGONS IN MODEL, 1.LE.M.LT.100, READ FROM TAPE20.
C      DENSITY(J) = ANOMALOUS DENSITY OF POLYGON J, F5.2,
C                   READ FROM TAPE20.
C      G(J) = ANOMALOUS GRAVITY FOR POLYGON NUMBER J.
C      N(J) = NUMBER OF SIDES ON POLYGON NUMBER J, I2, READ FROM TAPE20.
C      J = COUNTER FOR LOOPS INVOLVING POLYGONS, 1.LE.J.LE.M.
C      I = COUNTER FOR LOOPS INVOLVING SIDES OF POLYGON,
C          1.LE.I.LE.N(J).
C      XRELERT(J,I) = X-COORDINATE OF APEX NUMBER I ON
C                     POLYGON NUMBER J, RELATIVE TO THE
C                     EARTH.  SET TO NEGATIVE INFINITY
C                     IF USER SETS IT TO 0.  USER IS NOT
C                     NOTIFIED.  F5.1.  READ FROM TAPE20.
C      Z(J,I) = Z-COORDINATE OF APEX NUMBER I OF POLYGON
C               NUMBER J, F5.2, READ FROM TAPE20.
C      STAGRV = ANOMALOUS GRAVITY AT STTTATION K
C             = SUM OF ALL TTHE G(J) FOR STATION K.
C      IPLUS1 = I + 1 IF I.LT.N(J)
C             = 1     IF I.EQ.N(J).
C      X1 = X(I) RELATIVE TO GRAVITTY STTATION NUMBER K.
C      X2 = X(I + 1) RELATIVE TO GRAVITY STTATTION NUMBER K.
C      THETA1 = ANGLE FROM HORIZONTAL TO APEX(I),
C               MEASURED CLOCKWISE, WITH ORIGIN AT STA(K).
C      THETA2 = ANGLE FROM HORIZONTAL TO APEX(I + 1),
C               MEASURED CLOCKWISE, WITH ORIGIN ATT STA(K).
C      PHI = SLOPE OF TTHE SIDE OF THE POLYGON  BETWEEN
C            APICES I AND I + 1, MEASURED CLOCKWISE FROM
C            HORIZONTAL.
C      A = DISTANCE FROM STA(K) TO ORIGIN OF PHI, CAN BE
C          NEGATIVE.
C      SUMGRV = SUM OF STAGRV'S.
C      GRV(K) = CALCULATED GRAVITY AT STATION NUMBER K.

READY 10.01.18
```

```
LIST,15200-20500,NS.
C       AMNGRV = MEAN OF ALL CALCULATED GRAVITIES.
C       SMBGGR = SIMPLE BOUGUER GRAVITY
C              = GRV(K) - AMNGRV - MEAN OF ALL L OBSERVED GRAVITIES.
C   OBGA(K) = THE OBSERVED BOUGUER GRAVITY ANOMALY AT STATION NUMBER K.
C   OBMNGR = THE MEAN OF THE OBSERVED GRAVITY ANOMALIES ON TAPE40.
C   SBGR(K) = THE SIMPLE BOUGUER GRAVITY ERROR AT STATION NUMBER K.
C           = CALCULATED ANOMALOUS GRAVITY - OBSERVED ANOMALOUS GRAVITY.
C           = SBGGR - OBGA(K).
C
C     DECK STRUCTURE
C       TAPE10
C         STA(1), F5.1.
C         STA(2), F5.1.
C               .
C               .
C               .
C         STA(K), F5.1.
C               .
C               .
C               .
C         STA(L), F5.1.
C       TAPE20
C         OBMNGR, F6.2
C         L, I2.
C         M, I2.
C         DENSITY(1), F5.2.
C         N(1), I2.
C         X(1, 1)(F5.1), Z(1, 1)(F5.1).
C         X(1, 2)(F5.1), Z(1, 2)(F5.1).
C                       .
C                       .
C                       .
C         X(1, I)(F5.1), Z(1, I)(F5.1).
C                       .
C                       .
C                       .
C         X(1, N(1))(F5.1), Z(1, N(1))(F5.1).
C         DENSITY(2), F5.2.
C         N(2), I2.
C         X(2, 1)(F5.1), Z(2, 1)(F5.1).
C         X(2, 2)(F5.1), Z(2, 2)(F5.1).
C                       .
C                       .
C                       .
C         X(2, I)(F5.1), Z(2, I)(F5.1).
C                       .
C                       .
C                       .
C         X(2, N(2))(F5.1), Z(2, N(2))(F5.1).
C
C                         .
C
C
C                         .

READY 10.02.40
```

```
LIST,20800-25500,N3.
C
C
C                          .
C
C        DENSITY(J), F5.2.
C        N(J), I2.
C        X(J, 1)(F5.1), Z(J, 1)(F5.1).
C        X(J, 2)(F5.1), Z(J, 2)(F5.1).
C                      .
C                      .
C                      .
C        X(J, I)(F5.1), Z(J,I)(F5.1).
C                      .
C                      .
C                      .
C        X(J, N(J))(F5.1), Z(J, N(J))(F5.1).
C
C                          .
C
C
C                          .
C
C
C                          .
C
C        DENSITY(M), F5.2.
C        N(M), I2.
C        X(M, 1)(F5.1), Z(M, 1)(F5.1).
C        X(M, 2)(F5.1), Z(M, 2)(F5.1).
C                      .
C                      .
C                      .
C        X(M, I)(F5.1), Z(M, I)(F5.1).
C                      .
C                      .
C                      .
C        X(M, N(M))(F5.1), Z(M, N(M))(F5.1).
C
C      TAPE40
C        OBGA(1)
C        OBGA(2)
C           .
C           .
C           .
C        OBGA(K)
C           .
C           .
C           .
C        OBGA(L)
C
C    SUBPROGRAMS
C      SUBROUTINES
C        SUBROUTINE LINE
C

READY 10.03.53
```

```
LIST,26000-31300,NS.
C     PROGRAMMER
C       DAVE PADDOCK
C
C     DATE WRITTEN
C       81 W
C        VERSION 133  82MAY


      DIMENSION STA(100),DENSITY(100),N(100),SBGR(100),
     +XRELERT(100,100),Z(100,100),GRV(100),OBGA(100)
      INTEGER ANS
      PI=3.141592654
      SUMGRV=0.
      RMS=0.

C INTERACTIVE INPUT OF DESIRED OUTPUT AND DEBUG OPTION.

      WRITE 2
2     FORMAT(* VERSION?*)
      READ 4,IO
4     FORMAT(I1)
5     CONTINUE
      WRITE 6
6     FORMAT(* DEBUG ALOG?  Y OR N.  *)
      READ 8,IDEBUG
8     FORMAT(A1)
      IF(IDEBUG.NE.1HY.AND.IDEBUG.NE.1HN)GOTO 5

C INPUT FROM TAPE20.

      READ(20,9)OBMNGR
9     FORMAT(F8.2)
      READ(20,10)L
10    FORMAT(I2)

      WRITE 20
20    FORMAT(* L OK*)
      WRITE(50,10)L
      CALL LINE(STA, L,OBGA)
      READ(20,30)M
30    FORMAT(I2)
      WRITE 40
40    FORMAT(* M OK*)
      WRITE(50,30)M
C     DO WHILE.
      DO 150J=1,100
      IF(J.GT.M)GOTO 160
      READ(20,50)DENSITY(J)
50    FORMAT(F5.2)
      WRITE 60,J
60    FORMAT(* P*,I2,* OK*)
      WRITE(50,50)DENSITY(J)
      READ(20,70)N(J)
70    FORMAT(I2)

READY 10.04.58
```

```
LIST,31400-36700,NS.
      WRITE 60,J
60    FORMAT(* N*,I2,* OK*)
      WRITE(50,70)N(J)
C      DO WHILE.
      DO 130I=1,100
      IF(I.GT.N(J))GOTO 140
      READ(20,100)XRELERT(J,I),Z(J,I)
100    FORMAT(2F5.1)
      WRITE(50,100)XRELERT(J,I),Z(J,I)
130   CONTINUE
140   CONTINUE
C      END DO WHILE.
      WRITE 145,J
145   FORMAT(* XZ*,I2,* OK*)
150   CONTINUE
160   CONTINUE
C     END DO WHILE.

C CALCULATE GRAVITY.
C      DO WHILE.
      DO 300K=1,100
      IF(K.GT.L)GOTO 310

C INITIALIZE STATION GRAVITY.
      STAGRV=0.
C      DO WHILE.
      DO 270J=1, 100
      IF(J.GT.M)GOTO 280

C INITIALIZE POLYGON GRAVITY.

      G=0.
C      DO WHILE.
      DO 250I=1,100
      IF(I.GT.N(J))GOTO 260
      IPLUS1=I+1
C      IF THEN.
      IF(IPLUS1.LE.N(J))GOTO 165
      IPLUS1=1
165   CONTINUE
C      END IF THEN.
      X1=XRELERT(J,I)-STA(K)
      X2=XRELERT(J,IPLUS1)-STA(K)
C      IF THEN.
      IF(X1)192,188
188   CONTINUE
C      IF THEN.
      IF(X1.EQ.Z(J,I))GOTO 240
      THETA1=PI/2
C      IF THEN.
      IF(X2)169,240
169   CONTINUE
      THETA2=ATAN2(Z(J,IPLUS1),X2)
C      IF THEN.

READY 10.06.01
```

```
LIST,36800-42100,NS.
      IF(Z(J,I)-Z(J,IPLUS1))190,209
190   CONTINUE
      A=X2+Z(J,IPLUS1)*((X2-X1)/(Z(J,I)-Z(J,IPLUS1)))
      PHI=ATAN2(Z(J,IPLUS1)-Z(J,I),X2-X1)
      G=G-A*SIN(PHI)*COS(PHI)*(THETA2-PI/2+TAN(PHI)*
     +ALOG(COS(THETA2)*(TAN(THETA2)-TAN(PHI))))
      GOTO 240
C END IF THEN.
192   CONTINUE
C      END IF THEN.
C      IF THEN.
      IF(X2)200,195
195   CONTINUE
C      IF THEN.
      IF(X2.EQ.Z(J,IPLUS1))GOTO 240
      THETA1=ATAN2(Z(J,I),X1)
      THETA2=PI/2.
C      IF THEN.
      IF(Z(J,I)-Z(J,IPLUS1))198,209
198   CONTINUE
      A=X2+Z(J,IPLUS1)*((X2-X1)/(Z(J,I)-Z(J,IPLUS1)))
      PHI=ATAN2(Z(J,IPLUS1)-Z(J,I),X2-X1)
      G=G+A*SIN(PHI)*COS(PHI)*(THETA1-PI/2+TAN(PHI)*
     +ALOG(COS(THETA1)*(TAN(THETA1)-TAN(PHI))))
      GOTO 240
C      END IF THEN.
200   CONTINUE
      THETA1=ATAN2(Z(J,I), X1)
205   CONTINUE
      THETA2=ATAN2(Z(J,IPLUS1), X2)
208   CONTINUE
C      IF THEN.
      IF(THETA1.EQ.THETA2)GOTO 240
C      IF THEN.
      IF(Z(J,I).NE.Z(J,IPLUS1))GOTO 210
209   CONTINUE
      G=G+Z(J,I)*(THETA2-THETA1)
      GOTO 240
C      END IF THEN.
210   CONTINUE
C      END IF THEN.
C      IF THEN.
      IF(X1.NE.X2)GOTO 230
C      IF THEN ELSE.
      IF(XRELERT(J,I).NE.0.)GOTO 220
      G=G+Z(J,I)*(PI-THETA1)+Z(J,IPLUS1)*(THETA2-PI)
      GOTO 240
220   CONTINUE
      G=G+X1*ALOG(COS(THETA1)/COS(THETA2))
      GOTO 240
C END IF THEN ELSE.
230   CONTINUE
C      END IF THEN.
      PHI = ATAN2(Z(J, IPLUS1) - Z(J, I), X2 -X1)

READY 10.07.29
```

```
LIST,42200-47500,NS.
      A =X2 + Z(J, IPLUS1) * ((X2 - X1) / (Z(J, I) - Z(J, IPLUS1)))
C IF THEN.
      IF(IDEBUG.NE.1HY)GOTO 236
C IF THEN.
      IF(COS(THETA1)*(TAN(THETA1)-TAN(PHI))/
     +(COS(THETA2)*(TAN(THETA2)-TAN(PHI))).LE.0.)GOTO 232
C IF THEN.
      IF(COS(THETA2)*(TAN(THETA2)-TAN(PHI)).NE.0.)GOTO 236
232   CONTINUE
      WRITE 234,XRELERT(J,I),Z(J,I),XRELERT(J,IPLUS1),Z(J,IPLUS1),STA(K)
234   FORMAT(* X=*,F5.1,*Z=*,F5.1,*X=*,F5.1,*Z=*,F5.1,*S=*,F6.2)
236   CONTINUE
C END IF THEN.
C END IF THEN.
C END IF THEN.
      G=G+A*SIN(PHI)*COS(PHI)*(THETA1-THETA2+
     +TAN(PHI) * ALOG(COS(THETA1) * (TAN(THETA1) - TAN(PHI))/
     +(COS(THETA2) * (TAN(THETA2) -TAN(PHI)))))
240   CONTINUE
C      END IF THEN.
C      END IF THEN.
C      END IF THEN.
C      END IF THEN.
C      END IF THEN.
250   CONTINUE
260   CONTINUE
C      END DO WHILE.

C CHANGE UNITS TO MILLIGALS.

      G=2.*6.67*DENSITY(J)*G
      STAGRV=STAGRV+G
270   CONTINUE
280   CONTINUE
C      END DO WHILE.
C IF THEN.
      IF(IO.NE.1)GOTO 295
      WRITE 290,K,STAGRV
290   FORMAT(* STAGRV(*,I2,*) = *,F4.0)
295   CONTINUE
C END IF THEN.
      SUMGRV=SUMGRV+STAGRV
      GRV(K)=STAGRV
300   CONTINUE
310   CONTINUE
C      END DO WHILE.

C MANIPULATE GRAVITY FOR DESIRED OUTPUT.

      AMNGRV=SUMGRV/L
      WRITE 311,AMNGRV
311   FORMAT(F5.0)
C    DO WHILE.
      DO 315K=1,L

READY 10.08.45
```

```
LIST,47600-52900,NS.
      SMBGGR=GRV(K)-AMNGRV+OBMNGR
      SBGR(K)=SMBGGR-OBGA(K)
      RMS=RMS+SBGR(K)*SBGR(K)
C IF THEN.
      IF(IO.NE.2)GOTO 314
      WRITE 312,K,SMBGGR
312    FORMAT(* SMBGGR(*,I2,*) = *,F5.1)
314   CONTINUE
C END IF THEN.
315    CONTINUE
C    END DO WHILE.
C      DO WHILE.
C IF THEN.
      IF(IO.NE.3)GOTO 319
      DO 318K=1,L
      WRITE 318,STA(K),SBGR(K)
318   FORMAT(* *, F5.1,* = *,F6.1)
318   CONTINUE
319   CONTINUE
C END IF THEN.
      RMS=SQRT(RMS/(L-1))
      WRITE 410,RMS
410   FORMAT(* RMS ERROR = *,F5.1)
C      END IF THEN.
      END
      SUBROUTINE LINE(STA,L,OBGA)
      DIMENSION STA(100),OBGA(100)
      DO 1020K=1,100
      IF(K.GT.L)GOTO 1030
      READ(10,1010)STA(K)
1010  FORMAT(F6.2)
      IF(STA(K).NE.0.)GOTO 1014
      WRITE 1012,K,STA(K)
1012  FORMAT(* STA(*,I2,*) = *,F6.2,*  CHANGE IT.*)
1014  CONTINUE
      READ(40,1015)OBGA(K)
1015  FORMAT(F6.2)
1020  CONTINUE
1030  CONTINUE
      RETURN
      END

READY 10.09.44
```

APPENDIX 5

Bayley, R. W., 1959, Geology of the Lake Mary Quadrangle: U.S. Geol. Survey Bull. 1077, 112 p., 1:24,000. (ground magnetic).

Case, J. E., and Gair, J. E., 1965, Aeromagnetic map of parts of Marquette, Dickinson, Baraga, Alger, and Schoolcraft Counties, Michigan and its geologic interpretation: U.S. Geol. Survey Geophysical Investigations Map GP467, 10 p., 1:62,500 (aeromagnetic).

Chenier, F. J., 1979, Report of seismic and boring survey, U.S. 2 and U.S. 141 from state line to M-69, Crystal Falls. Mastadon and Crystal Falls townships and City of Crystal Falls, Iron County. Control section 36051, Job Number 05444: Michigan Department of Transportation (till thickness and surface geology).

Dutton, C. E., and Linebaugh, R. E., 1967, Map showing Precambrian geology of the Menominee iron-bearing district and vicinity, Michigan and Wisconsin: U.S Geol. Survey. Miscellaneous Geologic Investigations Map I-466, 1:125,000 (surface geology).

James, H. L., Dutton, C. E., Pettijohn, F. I., and Weir, K. L., 1968, Geology and ore deposits of the Iron River-Crystal Falls district, Iron County, Michigan: U.S. Geol. Survey Prof. Paper 570, 134 p., 1:24,000. (ground magnetic).

James, H. L., Pettijohn, F. J., and Clark, L. C., 1970, Geology and magnetic data between Iron River and Crystal Falls, Michigan: Michigan Geol. Survey, Report of Investigation 7, 17 p. (till thickness, surface geology, and magnetics).

Kerkhoff, G. O., 1965, Report of seismic, resistivity, and boring survey, U.S. 2 relocation, Iron River-Crystal Falls Road Control Section Mb36022C: Michigan State Highway Department, Office Memorandum, (till thickness and surface geology).

Mallott, D. F., 1969, Report of seismic and boring survey, U.S. 141 relocation, Crystal Falls to Amasa Control Section 3605B: Michigan Department of State Highways, Office Memorandum. (till thickness and surface geology).

Meshref, W. M., and Hinze, W. J., 1970
aero
Geol. Survey, Report of Investigation 12, 25 p., 1:250,000. (aeromagnetic.)

Michigan Department of Natural Resources, 1979, East Part Iron County, 1:170,000. (station location)

Michigan Department of Natural Resources, various years, photocopied well log reports. (till thickness and surface geology)

Michigan Department of Transportation, no date, Plans of Control Section 36051, Job Number 05444. (helps in interpretation of Chenier, 1979)

Pettijohn, F. J., 1970, Geology and magnetic data for northern Crystal Falls area, Michigan: Michigan Geol. Survey, Report of Investigation 8, 23 p. (till thickness surface geology, and magnetics)

_____, 1972, Geology and magnetic data for southern Crystal Falls area, Michigan: Michigan Geol Survey, Report of Investigation 9, 31 p. (till thickness, surface geology, and magnetics)

Pettijohn, F. J., Gair, J. E., Weir, K. L., and Prinz, W. C., 1969, Geology and magnetic data for Alpha-Brule River and Panola Plains area, Michigan: Michigan Geol. Survey, Report of Investigation 10, 12 p. (till thickness, surface geology and magnetics)

Ruckford Map Publishers, 1979, Land Atlas and Plat Book, Iron County, Michigan: 58 p. (station location)

United States Geologic Survey, 1945 (photorevised 1975), Amasa Quadrangle, Michigan, Iron Co., 7.5 Minute Series (Topographic): 1:24,000. (station location).

_____, 1944, Michigan (Iron County) Crystal Fall Quadrangle, 7 1/2-Minute Series: 1:24,000.

_____, 1962, Florence East Quadrangle, Wisconsin-Michigan, 7.5 Minute Series (Topographic): 1:24,000. (station location)

_____, 1962, Florence West Quadrangle, Wisconsin-Michigan, 7.5 Minute Series (Topographic): 1:24,000. (station location)

_____, 1944, Michigan-Wisconsin, Fortune Lakes Quadrangle, 7 1/2-Minute Series: 1:24,000. (station location).

_____, 1961, Iron River, Michigan: Wisconsin: U.S. Geol. Survey Map NL 164, 1°x2°, 1:250,000. (station location).

_____, 1945, Michigan (Iron County), Kelso Junction Quadrangle, 7 1/2-Minute Series: 1:24,000. (station location).

_____, 1956 (photo revised 1975), Kiernan Quadrangle, Michigan-Iron Co., 7.5 Minute Series, NW/4 Sagola 15' Quadrangle: 1:24,000. (station location).

_____, 1956, Lake Mary Quadrangle, Michigan-Iron Co., 7.5 Minute Series (topographic), SW/4 Sagola 15' Quadrangle: 1:24,000. (station location).

_____, 1962, Naults Quadrangle, Wisconsin-Michigan, 7.5 Minute Series (topographic): 1:24,000.

_____, 1955, Ned Lake Quadrangle, Michigan, 15 Minute Series (topographic): 1:62,500. (station location).

_____, 1955, Witch Lake Quadrangle, Michigan, 15 Minute Series (topographic): 1:62,500. (station location).

Weir, K. L., 1971, Geology and magnetic data for northeastern Crystal Falls area, Michigan: Michigan Geol. Survey, Report of Investigation 11, 14 p. (till thickness, surface geology, and magnetic).